



**Acoustic Tracking of Juvenile Chinook
Salmon Movement in the Vicinity of
Georgiana Slough, Sacramento River,
California – 2003 Study Results.**

By Aaron Blake and Michael J. Horn

Draft Report

U.S. Department of the Interior
U.S. Geological Survey

DRAFT

Contents

Conversion Factors	v
SI to Inch/Pound	v
Datums Referenced.....	v
Abbreviations and Acronyms	v
Acknowledgements.....	vii
Executive Summary	9
1.0 Introduction.....	12
1.1 Background.....	12
1.2 Synopsis of 2001 DCC Study Results	14
1.3 Entrainment Zone Conceptual Model.....	15
1.3 Purpose and Scope	16
2.0 Methods.....	17
2.1 Acoustic Configuration.....	17
2.2 Mass Releases	18
2.3 Acoustic Data Collection	19
2.4 Generation of Fish Density Distributions	20
2.5 Fish Density Distribution Signals	23
2.6 Physical Data	24
2.7 Determination of Salmon Analysis Period	26
2.7 Analytical Techniques	28
3.0 Results and Discussion	31
3.1 Timing of fish detections Entering the Control Volume	31

3.2 Timing of Fish Detections Leaving the Control Volume	36
3.3 Patterns in the Spatial Distribution of Fish Entering the Control Volume	38
3.4 Patterns in the Spatial Distribution of Fish Leaving the Control Volume	42
3.5 Predicting Entrainment	46
4.0 Conclusions	50
4.1 Effectiveness of the Control Volume Approach	50
4.2 Relative Measures of Georgiana Slough Entrainment	51
4.3 Management Implications	52
4.0 References	53

DRAFT

Conversion Factors

SI to Inch/Pound

Multiply	By	To obtain
Length		
centimeter (cm)	0.3937	inch (in.)
millimeter (mm)	0.03937	inch (in.)
meter (m)	3.281	foot (ft)
kilometer (km)	0.6214	mile (mi)

Temperature in degrees Celsius (°C) may be converted to degrees Fahrenheit (°F) as follows:

$$^{\circ}\text{F}=(1.8\times^{\circ}\text{C})+32$$

Datums Referenced

Vertical coordinate information is referenced to the North American Vertical Datum of 1988 (NAVD 88)

Horizontal coordinate information is referenced to the North American Datum of 1983 (NAD 83)

Altitude, as used in this report, refers to distance above the vertical datum. Depth, as used in this report, refers to distance below the free surface, in meters, measured at the time of interest.

Abbreviations and Acronyms

bl/s body length per second

dB decibel

kHz kilohertz

M_H horizontal first moment

M_V vertical first moment

V	volt
ADCP	acoustic Doppler current profiler
COM	center of mass
CVP	Central Valley Project
CWT	coded wire tag
DAG	Dagmar's Landing measurement site.
DCC	Delta Cross Channel
FDDA	Fish Density Distribution Analysis
GS	Georgiana Slough measurement site
NAVD 88	North American Vertical Datum of 1988
PSD	Power Spectral Density
SACDS	Sacramento River measurement site downstream of the Sacramento River – Georgiana Slough junction.
STD	Standard deviation
SWP	State Water Project
USFWS	U.S. Fish and Wildlife Service
USGS	U.S. Geological Survey

Acknowledgements

The authors wish to acknowledge IEP and CALFED for the financial support of this work. Ron Ott and Kim Taylor at CALFED were instrumental in securing funding on short notice. Thanks to the California Department of Water Resources, Conveyance Program, for contract administration. Pat Brandes and Paul Cadrett, USFWS, were instrumental in arranging, delivering, and releasing the juvenile salmon used in this investigation. Thanks finally to Chris Enright and all of the men and women from DWR who were brought in on short notice to help in the field.

This study would never have been possible without the hard work of the USGS Bay Delta Project's dedicated team. Jon Burau (USGS) spent long hours planning and organizing this study, and kept the study on track despite an incredibly tight deadline. Jim George (USGS) created all of the custom hardware for the transducers, designed and fabricated the deployment tools, and was a constant source of ideas and solutions. Jay Cuetara (USGS) worked extremely hard to ensure that equipment deployment and recovery went smoothly. Jon Yokomizo (USGS) conducted ADCP surveys of the study area, and tested and debugged bathymetry survey software. Jay Cuetara and Jim DeRose (USGS), along with Jon Yokomizo, dove in often hazardous river conditions to help deploy and recover instrumentation.

**Acoustic Tracking of Juvenile Chinook
Salmon Movement in the Vicinity of
Georgiana Slough, Sacramento River,
California – 2003 Study Results.**

By Aaron Blake, And Michael J. Horn

DRAFT

Executive Summary

In the winter of 2003 a pilot study of juvenile salmon movement was conducted in the junction of the Sacramento River and Georgiana Slough. This study was conducted to evaluate the performance of technologies and techniques for studying juvenile salmon transport, this study included the use of active hydroacoustics to create an acoustic control volume around the Georgiana Slough – Sacramento River junction. Split-beam hydroacoustic target tracking systems were deployed in the Sacramento River upstream of the junction at Dagmar’s Landing, in Georgiana Slough immediately downstream of the junction, and in the Sacramento River downstream of the junction. These transducers were used to record the position and movement of fish passing through the study area over a 48 hour period. Large numbers of hatchery juvenile chinook salmon were released upstream of the junction, which provided a strong signal of salmon movement for 29 hours of the data acquisition period.

The data obtained from these acoustic transducers showed consistent patterns in the location and timing of fish detections at the measurement sites. At Dagmar’s Landing there was strong evidence that the horizontal location of fish density could be predicted by physical signals such as upstream water velocity, and the amount of flow entering Georgiana Slough. When considered in the context of the study area’s geometry, the nature of these predictive relationships suggest that increases in the strength of secondary circulation currents causes fish density to move towards the outside of the Sacramento River bend upstream of Georgiana Slough. In addition, analysis of pulses in fish

detections at Dagmar's Landing indicated that most release fish were holding upstream of the junction for around 2 hours, and that many fish appeared to hold upstream until dusk. Almost all fish detected at Dagmar's Landing were within 1.5 meters of the river surface, and there was a very clear difference in the depth of fish detected during the day and the depth of fish detected at night. Overall, the hydroacoustics at Dagmar's landing provided very clear measurements of the non uniform distribution of fish density in the river cross section at the measurement site, and excellent statistics on fish density distributions over the 29 hour salmon analysis period.

The data collected in the downstream junctions showed little correlation between processes controlling the location of fish entering the junction, and the location of fish leaving the junction. The location and timing of fish entering the junction did appear to impact the timing of fish detection in the downstream junctions (e.g. entrainment), but had little effect on the location of the detected fish. Entrainment in Georgiana Slough appears to be determined by a complex interaction between the location of fish at Dagmar's Landing, and the tidally controlled Eulerian velocity fields within the junction, but lacking velocity field data, these relationships could not be predicted. Fish detected in Georgiana Slough were almost uniformly distributed, with a few significant spikes in fish density detections in portions of the beams nearest the river surface. It is likely that fish were moving above the beams in the majority of the Georgiana Slough cross section, so Georgiana Slough detections can be used only as a lower-bound estimate of entrainment. Even so, when detections in Georgiana Slough are normalized for detection effort (acoustic beam volume), or for the relatively small volume of water moving

through the junction during the study period, the level of detections in the junction suggest that there are significant numbers of fish entering Georgiana Slough

The location of fish density in the cross section of the Sacramento River downstream of the junction was consistently skewed towards the outside of the channel, and did not fluctuate significantly over the duration of the study. As at Dagmar's Landing, the vast majority of fish detected at the Sacramento River downstream site were within 1.5 meters of the river surface, but, unlike the Dagmar's Landing data, the depth of fish detections did not show a physically significant change between day and night periods. Predictive relationships for entrainment in the Sacramento River downstream of the junction were heavily dependent on the number of fish detected at Dagmar's Landing, but these relationships improved significantly when the location of fish density at Dagmar's Landing, and water velocity in the Sacramento River were included.

Analysis of the hydroacoustic data showed the advantages of the control volume approach for acquiring very detailed statistics and time series data on the location of fish entering and exiting the study junction. However, the inability of this technique to resolve patterns in the timing of fish movement, and its inability to directly measure the movement of fish between acoustic measurement sites are major limitations. It is recommended that future studies that utilize fixed station hydroacoustics also include the use of Lagrangian techniques such as acoustic tag tracking.

The data collected during this study supported the entrainment zone conceptual model of juvenile transport developed during the analysis of the 2001 Delta Cross Channel study data. The 2003 data provided additional evidence that the location of fish entering a junction below a bend is influenced by the strength of secondary circulation patterns upstream of the junction. In addition, the Georgiana Slough data showed that entrainment in a branch of interest cannot be predicted based on the distribution of flow in the junction. These findings reinforce the importance of considering the interplay between channel geometry, hydrodynamic processes and fish behavior when designing or reconfiguring diversions and intake structures. In addition, the evidence of juvenile holding behavior and preferential selection of outmigration periods suggests that juvenile entrainment in diversions could be reduced through diurnal gate operations. Because of the complexity of the observed relationships, it is recommended that a coupled three dimensional hydrodynamic and fish behavior model be developed as soon as possible, so that future research can be used to improve the predictive capabilities of such a model.

1.0 Introduction

1.1 Background

The Sacramento River is a large alluvial system that drains the northern half of California's Central Valley, from its headwaters near Mt. Shasta, to its terminus at the mouth of the Sacramento-San Joaquin Delta (fig. 1). The Sacramento River supports four distinct populations of Chinook salmon, one of which is listed as a Federally Endangered Species. These species spawn and rear in the alluvial gravel beds of the

Sacramento River's tributaries then migrate south down the Sacramento River, through the Sacramento-San Joaquin River Delta and then San Francisco Bay before passing through the Golden Gate where they begin the marine portion of their life cycle. Unlike most other river systems where dams are the dominant human control on salmon outmigration, many of the problems associated with juvenile out-migrant survival in the Sacramento River arise from in-Delta mortality (Newman and Rice, 1998), which is affected by numerous diversions, changes in flow routing, large-scale pumping plants, and complex interactions and tidal influences between them. Concerns for in-Delta mortality has lead to a variety of water management operational constraints aimed at limiting losses of outmigrating salmon. In the fall of 1999 the Delta Cross channel was closed to protect salmon outmigrants. This closure created a rapid increase in western Delta salinities which precipitated a reduction in exports at the State Water Project (SWP) and Central Valley Project (CVP) pumping plants located in the southern Delta to comply with State Water Resources Control Board mandated maximum salinity levels in the western Delta (see <http://www.waterrights.ca.gov/baydelta/d1641.htm>). Because of this conflict between water supply, water quality and fisheries management in the operation of the Delta Cross Channel (DCC), CALFED and the various water project and fisheries agencies embarked on a series of field investigations aimed at improving our understanding of the dynamics that control juvenile salmon movement in junctions that are strongly influenced by the tides. During the winter of 2001 a multidisciplinary research team conducted a study of juvenile salmon entrainment in the DCC, which is the most significant man-made diversion on the lower Sacramento River. The results of this study, described in Horn and Blake (2003), suggest that juvenile salmon movement

through tidal junctions is controlled by interactions between biological and physical processes, and that it may be possible to quantify and predict these interactions.

Although these results were promising, the study was limited by an inability of the acoustic configuration to accurately measure the movements of fish in all branches of DCC junction. In order to build on the foundation of the 2001 study, researchers planned a large scale study of juvenile salmon movement in the Sacramento River in the general vicinity of the DCC area. This study includes the use of the same active acoustic technology employed in the 2001 study, as well as a variety of new fish tracking and velocity measurement technologies. In order to evaluate the performance of these technologies, and to test capabilities of split beam active hydroacoustics, a pilot study of salmon movement was conducted in the junction of the Sacramento River- Georgiana Slough in the winter of 2003/2004.

1.2 Synopsis of 2001 DCC Study Results

Analysis of acoustic fisheries data and water velocity data collected in the Sacramento River at the DCC in the fall of 2001 indicated that the location of juvenile salmon within the Sacramento River cross section was heavily influenced by the water velocity patterns in the vicinity of the DCC (Horn and Blake, 2003). Quantitative measurements of the distribution of fishes detected by the acoustics were made via Fish-Density Distribution Analysis (FDDA) techniques developed by the U.S.G.S. (ibid). FDDA showed that fish were non-uniformly distributed in the Sacramento River cross section, biased towards the left-upper half of the water column (outside of bend) of the Sacramento River. Time series analysis of FDDA data showed the across-channel bias of detected fish to be

correlated with the tidally varying flow in the Sacramento River upstream of the DCC, and the vertical position of the fish within the water column to be inversely correlated with light measurements (ibid). Maps of water velocities measured in the DCC junction area during the study show evidence of secondary circulation patterns in the river bend above the junction, suggesting that the outwards bias in the juvenile salmon distribution could evolve from an interaction between the secondary circulation that occurs in bends (basic hydrodynamics) and the surface orientation of juvenile salmon (simple models of behavior).

1.3 Entrainment Zone Conceptual Model

These observations led to the formulation of the “entrainment zone” conceptual model for juvenile salmon transport in tidal junctions. This model proposes that entrainment in a complex, tidally varying junction is controlled by the interaction between velocity distributions acting on outmigrants in a Lagrangian frame of reference up-current of a junction, and Eulerian referenced (tied-to-the-local geometry) velocity fields acting on juvenile salmon when they enter and pass through a junction. This model explicitly couples processes that occur upstream of the junction with processes that occur in the junction by proposing that at any given instant in time, the velocity patterns within a given junction dictate a spatial entrainment zone for each downstream branch, but that the number of fish entering each entrainment zone is determined by the interaction between fish behavior and upstream hydrodynamic processes. Thus, strong advection dominates the horizontal movement of juvenile salmon over short time and length scales, but much weaker processes acting over longer distances upstream of a junction can have

significant impacts on the spatial distribution of fish as they enter a junction, and thus can have significant influence on the entrainment characteristics of a given junction.

1.3 Purpose and Scope

During the winter of 2003, USGS researchers conducted a pilot study of emerging technologies and techniques for monitoring juvenile salmon movement in tidal junctions. One aspect of this study was the deployment of multiple active split-beam hydroacoustic target tracking systems to create a “control volume” around a junction. A control volume approach, using multiple instruments, gave investigators the capability of testing this equipment’s ability to measure the position, movement, and entrainment of mass releases of juvenile Chinook salmon entering and leaving a junction of interest. The data from the active acoustics were post processed using the FDDA techniques developed in Horn and Blake (2003), and then further analyzed to examine patterns in fish movement to test the entrainment zone conceptual model developed using the 2001 DCC data. This paper presents the results of the analysis of data obtained from the split-beam hydroacoustic target tracking systems; future works will seek to synthesize the analysis of the hydroacoustic data with the analysis of the other types of data collected during the 2003 study.

2.0 Methods

2.1 Acoustic Configuration

The split-beam acoustic portion of the Georgiana Slough pilot study was designed to test the feasibility of creating an acoustic “control volume” around a junction to measure the fate of fish entering the study area. To this end, two side looking, split-beam acoustic transducers were located in each branch of the Sacramento River – Georgiana Slough junction (figs 2, 3, 4). All transducers were BioSonics DTX systems equipped with HPR sensors. In order to avoid interference between transducers, each junction measurement site used one 199.2 Hz transducer and one 430 Hz transducer, with beam widths of about 6 degrees. At the Georgiana Slough (GS) measurement site, the Sacramento River Downstream (SACDS) measurement site, and on the Southeast bank of the Dagmar’s Landing (DAG) measurement site, transducers were mounted on platforms driven into the river bank ~2.5 meters below the water surface during the week of December 10th, 2003. At the Northwest side of the Dagmar’s Landing measurement site, one transducer was mounted 2.5 meters below the river surface on a pole attached to a moored houseboat. Transducers were attached to their mounting plates on remotely controlled pan-tilt systems. Each transducer was rotated to be roughly perpendicular to the river cross-section, and tilted to achieve maximum range. These mounting procedures resulted in acoustic beam patterns in each junction branch that provided beam coverage in the majority of the cross-section, with poor coverage near the banks and river bottom (figs. 3, 4, 5). Because the 2001 DCC study indicated that juveniles were located in the upper portion of the water column, beams were biased to provide better coverage near the river

surface, and as a result, there was no beam coverage at any site in the bottom 2 meters of the river cross-section.

After each transducer was positioned, its location and orientation were estimated to allow geo-referencing of the fish track data. The horizontal location of each transducer was measured with a handheld DGPS during deployment, and the vertical location of each transducer was estimated by subtracting its depth from water surface elevations measured at the USGS Walnut Grove Above (WGA) gauging station located on the Sacramento River upstream of the study site (see <http://baydelta.wr.usgs.gov/> for station location, station specifications, and data). Unfortunately, the exact deployment time of each transducer was not recorded, so transducer elevations were only accurate to about 0.5 meters. The elevation of the boat mounted transducer was calculated by subtracting 2.5 meters from the WGA stage record at the start time of each fish track, and can be considered accurate to 0.1 meters for each fish track. The heading, pitch, and roll of each transducer was measured with an internal compass and electrolytic tilt sensors, and recorded in the Echo View data files.

2.2 Mass Releases

During the study period mass-releases of coded wire tagged juvenile Chinook salmon were released upstream of the study site over a period of about 35 hours. Approximately 40,000 sub-yearling Chinook salmon from Coleman National Fish Hatchery were trucked to Vorden, CA, then pumped into floating net pens in the Sacramento River. Fish were acclimated for a period of about 24 hours prior to the beginning of mass-releases (fig 6).

Four groups of 10,000 fish were released between the afternoon of December 21, 2003, and the evening of December 22, 2003, with two releases occurring during the day and two at night. Releases were timed to allow for the arrival of fish (based on the assumption that juvenile salmon would travel at approximately the same velocity as the water) at the study site during peak ebbs, peak floods and tidal slack water. All fish were injected with coded wire tags (CWTs). A set of passive drifters equipped with D-GPS loggers were released with each group to track the movement of the parcel of water in which fish were released (fig 6).

2.3 Acoustic Data Collection

Beginning several hours before the mass releases, transducer data were recorded using Sonar Data's Echo View Visual Acquisition Software V4 (fig 7). The transducers acquired data at a rate of 5 pings per second and logged continuously to Dell laptop computers communicating over a wireless LAN, with one laptop per measurement site recording data from both transducers. Data-collection ranges were set from 33m to 90m depending on each beam's range (fig 3). Data thresholding was squared, water temperatures were left at the default value of 20⁰ Celsius (C), and sensitivity was set to -57 decibels (dB). Visual on-screen display was set to -40LogR, which is used for target-strength estimation and echo counting. Data was continuously logged using these settings, from several hours before the mass releases began to about 24 hours after the last release was made. After the study, echo-processing and trace formation was performed using Sonar Data's Echo View v4 as described in Blake and Horn (2003).

2.4 Generation of Fish Density Distributions

After echo-processing the ASCII output files produced by Echo View were loaded into Matlab software for FDDA. Using the position and orientation estimates for each transducer, each recorded fish track was geo-referenced, and assigned a Truncated Julian Day (TJD) time stamp calculated for the track's center point. The date and time of fish track points are recorded by Echo View based on the date and time set in the operating system of the acquisition computer, so it is important to verify that they are corrected. It was initially thought that the Sacramento Downstream measurement site computer was set to Mountain Time, one hour behind the other units, but after initial processing, pulses in the number of fish detected at the Sacramento River Downstream site were found to consistently lag those at the other sites by one hour. As a result, data from SACDS were reprocessed using Pacific Standard Time to match the other sites. Fish track points were geo-referenced based on recorded range and beam angle data as described in Horn and Blake (2003), and track positions were stored in UTM coordinates using the WGS84 horizontal datum, and NAVD88 vertical datum. Surveyed stage data used as the vertical reference for computing instrument elevations was converted from NGVD29 to NAVD88 using a vertical offset for the study area computed by VERTCON v2.0 (NGS, 2004).

After fish tracks were time-stamped and geo-referenced, tracks were filtered based on the track's mean target strength and mean elevation. The maximum surface elevation during the study was 2.47 meters NAVD88, so tracks having a mean elevation of greater than 3 meters NAVD88 were assumed to have incorrect position data (possibly due to transducer beam side-lobe interactions), and were not used for the analysis. Target

strength distributions from each beam were examined to determine if fish tracks could be filtered based on mean target strength to limit the analysis to juvenile salmon sized fish. Target strength distributions for the Georgiana Slough site (GS), for Sacramento River downstream (SACDS) beam 1, and for Dagmar's Landing (DAG) beam 1 match expectations for a riverine environment, with a normal-skew-left distribution and a mean of about -40dB, corresponding to fish size on the order of 0.05 meters (fig 8). The distributions for DAG beam 2 and SACDS beam 2 stand out with normal distributions that have a mean of about -30dB, which corresponds to fish an order of magnitude larger, about .5 meters. Because these two transducers were sampling very similar portions of the river to their counterparts, one would expect them to have similar target strength distributions; the order of magnitude difference in distribution means, and the difference in distribution shapes, suggests that these two transducers were incorrectly calibrated and reporting erroneous signal strengths. As a result, data from both GS transducers, the SACDS 1 transducer, and the DAG 1 transducer were filtered based on target strength, and the data from the DAG 2 and SACDS 2 transducers were not. For the filtered data, the minimum allowable target strength was set to -55 dB, which is the theoretical detection limit for the transducers, and the maximum allowable size was set to -33 dB, which corresponds to a fish size on the order of .2 meters. The filter range was set intentionally broad, as the relationship between target strength and fish size is inexact, so the result of the filtering was to minimize the contribution of information from fish that are significantly larger than juvenile salmon, and the removal of track information from debris or boats.

Filtered fish tracks from each site were grouped into 5 minute temporal bins, so that fish-track information could be summarized in discrete temporal increments. Five minute increments were chosen as a tradeoff between having enough fish in each bin for developing summary statistics, and keeping bins small enough to maintain temporal resolution consistent with the tidal timescale variation in the velocity fields in the junction. Horizontal and vertical binning patterns were developed for each branch using the techniques described in Horn and Blake (2003). Bins were laid out with 2 meter wide horizontal bins, and 1 meter vertical bins (figs 9, 10, 112), and ordered so that bin 0 for each site was on the river right bank with bin numbers increasing to the river left bank. Bin volume distributions were calculated for the Sacramento downstream site and the Georgiana Slough site as described in Horn and Blake (2003)(figs 12, 13). Calculating a bin volume distribution for the Dagmar's Landing site was more complicated because DAG beam 1 was mounted a fixed distance below the river surface, so the amount of beam coverage in each bin varied with stage. To solve this problem a beam volume distribution was calculated for 5 stage values evenly spaced from the maximum to the minimum stage measured during the study, and the beam volume distribution for any other stage was estimated by linearly interpolating between these values:

$$[BV_{s_n}] = [BV_{s_{low}}] + \left(\left([BV_{s_{high}}] - [BV_{s_{low}}] \right) \times \frac{(s_n - s_{low})}{(s_{high} - s_{low})} \right) \quad (2.1)$$

Where [BV] is the beam volume matrix for a given stage, s_n is the stage of interest, and s_{low} and s_{high} are lower and upper stages at which beam volume distributions were calculated. After initial analysis, it was desirable to attach the vertical bin reference to the water surface elevation, so that the distribution of targets at each depth could be compared for different stage values. Beam volume distributions for these depth

referenced bins were computed using the methods developed for Dagmar's Landing beam 2.

2.5 Fish Density Distribution Signals

Once binning patterns were established and beam volume distributions were calculated, fish density distributions were computed for each temporal bin, and various statistics of these distributions were calculated to create time series for further analysis. Fish density distributions and statistics in each temporal bin were calculated for four classifications: all detected tracks, all downstream moving fish, all upstream moving fish, and all milling fish. Fish tracks were categorized as upstream moving, downstream moving, or milling by the angle in R^3 between each track's net movement vector, and a preset downstream direction vector (set during spatial binning), calculated using the vector inner product. Tracks that were within 80 degrees R^3 of the downstream vector were classified as downstream moving, tracks that were between 110 and 180 degrees R^3 from the downstream vector were classified as upstream moving, and tracks that were between 81 and 109 degrees R^3 from the downstream vector were classified as milling. These angle ranges were set to limit milling fish classifications to fish that were explicitly moving transverse to the direction of mean flow, because net movement vectors calculated by Echo View were observed to be noisy, and tended to exaggerate the cross-stream component of fish movement. Time series statistics calculated for each group included the total number of fish in each temporal bin, the horizontal and vertical first moments for each temporal bin's fish density distribution, the horizontal and vertical second moments for each temporal bin's fish density distribution, and the depth of the vertical first

moment. Horizontal and vertical first moments were calculated as described in Horn and Blake (2003), vertical first moment depth was calculated by subtracting the elevation of the vertical first moment for each temporal bin from an interpolated stage record (USGS WGB see <http://baydelta.wr.usgs.gov/> for flow and stage data and station information), and horizontal and vertical second moments were calculated as follows:

$$X_2 = \frac{\sum_{i=1}^{nibins} \left[(X_i - X_1)^2 \sum_{k=1}^{nkbins} M_{i,k} \right]}{\sum_{i=1}^{nibins} \sum_{k=1}^{nkbins} M_{i,k}} \quad (2.2, 2.3)$$

$$Z_2 = \frac{\sum_{k=1}^{nkbins} \left[(Z_i - Z_1)^2 \sum_{i=1}^{nibins} M_{k,i} \right]}{\sum_{i=1}^{nibins} \sum_{k=1}^{nkbins} M_{i,k}}$$

where X_1 , and Z_1 are the horizontal and vertical first moments, X_2 , and Z_2 are the horizontal and vertical second moments, and $M_{i,k}$ is the fish density detected in the i,k bin. The second moments for a fish density distribution are a measure of the spatial variability in the distribution of fish in a study area for a period of time, with units of meters squared.

2.6 Physical Data

A variety of physical data signals were used in the analysis of fish density distribution information. Stage data for the study was obtained from the USGS Walnut Grove Below (WGB) gauging station (figs 14, 15), located on the Sacramento River about 1.5 km below the study area, and converted to NAVD88 as described above. Fifteen minute averaged discharge and mean cross-sectional averaged velocity were obtained for the

Sacramento River above the study area from the USGS Walnut Grove Above (WGA) gauge, located about 10 km upstream of the study site near Vorden, CA (figs 14, 15). Fifteen minute averaged discharge and mean cross-sectional averaged velocity for Georgiana Slough were obtained from the USGS Georgiana Slough (GS) gauging station, located about 100 meters downstream from the fisheries acoustics (figs 14, 15). Fifteen minute data for the Sacramento River downstream of the junction was also obtained from WGB. In order to analyze these signals in conjunction with the fish density distribution signals, data from each of these sites was linearly interpolated to the center time of the temporal bins established for the fish density distribution analysis (fig 15). A time series of the percent of flow entering the study control volume at Dagmar's Landing that entered Georgiana Slough (PDAGQ) was calculated by dividing the interpolated GS discharge values by the interpolated WGA discharge values (fig 15). The passive drifters released with each group of salmon were removed from the river about .25 km upstream of the Dagmar's Landing site (fig 2), and the date and time of their removal was recorded. This data was used to create an array of drifter arrival times for each mass release. These times are a rough estimate of the time at which the parcel of fluid the fish were released into reached the study site, and were used in the analysis of fish outmigration patterns.

A meteorological monitoring station was deployed in the study area prior to the mass releases, but did not function properly during the study. As a result, an approximate light signal was constructed using sunrise and sunset times obtain from a Garmin Fortrex 101 GPS for the study period. Sunrise and sunset times were assumed to be at the center of a

1 hour transition from a light value of 1.0 to a light value of 0.0 (fig 16). In order to obtain a broader estimate of periods with a high probability of crepuscular light conditions, a crepuscular signal was constructed by normalizing the 2hr, 5 minute rolling variance in the light signal (fig). Although crude, these two signals were used to classify temporal periods as high probability of daylight conditions, high probability of night conditions, and high probability of crepuscular conditions. During the study the weather was cloudy and occasionally drizzling with a new moon, so it is likely that this classification method under predicts the number of periods with crepuscular light conditions, but predicts periods with night conditions well.

2.7 Determination of Salmon Analysis Period

Fish density distributions and associated time series statistics for each classification of fish track were calculated for every temporal bin during the entire study period. As a result, these signals contain information on the movements of both released salmon, and “background” fish that naturally occur in the river. Thus, the fish track signals can be thought of as the sum of two separate processes:

$$Fish(t) = Salmon(t) + \omega_{salmon} + Residents(t) + \omega_{residents} \quad (2.4)$$

a behavior and noise signal from the introduced salmon, and a behavior and noise signal from the resident fishes. The goal of the mass-release methodology used in this study is to introduce a large enough number of salmon into the study area to dominate the observed fish signal,

$$Fish(t) = Salmon(t) + \omega \quad (2.5)$$

where the noise term, w , includes the signal from resident fishes, and noise in the salmon behavior signal. In order for this methodology to be effective, analysis of the fish data signals must be restricted to periods when it is likely that the fish movement signal is dominated by information from released salmon. Figure 17 shows the number of fish detected at Dagmar's Landing over time, with the daylight signal, drifter arrival times, and the start and end times of the selected analysis period in the upper axes. One can see that before and after the selected analysis period, very few fish were detected in the study area, with background levels of 5-15 fish per five minute bin. For most of the analysis period, there were over 200 fish detected per 5 minute bin, with the mean number of detections at 134 fish per five minute bin; if the average background level of about 10 fish per bin was consistent through the study period, then the mean contribution of background fish per temporal bin was around 7% of the total signal.

The lower axes of Figure 17 shows the Dagmar's Landing horizontal first moment signal, along with the 35 minute rolling standard deviation in the first moment signal, and the standard deviation of the second moment signal. The standard deviation of the second moment signal shows the amount of spread in the fish density distribution in a five minute period, in meters, while the 35 minute rolling standard deviation of the horizontal first moment shows the amount of change in the center of mass of fish density over a 35 minute period, in meters. Thus, these two signals show the evolution of the amount of spatial variance in the fish density, and changing consistency in the mean location of fish density.

As the number of fish detected at Dagmar's Landing increases, the temporal standard deviation and the second moment signals decrease significantly. This trend is quantified in figure 18, which shows the exponential decrease in the temporal variance in the Dagmar's Landing horizontal first moment signal as the number of fish detected increase. The temporal variance approaches its asymptote at about 50 fish per five minute bin – for this reason, the start of the salmon analysis period was chosen as the first bin before the Dagmar's Landing number of fish signal reached 50. In general, low temporal standard deviation in the horizontal moment signal means that changes in the fish position in the river are happening smoothly, and coherently, over time. In contrast, a large temporal standard deviation indicates that fish position in the river cross section is changing randomly over time. Thus, the fact that the standard deviation of the horizontal first moment signal is low during the selected analysis period, and fairly large on either end of the analysis period (fig 19), supports the assumption implicit in (eq. 2.5), and is a strong indication that fish density distributions from the analysis period are indicative of salmon movements.

2.7 Analytical Techniques

Analysis of fish density distributions, distribution statistics, and physical signals was performed in Matlab®, using a mixture of prepackaged routines and custom algorithms. In order to keep all signals on the same temporal spacing, time periods for any signal that didn't contain data were assigned nan values. These occurred if the base distribution used to generate the statistic contained periods where no fish were detected. Some analysis were performed with nans left in the signals – in those cases time periods with

nans were thrown out of the analysis. However, some analysis, such as the calculation of correlations and power spectral densities, required all signals to contain real data at every time step. In order to meet this constraint without introducing spurious frequency content, nans in each signal were replaced with white noise drawn from a distribution with the signals mean and variance:

$$X_n = \mu + 2(\text{randn} - .5) \frac{\sqrt{12\sigma^2}}{2} \quad (2.6)$$

where μ is the signal mean, σ^2 is the signal's variance, and *randn* is a computer generated, uniformly distributed random number of mean 0 and variance 1. Figures 20 and 21 illustrate the importance of using noise to fill in missing data, rather than using zeros or interpolated values.

Cross Correlation Function (CCF) output were calculated without wrapping, and scaled by the product of the square roots of the component signal's autocorrelations. Power spectral density functions for signals were calculated using Welch's method (Welch, 1967), as implement in the Matlab Signal Processing Toolbox V6.4, with the signal divided into two contiguous, non-overlapping 13.2 hour segments, and a hamming window applied to each segment to reduce spectral leakage. These parameters provided the best tradeoff between resolution and decreased uncertainty in the PSD. Confidence intervals were calculated for the PSDs at the 90% level. Stepwise multiple regressions were performed using the Matlab Stepwise Regression Tool from the Matlab Statistics Toolbox, V5.1. The acceptance P value was set at 0.05, and the rejection P value was set to 0.10. Unless otherwise noted, P values for simple regression statistics given in the text are practically 0.0.

The Monte Carlo simulation used for analysis of arrival time distributions simulated fish arrival times using a simple model of juvenile outmigration:

$$T_{r,n} = T_r + \frac{D}{(u_w - u_n)} + H_n \quad (2.7)$$

where $T_{r,n}$ is the arrival time of fish n , released upstream at Vorden, C.A. with release group r . In this model T_r is the release time for release group r , D is the river distance from the release point to the Dagmar's Landing measurement site, u_w is the Lagrangian mean water velocity in the Sacramento River between the release site and Dagmar's Landing, u_n is the positive rheotaxis swim speed of fish n , and H_n is the holding time of fish n . Using a Monte Carlo approach u_n and H_n were randomly generated numbers; u_n was drawn from normal distributions, and H_n was drawn from Gamma distributions. H_n distributions were generated using the `gamrnd` function as implemented in the Matlab Statistics Toolbox V5.1. The PDF of the complete gamma distribution is defined by:

$$P(x) = \frac{1}{b^a \Gamma(a)} x^{a-1} e^{-\frac{x}{b}} \quad (2.8)$$

where Γ is the standard gamma function. The shape and magnitude of gamma distributions were fit by changing parameters b and a , and the normal distributions were parameterized by changing the distribution's mean and standard deviation.

3.0 Results and Discussion

3.1 Timing of fish detections Entering the Control Volume

Analysis of the patterns of fish detection at each branch of the control volume focused on two considerations; patterns in fish arrival at the entrance to the control volume, and patterns in the numbers of fish leaving the control volume in each downstream branch.

Patterns in the timing of fish arrivals at Dagmar's Landing are important to understanding the timing of fish leaving the control volume, but also contain information on the downstream movement behaviors of the released fish. Figures 17 and 22 show time series of downstream moving fish detections at Dagmar's Landing along with fish release times and drifter arrival times. Elevated levels of fish detection at the Dagmar's Landing measurement site begin about 1 hour after the arrival of the drifters from release 1 with a sharp spike in the number of detections that slowly decays to a minimum around 0.85 days after the first release, then increases to another pulse around 1.15 days after the first release. Superimposed on top of this general trend are broad, noisy pulses in the number of detections around the time of the arrival of drifters from releases 2 and 3. The arrival of the drifters from release 4 is followed by what could be a small pulse of about 40 fish.

The general pattern of detections at Dagmar's Landing is likely due to interactions between a variety of factors, including variable swimming speeds, variable predation rates, changes in the detection efficiency of the transducer configuration with changing surface elevation, and the timing of holding and out migration behaviors of the release fish. One hypothesis that explains the general trends in fish detections at Dagmar's Landing is that large numbers of the release fish tended to hold along the banks of the

Sacramento River upstream of the study site, and then gradually move downstream after holding for some period of hours. If fish did tend to hold for a significant period after release, then it's likely that some subset of the fish would remain in refuge habitat until evening crepuscular conditions that would stimulate the beginning of a crepuscular or nighttime migration period. This would explain the extremely large numbers of fish observed in the study area after the first release, which occurred at the beginning of the evening crepuscular period, the declining numbers of fish observed through the following night and day, and also the pulse of fish observed moving through the study area during the subsequent evening crepuscular period. Although it is impossible to test this hypothesis without upstream tracking data, it is in agreement with existing work on Chinook outmigration on the Columbia River System, which suggests that less smolted juveniles tend to migrate for short evening periods following the crepuscular decrease in sunlight, (Northwest Power and Conservation Council, 2000), and is consistent with data from the 2001 study, which suggested that large numbers of the released fish were holding upstream of the Delta Cross Channel until evening crepuscular periods (Blake and Horn, 2003).

Although it is impossible to determine the extent to which holding behavior dominated the Dagmar's Landing fish detection signal, pulses in the signal contain evidence that some fish from each release were holding above the study site for short periods of time. In order to examine the pulses visible in the overall fish detection signal in increased detail, a pulse signal was constructed by detrending the fish detection signal for the analysis period and setting the negative values to zero (fig 23). The detrending was

accomplished by fitting a 5th order polynomial to the fish detection signal, offsetting this fit by the mean of the absolute value of the fit residuals, and subtracting the result from the detection signal (fig 23). The pulse signal shows fairly distinct and relatively broad pulses following the arrival of drifters 1, 2, and 3, and a smaller pulse of about the same width following the arrival of drifter 4. There is also a very significant pulse at the end of the signal that corresponds very strongly in duration to the approximate crepuscular signal, reinforcing the hypothesis that this pulse represents fish that had waited to begin outmigration during dusk conditions.

The problem of making inferences about outmigration behavior from the observed pulses in fish detections is a classic Bayesian dilemma; the detection data contains information on population distributions, namely swim speed and holding time behaviors, but there is not enough information on the population to explicitly resolve these distributions. Lacking the data for an explicit solution, stochastic techniques were used to investigate the relationship between holding time, swimming speed, and the measured fish detections. Using a Monte Carlo approach, the holding and swimming behaviors of any single fish were considered to be random, but it was assumed that the distribution of these behaviors across the entire population could be described by real but unknown probability density functions. Arbitrary initial values were used to parameterize the probability distributions described in section 2.7, and these distributions used to generate a large number of fish ($O \sim 10^4$) with independent swim speeds and holding times. Using equation 2.7, arrival time at Dagmar's Landing was calculated for each simulated fish and used to assign the simulated fish to temporal bins in the same manner as the real

targets. The resulting fish detection signal was compared with the actual pulse signal, and the swim speed and distribution parameters were adjusted and the process repeated.

The Bayesian Monte Carlo cycle of probability distribution parameterization, population simulation, simulation evaluation, and population re-parameterization converged towards solutions having a significant mean holding time, on the order of two hours. While it is impossible to pick a specific holding time – swim speed combination as the best fit, the simulation process provided valuable information on the influence of holding time and swim speed population parameters on fish travel time. Figures 24 and 25 show snapshots of this process, beginning with curves generated with normal swim speed distributions and no holding time (fig 24), and ending with curves generated with normal swim speed distributions, and holding times drawn from gamma probability distributions (e.g. 2.7, fig 25). The most important observation from this process, illustrated in Figure 25, is that realistic swim speed distributions alone cannot produce arrival time pulses that match observations. The pulses in Figure 24 have an average width of only 15-20 minutes, and more closely match the noisy spikes in the pulse values than the actual pulses. The histograms in the lower axes of Figure 24 illustrate this concept, with a realistic swim speed distribution and corresponding arrival time distribution contrasted with a swim speed distribution that produced an arrival time distribution of about the same width as the observed pulses, using a mean Lagrangian water velocity of .54 m/s. It is highly unlikely that significant numbers of fish were exhibiting positive rheotaxis swim speeds on the order of 2.5 bl/s or greater (Nelson, 1994), so it can be concluded that some type of holding behavior is probably occurring. The arrival curves in Figure 25 are a

much better fit to the shape and width of the observed pulses at realistic rheotaxis swim speeds using holding times drawn from gamma distributions ($a=3$, $b=.025$). One can see that the swim speed acts as an offset to the arrival pulse, with the width and the shape of the pulse almost completely determined by the holding time distribution. The relative impact of the swim speed decreases with increasing Lagrangian mean water velocity, as is seen in the difference between the curves for release 1 and release 2. The relative contribution of the swim speed distribution and the holding time distribution on the resulting arrival time distribution is shown for four different water velocities in Figure 26. At water velocities greater than about 6 times the swim speed, swim speed acts to shift an arrival time distribution set by the holding time distribution. As water velocity decreases towards about 3 times the swimming speed, swim speed shifts and stretches the distribution that is set by holding time. For water velocities less than three times mean swimming speed, both the width and shape of the arrival time distribution is significantly affected by the swim speed distribution. These observations are important, because they suggest a parameterization to predict the relative importance of swimming and holding behavior on the long term transport of juvenile salmon that is dependent only on maximum likely rheotaxis swim speed and mean water velocity. In addition, this analysis strongly suggest that the shape of local features in the detection signal at Dagmar's Landing are the result of holding behavior, and that the overall trends in Dagmar's Landing are likely to be as well.

3.2 Timing of Fish Detections Leaving the Control Volume

The analysis of fish detections at the downstream measurement sites focused on comparing the patterns in fish entering the control volume at Dagmar's Landing with patterns in the total number of fish leaving the control volume (SACDS and GS). Based on the relative magnitude of the individual branch detection signals (fig 22), one would expect SACDS detection to dominate the total downstream detection signal, with GS detections adding some additional variability. The total overall downstream detection signal shown in Figure 27 matches these predictions, with fewer numbers of fish detected leaving the control volume than entering, and an overall shape that is similar to both the DAG and SACDS detection signals. However, there are some time periods where GS detections have a significant impact on the shape of the downstream detection curve, effectively accentuating the pulses in total downstream detection following drifter arrivals.

Cross correlation coefficient functions (CCCF) that compare shared variance between the downstream detection signals are shown in Figure 28. The CCCF signals indicate that the total number of fish detected exiting the control volume is highly correlated with the number of fish detected entering the control volume (0.89), and that for the SACDS and total downstream signals the maximum cross correlation with the DAG signal occurs at 0 lag, which indicates that most fish that pass through the beams at Dagmar's landing pass through the SADDs within the same temporal bin, which means that most fish take between 2-4 minutes to pass through the control volume. The maximum in the DAG-GS CCF is at -35 minutes, with another peak at -5 minutes. The signal's peak at -35 minutes

is likely due to the low number of fish detected at GS relative to the variance in the DAG signal (fig 29), and the -5 minute peak indicates that fish leave the control volume in Georgiana Slough more than one temporal bin (4-8 minutes) after they enter. The slow decay of all CCCF functions is due to the relatively slow rate of change of the fish detection signals, and supports the idea that fish arrival times are temporally smoothed by holding behavior.

The high correlation between the DAG and downstream detection signals suggest that the control volume approach was successful in detecting the majority of fish when they entered and exited the control volume, and that many of the fish that contribute information to fish density distributions at the DAG measurement site are also contributing information to the fish density distributions at the downstream sites for the same temporal bin. This is supported by the fact that the cross correlation between DAG detections and the downstream detections signal is higher than the cross correlation between DAG detections and SACDS detections alone, which suggests that despite the very low numbers of fish detected at GS (figs 22, 29), the GS detection signal still shares significant information content with the DAG signal. This idea is supported by least squares regression analysis, which shows that, with outliers included, the DAG detection signal explains about 50% of the variance in the combined downstream detection signal, and 47% of the variance in the SADDS signal alone; with a few outliers removed, DAG detections explain 72% of the variance in the combined downstream detection signal, and 69% of the variance in the SACDS signal (figs 30,31).

3.3 Patterns in the Spatial Distribution of Fish Entering the Control

Volume

Patterns in the spatial distribution of fish entering the control volume at Dagmar's Landing were analyzed with the goal of drawing inferences about the interaction between upstream physical processes and fish behavior, and how these interaction affected the location of fish entering the control volume. Figure 32 shows the overall fish density distribution for Dagmar's Landing during the analysis period. The vast majority of fish were detected within 2 meters of the surface, with almost no detections below -2 meters (about 4 meters deep). Laterally, fish were centered on the middle of the channel, with an almost Gaussian pulse in fish density around bin 30, and a smaller, roughly Gaussian pulse in fish density near bin 40. The fact that there are two distinct, smooth pulses in the fish density distribution suggests that release fish may be exhibiting two separate modes of behavior, the dominant mode resulting in fish moving through the cross section near center channel, and a secondary mode that has fish moving down the edge of the rivers left bank shoal.

Time series statistics for the Dagmar's Landing fish density distribution are shown in figure 33, and distributions of these statistics are shown in figure 34. The most striking feature seen in these plots is the very clear, bimodal distribution in the depth of the DAG vertical first moment. There is a very clear change in depth that occurs during the evening about .75 days after the first release, with fish rising during the day. Separate daytime and nighttime vertical fist moment depth distributions were generated for

nighttime and daytime periods with low crepuscular values (fig 35), and a non-parametric Kruskal-Wallis test was performed to determine the probability that these two samples were drawn from the same distribution – this null hypothesis was rejected at a probability of 0.0 (P that null should be accepted). Both the daytime and the nighttime distribution have very low standard deviations of about .2 meters; the detected fish exhibited incredibly clear vertical orientation behavior during the analysis period. It is important to note that the direction of this migration is opposite of that the migration observed during the 2001 DCC studies, however, sediment loads during the 2003 studies were significantly higher than during the 2001 experiments, and there was a full moon during the 2001 studies, and a new moon during this analysis period. It is quite likely that the direction and magnitude of the observed vertical migrations could be parameterized based on down-welling radiation and light extinction profiles, and future studies should address this challenge.

The square root of the horizontal second moment signal, which represents the horizontal standard deviation of each density distribution, remained roughly constant at about 12 meter for the duration of the analysis period, while the horizontal moment signal fluctuated between -10 and +10 meters. These general trends in the horizontal signals indicate that center of mass of fish density moved within the site cross section, but the amount of spread in the fish density didn't change significantly through the study period. The auto correlation function for the Dagmar's Landing horizontal moment signal (fig 36) exhibits strong periodicity, with negative and positive peaks separated by about 12.5 hours. The behavior of the autocorrelation function indicates that the DAG horizontal

moment signal has a strong sinusoidal trend, and the approximately 12 hr period of the fluctuates suggests that there may be a tidal influence in the data. To follow up on these observations, spectral analysis was performed for the DAG horizontal moment signal, and the WGA cross sectional mean velocity signal (figs 37 and 38); the power spectral density function (PSD) for the DAG horizontal first moment signal reveals a distinct peak in energy at a frequency corresponding to a roughly 12 hour period, and the PSD for the WGA velocity signal shows significant peaks corresponding to 12hr and 24hr sinusoids. The fact that the WGA velocity signal and the DAG horizontal first moment signal share significant frequency components at the 12hour period strongly indicates that tidal fluctuations in velocity upstream of Dagmar's Landing influence the cross sectional location of the center of mass of fish density entering the control volume, even though the tidal signals in the velocities during this study period were relatively weak (non-reversing) compared to periods of low Sacramento River inputs.

The relationship between the WGA mean cross sectional velocity signal and the Dagmar's Landing horizontal moment signal was formalized through several phases of regression analysis (figs 40, 41, 42, 43, 44). Initially, a linear relationship was fit between WGA velocity and the DAG horizontal first moment (fig 40). This model predicted a weak positive relationship with an r^2 of about 0.1, and was used to identify outliers (fig 40). The identified outliers all occurred during crepuscular periods, and/or during periods of very low fish detection at the DAG measurement site; the timing of the outliers suggests that they were from time periods when non-salmon were having a significant impact on the observed fish density distribution. After these outliers were

removed the relationship improved to an r^2 of 0.2, with roughly uniformly distributed residuals (fig 41), indicating that a simple linear model was a good match to the shape of the relationship between WGA velocity and DAG horizontal first moments, but that it could only directly explain about 20% of the variance in the horizontal moment signal. This model was improved by using stepwise multiple regression analysis to identify additional relationships that could be used to predict the DAG horizontal first moment (figs 42, 43). Adding Georgiana Slough discharge and the depth of the DAG vertical first moment resulted in an r^2 of .4, and incorporating the DAG horizontal second moment improved the r^2 to .66. The final regression model provided a good fit to the data, with most residuals falling within 4 meters of the prediction – considering that the river cross section at the Dagmar’s Landing measurement site is about 120 meters wide, a 4 meter error in the predicted location of fish density center of mass is quite good. In addition, the shapes of model relationships are in accordance with the entrainment zone conceptual model, which suggests that parameters correlated with increasing secondary circulation strength should have a positive relationship with DAG horizontal first moments, and parameters correlated with decreasing secondary circulation should have a negative relationship. Simple scaling of the equations of motion predicts that the strength of secondary circulation structures increases with mean velocity (Fisher, 1969), and because increasing flow into Georgiana Slough effectively reduces the bend in the Sacramento river through the study area (fig 2), increased GS discharge should correlate with decreased secondary circulation strength. These hypothesis are consistent with the relationships shown in figure 42, and further, the negative relationship between depth and the residuals shown in figure 43 is consistent with the idea that outward strength of

secondary currents decreases with depth. The strong relationship between the horizontal first and second moments is probably explained by bimodal distribution of fish density shown in figure 32; it appears that the primary source of spatial variance in the fish density distribution for periods with a strong salmon signal is caused by the presence of significant numbers of fish moving through the area of the second peak in fish density, and thus, increased spatial variance tends to correspond to increased horizontal moment. If the bimodal density distribution is indicative of bimodal behavior, then the second moment component of the regression model is really a surrogate indicator of fish behavior mode. For example, tendency to migrate along the shoal could be influenced by degree of smoltification, so in this case, the second moment signal would be acting as a surrogate for behaviors related to the degree of smoltification (e.g. a mean gill ATPase data signal).

3.4 Patterns in the Spatial Distribution of Fish Leaving the Control Volume

Fish density distributions for the entire study period for the Sacramento River downstream measurement site and the Georgiana slough measurement site are shown in figures 45 and 46. Fish density in the Sacramento River cross section exiting the control volume was centered around bin 27, about 57 meters from the river right bank, and very clearly skewed towards the river-left bank. The SACDS horizontal first moment signal fluctuated slightly during the study period but is almost always significantly greater than zero (figs 47, 34), and in addition, the temporal distribution of the horizontal first

moment signal is skewed to the right (fig 34) which shows an increased tendency for the fish density distribution from any five minute period to be significantly skewed towards the river right bank. The mean of the SACDS horizontal standard (square root of the second moment signal) deviation signal was about the same as at DAG (fig 47), but tended to fluctuate less, having lower variance (fig 34) and a skewed left temporal distribution (fig 34), with a mode of around 6 meters of variability, meaning that fish densities at the SACDS site were significantly less likely to be as spread out as at the DAG site.

In contrast with fish density distributions observed at the Dagmar's Landing and Sacramento River downstream measurement sites, the overall fish density distribution for the Georgiana Slough measurement site showed fish density to be almost uniformly distributed in much of the river cross section, with a few dramatic pulses indicating detection "hot spots"; the two greatest pulses were in the upper edges of the river cross-section, and a third pulse at the bottom of the beams in the center of the cross section. The temporal distribution of the GS horizontal first moment is nearly uniform, which means that fish were about equally likely to pass through all portions of the Georgiana Slough measurement site cross section in any given five minute period (fig 34). Unfortunately, the most likely explanation for these results is that the majority of fish moving through Georgiana Slough were located in the upper meter of the measurement site cross section, and as a result, where the only beam coverage was on either edge. The two order-of-magnitude increase in the density of fish detected in the upper portions of

the beam support this explanation, and suggests that measurement bias has a significant effect on the fish density distributions from the GS measurement site.

The vertical first moment signals from both downstream measurement sites contain different patterns than the vertical first moment signal from the DAG measurement site. The depth of the vertical first moment at the SACDS site exhibited very little change over the study period (fig 48), but the temporal distributions of the square root of the vertical second moment signals from the two sites were similar, suggesting that the fish density at each site had about the same vertical variance during any given time period, but that the center of vertical fish density at the SACDS measurement site did not shift between day and night periods. The depth of the Georgiana Slough measurement site vertical first moment signal contained significantly more noise than the same signals from the other two sites, and the temporal distribution of the depth of the vertical first moment signal was nearly uniformly distributed. Thus, the patterns in the depth of the vertical first moment signal from the GS measurement site also suggests that either fish density was nearly uniformly distributed within the cross section, or, that the majority of the fish density in the GS cross section was not detected. Nighttime and daytime depth of vertical first moment signal temporal distributions were constructed from the signals at the two downstream sites using the same time periods that were used for the DAG analysis, and the same non-parametric test was performed on each set of distributions to evaluate the statistical significance of any differences in daytime and nighttime depth at each site (fig 49). Test statistics for each site were on the order of 10^{-6} , which suggests that there were statistically significant differences between the daytime and nighttime depth of fish

densities at each site. However, the magnitude of these differences were much smaller than the mean spatial standard deviation in the vertical first moment signal for each site (figs 49, 34), so these differences do not appear to be physically significant.

The behaviors of the horizontal first moment autocorrelation functions for each downstream site are in accordance with the other evidence about fish location at each measurement site (fig 36). The horizontal first moment signal from the SACDS measurement site is almost perfectly auto correlated with itself over the entire study period, evidence that the horizontal location of fish density in the SACDS measurement site cross section did not exhibit significant fluctuations over the course of the study. In contrast, the horizontal first moment signal from the GS measurement site is almost completely decorrelated with itself over the course of the study (fig 36); a strong indication that the fish detections for this site were randomly distribution. Spectral analysis of the horizontal first moment signals provided additional evidence of the trends in the autocorrelation functions; the SACDS horizontal first moment signal PSD showed all energy present at steady state, and the GS horizontal first moment signal PSD indicated a uniform distribution of energy throughout the spectra, reminiscent of the PSD for white noise. Taken together, the observations of patterns in the fish density distributions exiting the control volume suggest that junction acts as a filter that decouples the location of fish exiting the junction from processes affecting the location of fish entering the junction. This idea supports the entrainment zone concept, and suggests interesting corollaries between juvenile entrainment dynamics and linear systems theory.

3.5 Predicting Entrainment

The ultimate goal of the North Delta juvenile transport studies is to develop tools to predict the entrainment of juvenile salmon in tidal junctions, so it is appealing to try developing predictive relationships to explain entrainment in the downstream junction branches. That said, if the entrainment zone conceptual model is correct, then Eulerian velocity patterns in the junction area are an important factor controlling entrainment, and one would expect entrainment relationships that didn't include such information to be relatively weak. However, the process of exploring entrainment relationships without Eulerian velocity maps is still useful, as it could identify surrogate signals that contain information on the Eulerian velocity fields, and provide insights into the validity of the entrainment zone concept.

The null entrainment hypothesis used in the design of the North Delta juvenile transport studies is the “fish go with the flow” hypothesis; the number of fish in a downstream branch over a given time period is equal to the percentage of the upstream flow entering that branch multiplied by the number of fish entering the upstream branch. Figure 52 shows scatter plots testing this hypothesis for both Georgian Slough and the Sacramento River downstream. It is immediately clear that this hypothesis is not valid for predicting Georgiana Slough entrainment, linear regression of this data results in a r^2 value of .028, and a P value of .0028. The entrainment in SACDS appears to be a better fit, with a clear linear relationship between the null hypothesis predicted entrainment and the actual entrainment. However, this plot is really just a slightly skewed version of Figure 30, because most of the flow entering the control volume went down the Sacramento River,

(fig 53), and almost all of the fish detected exiting the control volume were detected in at the SACDS site (fig 29). Further, stepwise multiple regression analysis indicated that the best linear model of SACDS entrainment included DAG detections, DAG horizontal first moments, DAG vertical first and second moments, and WGB velocity information, but not the PDAGQ signal, indicating that this data set does not clearly support the null entrainment hypothesis, and probably shouldn't be used to test it.

The best model of Sacramento River entrainment was identified through stepwise multiple regression analysis that considered all physical signals and all DAG distribution signals without removing outliers provided an r^2 of 0.59, using; a positive fit with DAG detections, a negative fit with DAG horizontal first moments, a negative fit with DAG vertical first moments, and a positive fit with DAG vertical first moments squared and a positive fit WGB velocity (fig 54). Removing the outliers shown in figures 30 and 31 this relationship improves with an r^2 of 0.77. It is interesting that all of the outliers identified showed no common pattern in their distribution, except for the fact that they all fell within a very narrow band of Georgiana Slough flows. It is likely that the Eulerian velocity field associated with these Georgiana Slough flows contains additional information that would explain the outliers during this period. With or without outliers, the shape of the predictive relationships support the entrainment zone concept, because they indicate that entrainment in the Sacramento River increases as the center of mass Dagmar's Landing moves to river right (towards SACDS), and also increases as velocities into SACDS increase. The quadratic relationship between entrainment in SACDS and DAG vertical first moments is likely the result of the coupling between

DAG vertical position and the light signal – it seems that vertical first moments squared is acting as a surrogate for diurnal information.

Unlike entrainment in the Sacramento River downstream branch, entrainment in Georgiana Slough is not easily predicted using physical signals and descriptions of DAG distributions. Fish detections shown in figures 22 and 23 suggest that entrainment in Georgiana Slough is weakly correlated with drifter arrivals, but the signals show little other structure. Extensive multiple regression analysis and stepwise multiple regression analysis yielded no usable relationships between any linear or quadratic combination of physical signals (fig 55). This observation is not surprising, as the entrainment zone for Georgiana Slough probably changed nonlinearly in response to interactions between the flow in each junction, and even with velocity field measurements this process would be hard to capture in a 1 dimensional regression analysis. In an attempt to capture the three dimensionality of the entrainment process, time signals of the detected fish density in each bin were created, and stepwise multiple regression analysis was performed on the resulting matrix of 627, 316-point long signals (192,132 total data points). The results of this analysis are summarized in figure 56; the r^2 value of .42 and P value of 0.0 were dramatic improvements over prior regression attempts ($r^2 \sim 0.01$, $P \sim 0.001$), but the seemingly random locations of the selected signals, and the number of negative relationships, suggest that the regression could be the result of over fitting entrainment data to slightly trended noise signals. Despite the increased spatial information utilized in this approach, it is likely that the regression could not full capture the complexity of the entrainment processes, because the bins that influence Georgiana Slough entrainment

should vary depending on the velocity field in the junction. In an attempt to address this problem, convolutions were added to the regression process to shift information from each bin in the river cross section in response to the percentage of WGA discharge entering Georgiana Slough – these analysis yielded models with lower r^2 coefficients (~ 0.3), and patchy bin influences. Thus, the best predictive model of entrainment in Georgiana Slough is the one shown in figure 56, which explains about 40% of the variance in the detection signal. The difficulty of predicting Georgiana Slough entrainment supports the measurement bias hypothesis deduced from patterns in Georgiana Slough fish density distribution.

Although attempts at developing a predictive model for Georgiana Slough entrainment were not highly successful, the observation that the GS detections signal is fairly well correlated with the DAG detections signal (fig 28) suggests that a less restrictive bin-by-bin analysis of the Dagmar's Landing distributions in conjunction with the GS detection signal could yield insights into entrainment dynamics. The individual bin-signal analysis described above was performed using a cross correlation between each bin signal and the GS detection signal instead of a least squares regression. The results of this process using both the GS and SACDS signals are show in figures 57 and 58. These correlation distributions show areas of the Dagmar's Landing site cross section that have similar temporal variance patterns to the detection signal. It is likely that these distributions map the regions in the DAG cross section that have the most significant effect on the shape of each downstream detections signal, and as such, are a very intriguing finding that should be investigated further.

4.0 Conclusions

4.1 Effectiveness of the Control Volume Approach

Data collected during the 2003 pilot study provided a good assessment of the strengths and limitations of the acoustic control volume approach. Acoustic data from the Dagmar's Landing measurement site and the Sacramento River downstream measurement site provided exceptional measurements of both the temporal and spatial patterns of fish movement through these cross sections, and allowed for the creation of information rich time series data that could be used for advanced analyses. In addition, information from the control volume's upstream face was successfully combined with independent physical data to develop good predictors for the number of fish detected exiting the control volume downstream at the SACDS measurement site. However, the difficulty in interpreting the Georgiana Slough fish density distributions highlights the sensitivity of the control volume approach to the orientation of the acoustic beams, and the problems associated with an observation method that cannot measure fish movement within large control volumes. In addition, the difficulty of inferring outmigration behavior from detection time patterns highlights another significant weakness of this type of data. These results can be summarized by observing that the control volume approach is an inherently Eulerian measurement technique, and as such, is limited to measuring changes occurring at a fixed location. For this reason, active hydroacoustics are not well suited to the study of process that change throughout space, but are very well suited for measuring the evolution of processes at a fixed point over time. For this reason, it would

be ideal to combine an active acoustic control volume with other tools that can obtain Lagrangian data over several time/length scales; slow ping (0~.01hz) acoustic tags or radio tags to measure the presence/absence of fish upstream of the junction to detect holding and outmigrating behaviors, and fast ping (0~1hz) acoustic tags to measure fish movement within the junction control volume to better understand entrainment processes.

4.2 Relative Measures of Georgiana Slough Entrainment

Although it is impossible to know if a measurement bias resulted in under detection of fish entering Georgiana Slough, it is fairly certain that fish detections at Georgiana Slough don't over-predict entrainment. Thus, the Georgiana Slough detection signal can be considered a good lower-bound estimate of Georgiana Slough entrainment. When considered as an absolute number of fish detected, the number of fish moving into Georgiana Slough appears to be quite small in comparison with the SACDS site. However, it is important to consider that during the study period, the amount of Sacramento River water from upstream of the junction entering Georgiana Slough was quite small compared to the amount entering the Sacramento River below the junction (figs. 15, 53). In addition, the amount of beam volume at each measurement site increases by the cube of cross section width; Both the Dagmar's Landing and Sacramento River downstream measurement sites had an order of magnitude more beam coverage than the Georgiana Slough site. When one adjusts each of the control volume detection signals to normalize for either site flow or site beam volume, the entrainment rate in Georgiana Slough appears quite significant (figs 59, 60). Almost an order of magnitude more fish per cubic meter of beam were detected in Georgiana Slough than were detected

in the Sacramento River below the junction, and detections per cubic meter of river water were about the same at each site. In this context, the questionably low detection rates in Georgiana Slough during this study indicate that entrainment in Georgiana Slough could be significant. This conclusion is especially important when one considers that a much greater portion of Sacramento River discharge enters Georgiana Slough during periods of lower outflows, when the Sacramento River below the junction reverses and flows into Georgiana Slough.

4.3 Management Implications

The results of this analysis are in good agreement with the conclusions drawn from the 2001 study data, and provide additional support for the framework of the entrainment zone conceptual model. These two studies show that it is highly unlikely that fish are evenly distributed in the river cross section, and, as is clearly illustrated in figure 52, that entrainment in critical junctions doesn't seem to be predicted by the distribution of flow within the junction. The strength and nature of the predictive relationship developed for the location of fish at Dagmar's Landing provides strong support for the hypothesis that surface oriented fish are being moved to the outside of bends by secondary flow structures in the upstream channel. These results highlight the importance of considering the interplay between hydrodynamics and channel geometry when designing or modifying intake structures or diversion channels. In addition, the likelihood that juveniles are exhibiting significant holding time behavior has important implications for operation of diversions; taking water during crepuscular periods appears to pose a greater risk for juvenile entrainment than taking water during the day or late at night, and the

relative risk between these periods could decrease over time as juvenile smoltification progresses.

The entrainment zone concept implies that such complex interactions between fish behavior, hydrodynamic processes, and changing environmental conditions can be modeled using process based simulations. It is very likely that a hydrodynamic and fish behavior model could be used in a stochastic manner to predict entrainment risk in both real and hypothetical junctions to inform management decisions. The development of such a model is the logical next step in the study of juvenile transport in the Delta, and for the first time, is supported by the level of detail available from modern acoustic data. Active hydroacoustics can be used to develop very robust distributions of fish location that can be used to test model predictions using Monte Carlo techniques, and tag tracking data can be used to develop fine scale swimming behavior models. In order to gain maximum benefit from future field efforts this model development should begin immediately, so that uncertainties encountered in the modeling process can inform data collection efforts.

4.0 References

Fisher, H.B. The effect of bends on dispersion in streams. *Water Resource. Res.* 5. 496-

506

Horn, M.J., and Blake, A. 2003. Acoustic tracking of juvenile Chinook salmon

movement in the vicinity of the Delta Cross Channel. 2001 study results. USBR
Technical Memorandum No. 8220-04-04.

Nelson, W.R., L.K. Freidenburg, and D.W. Rondorf. 1994. Swimming performance of
subyearling chinook salmon. Pages 39-62 in D.W. Rondorf and W.H. Miller, (eds.).
Identification of the spawning, rearing, and migratory requirements of fall chinook
salmon in the Columbia River basin. Bonneville Power Administration, Annual Report
1992, Portland, Oregon.

Newman, K.B., and J. Rice. 1998. "Modeling the Survival of Chinook Salmon Smolts
Outmigrating Through the Lower Sacramento River."

Northwest Power and Conservation Council. 2000. "Return to the River." Council
Document 200-12 Portland, Oregon

Welch, P.D, "The Use of Fast Fourier Transform for the Estimation of Power Spectra: A
Method Based on Time Averaging Over Short, Modified Periodograms," IEEE Trans.
Audio Electroacoustics, Vol. AU-15 (June 1967), pp. 70-73. As cited in the Matlab
Signal Processing Toolbox documentation, version 6.4.

Figure 1. Map of the Sacramento River watershed and the Sacramento/San Joaquin Delta, California.

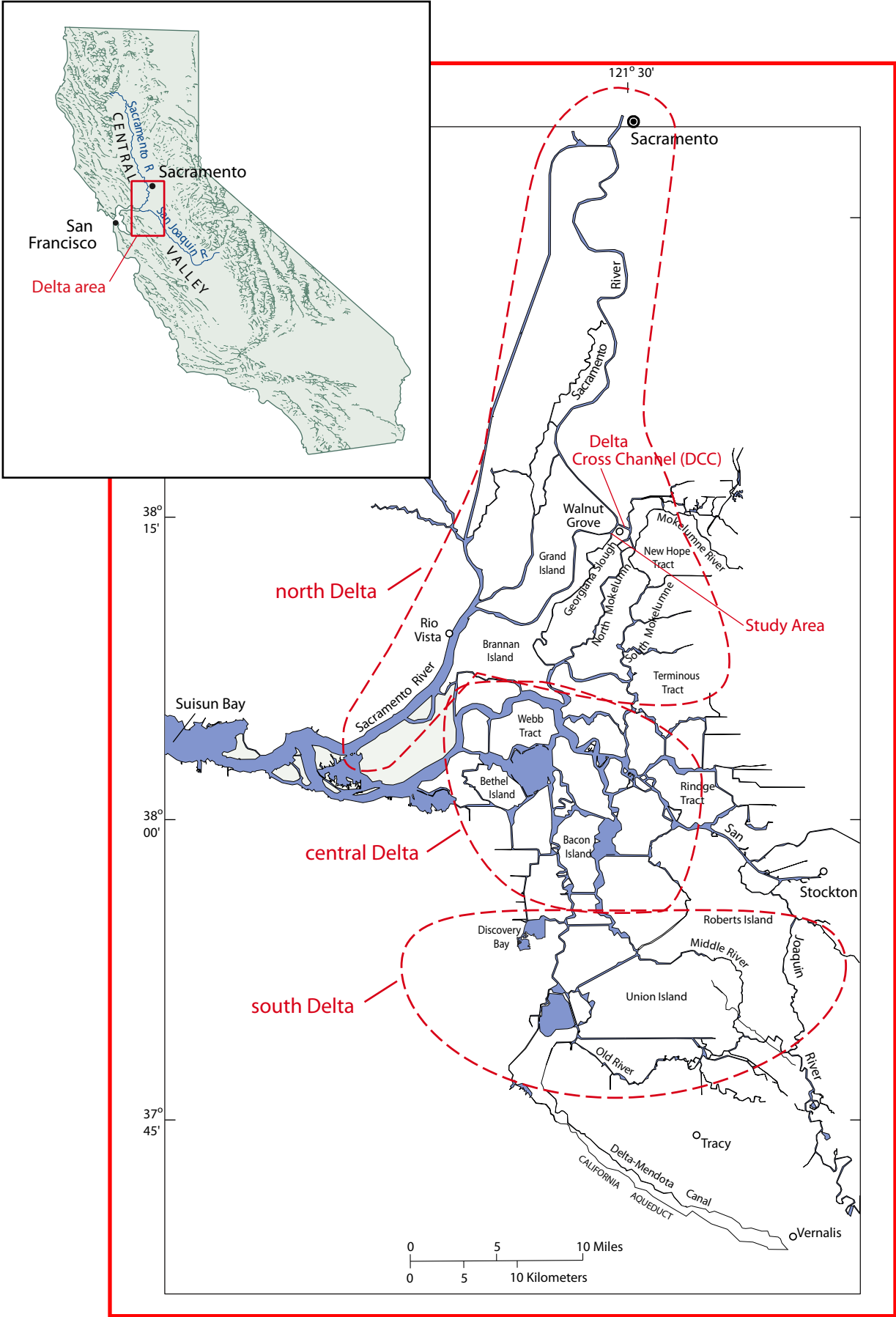


Figure 2. Study area with bathymetry and acoustic beams superimposed

Study Area

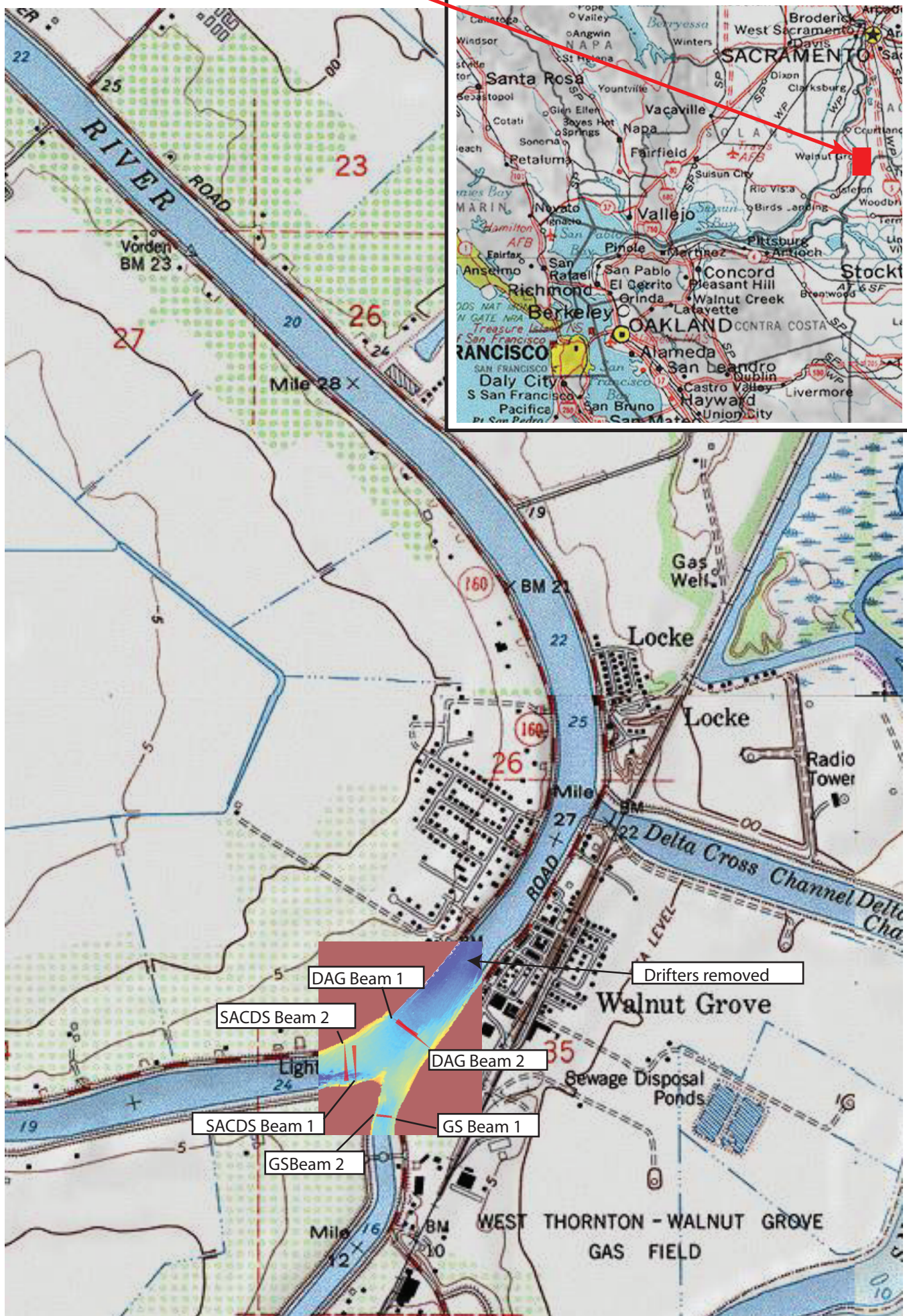


Figure 3. Bathymetric map of the Sacramento River - Georgiana Slough junction area with acoustic beams, and conceptual "control volume" around the junction area.

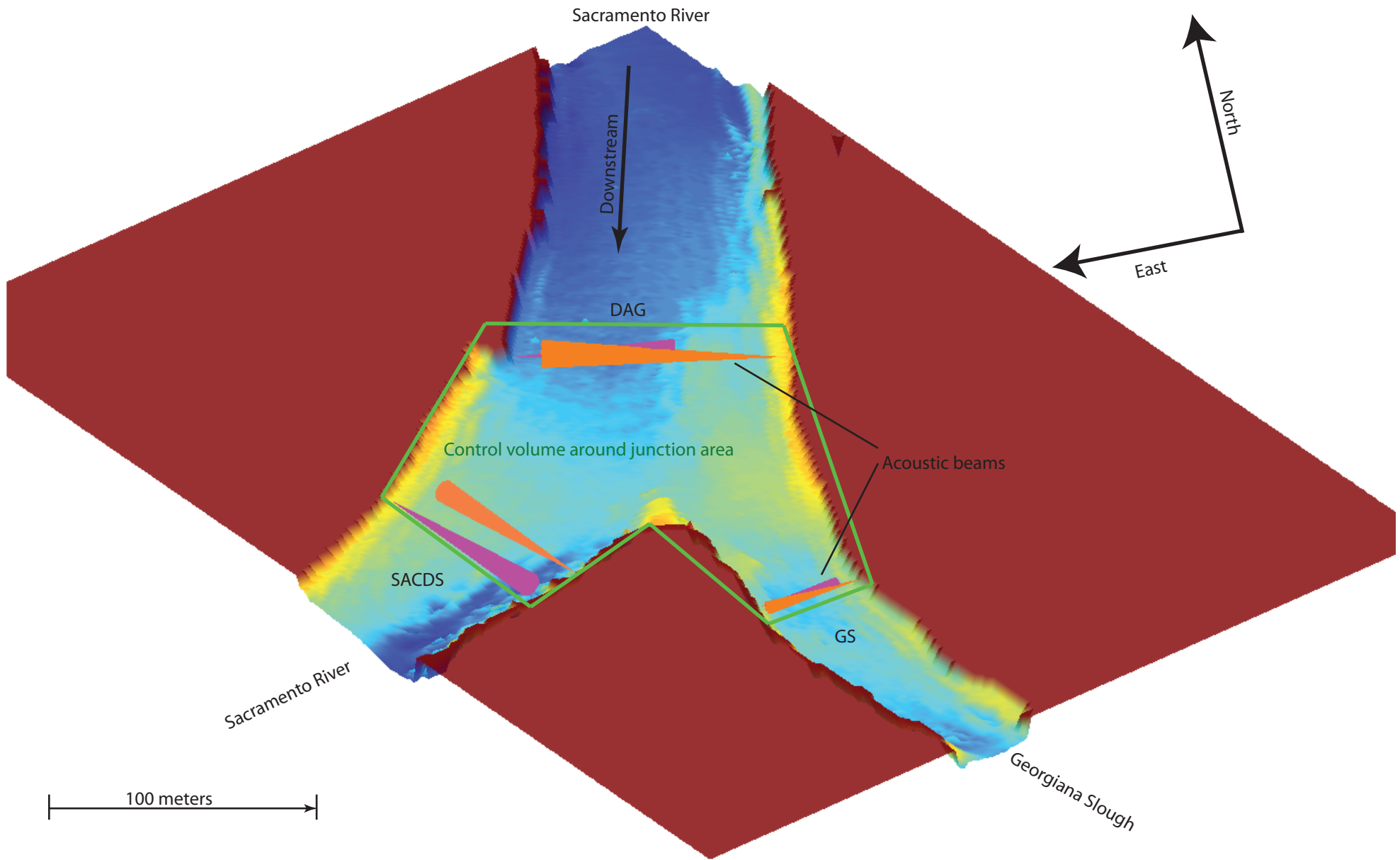


Figure 4. Fisheye view of the acoustic beam control volume around study site, viewed from the perspective of a fish moving downstream towards the Dagmars Landing beams. Beams are drawn in red, bathymetry is shaded by depth, the vertical scale is slightly exaggerated for illustrative purposes.

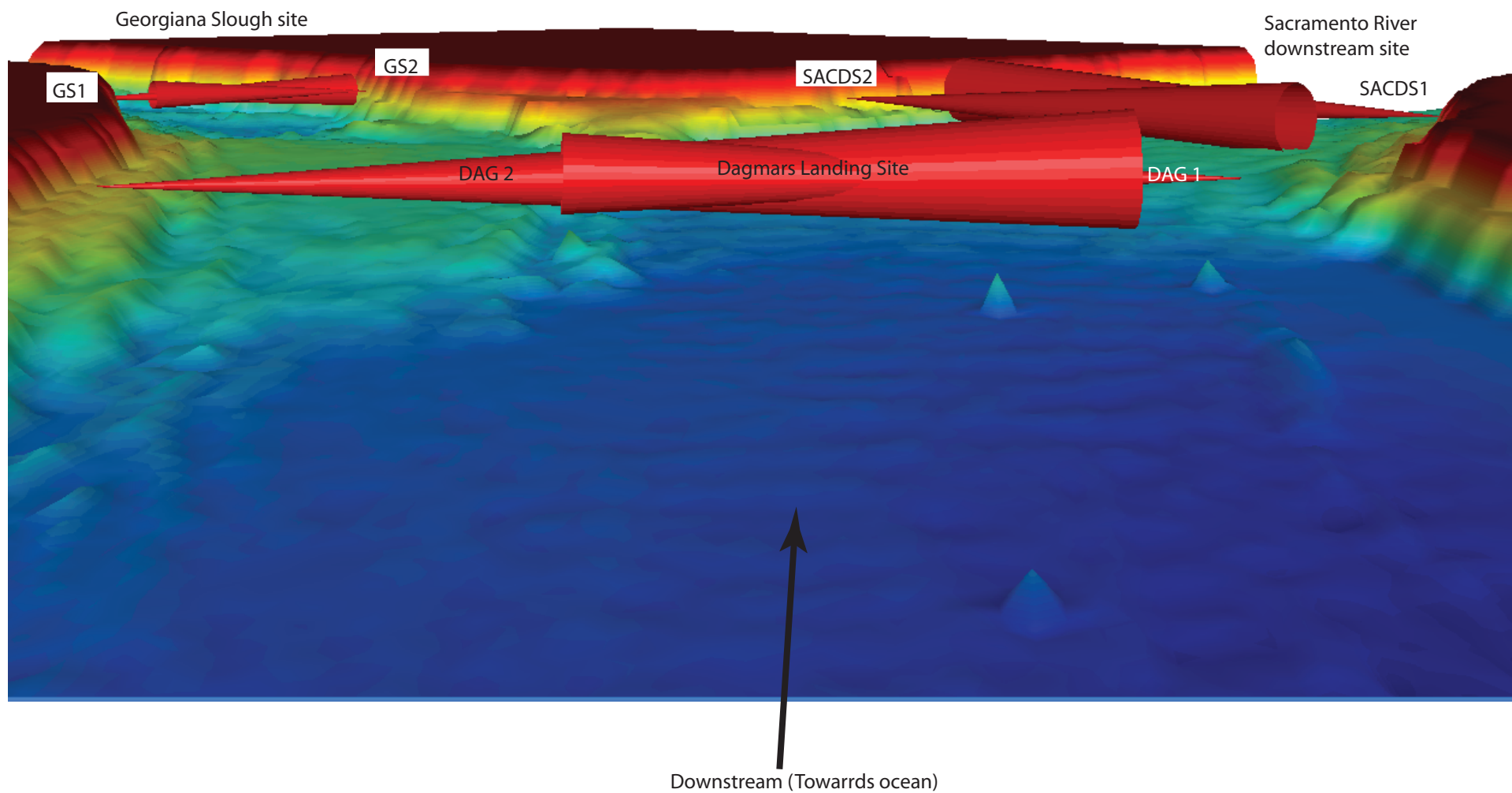


Figure 5. Measurement site river cross sections showing all the fish density detected for the analysis period. Fish density is shaded by magnitude. Areas in the cross sections with beam coverage, but no fish detections are shown in light pink. Areas of the river cross section that were wet during the study but didn't have beam coverage are shown in gray. The elevation of the river bottom is drawn in a thick black line. The elevation of maximum stage is drawn as a thick, horizontal blue line. The river cross section horizontal center (0.0 Horizontal first moment) is shown as a dashed green line. The fish density distribution center of mass (horizontal and vertical first moment) is located with dashed purple lines. The cross sections are aligned based on approximate streamlines at maximum flow into each junction, so that each downstream distribution is located underneath the portion of Dagmar's Landing expected to contribute the bulk of water entering it.

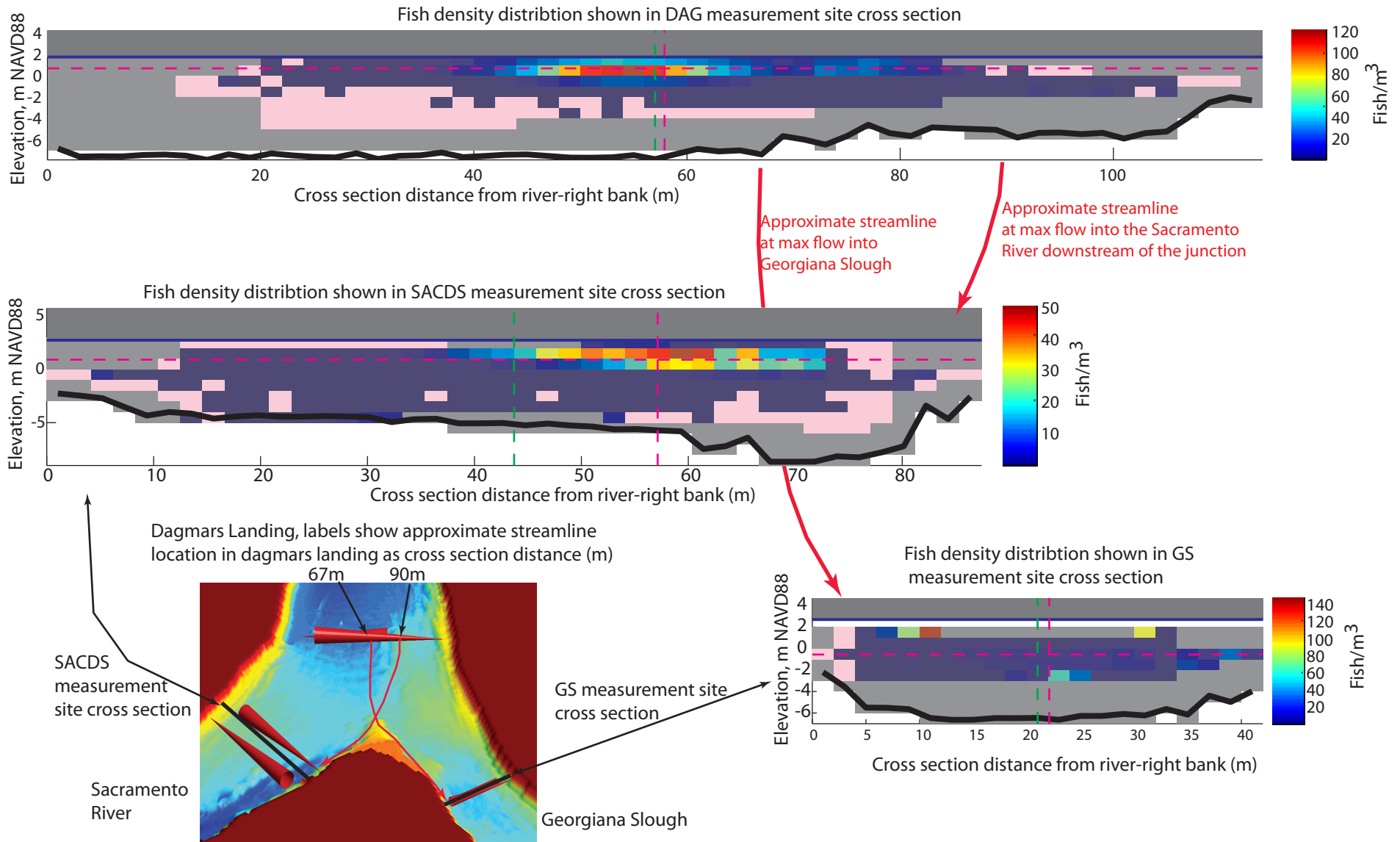


Figure 6. Illustrations of the salmon acclimation and release process.

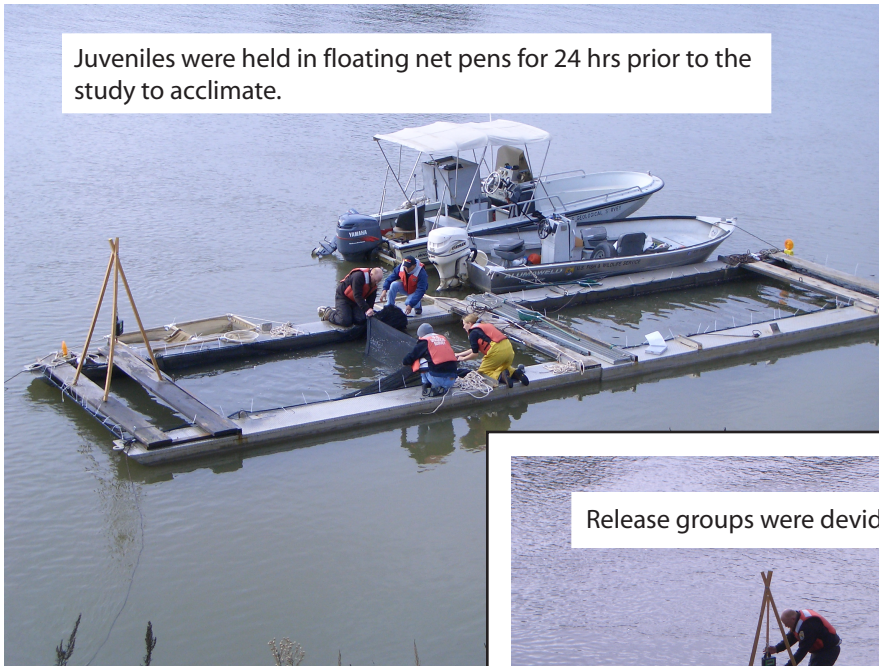


Figure 7. Example screen from BioSonics Visual Acquisition Software V4.

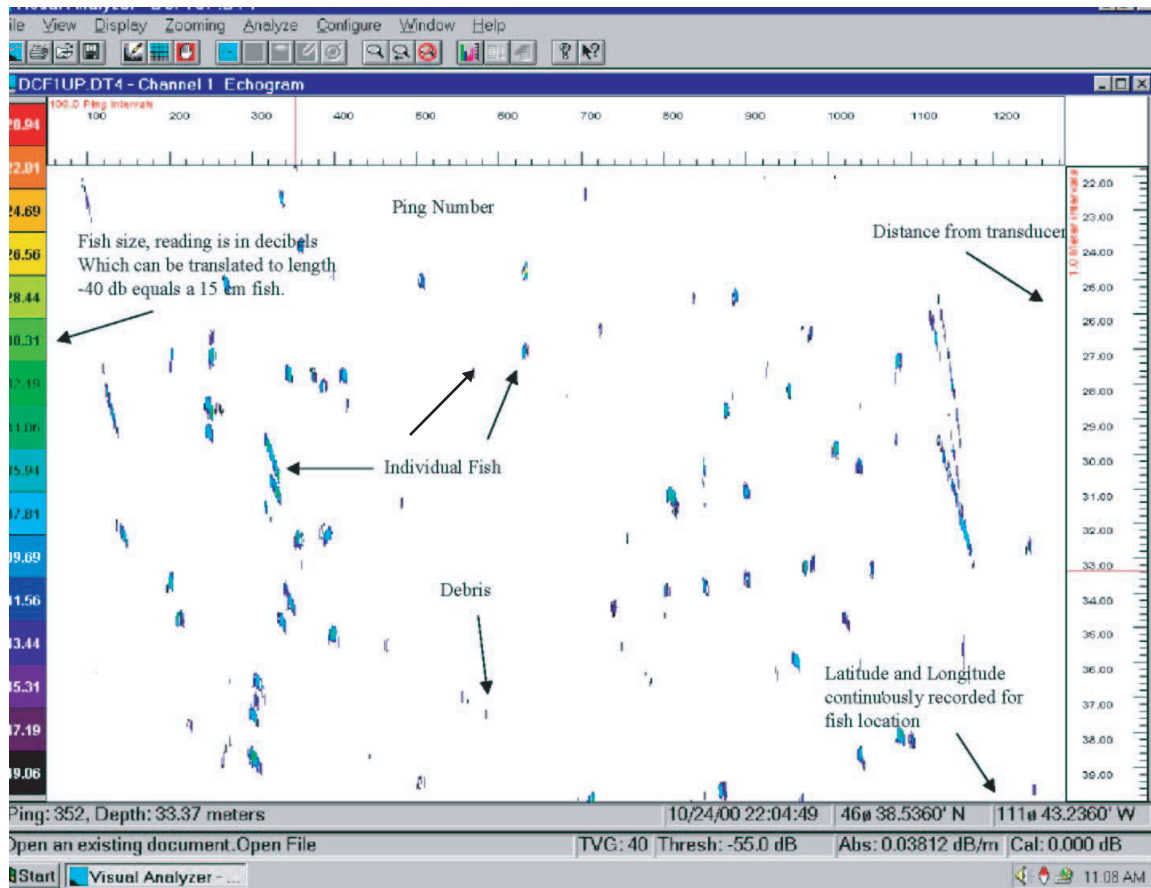


Figure 8. Target strength distributions for each transducer beam.

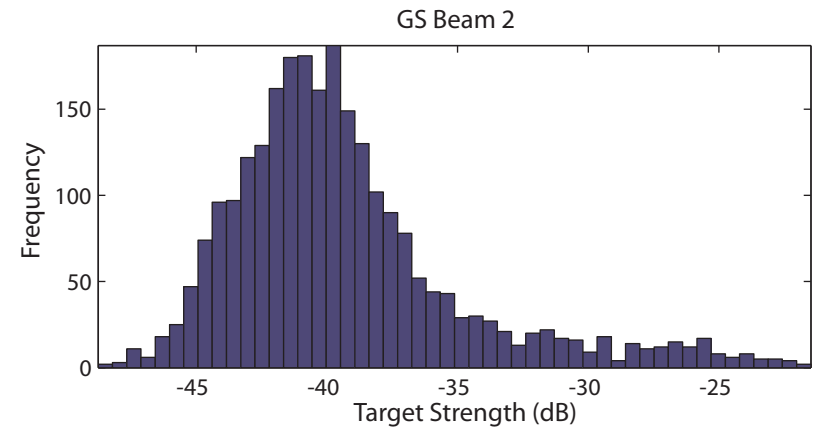
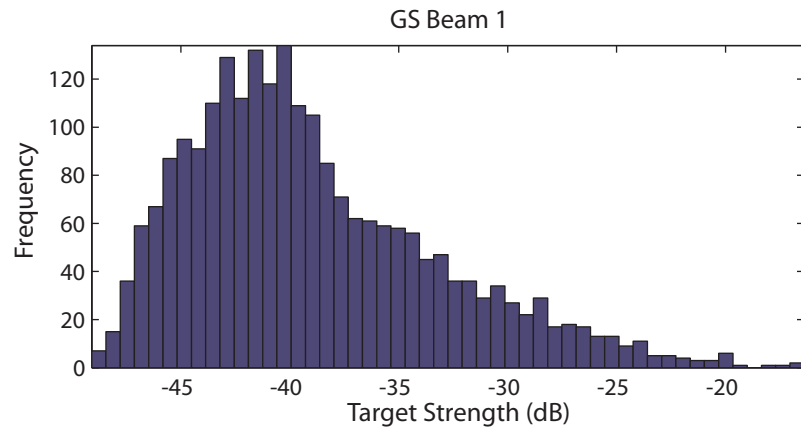
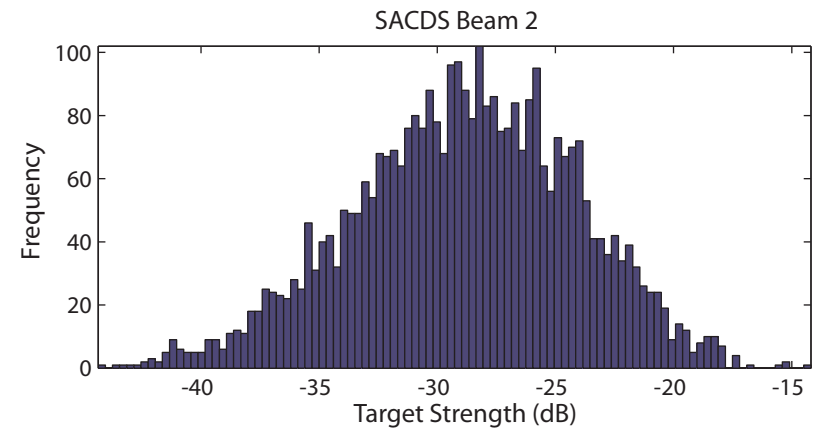
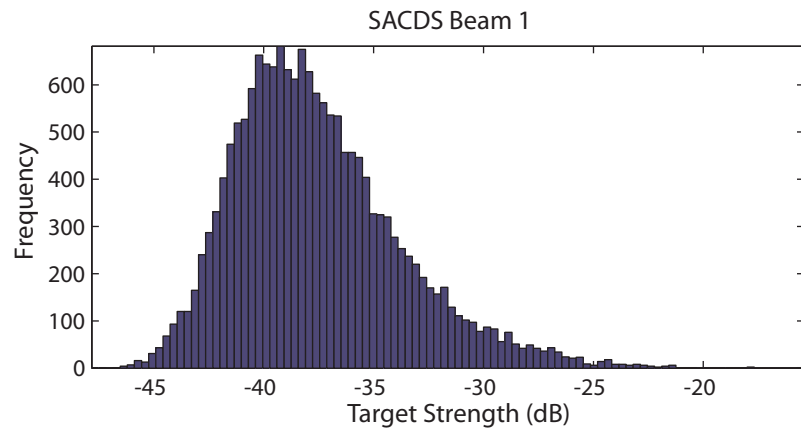
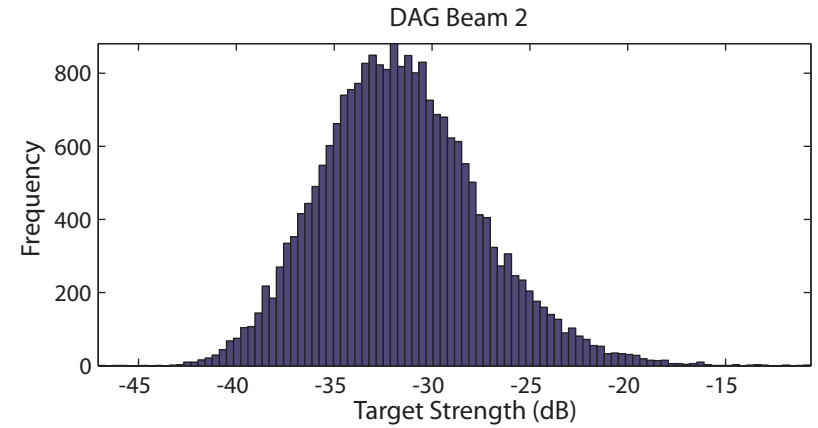
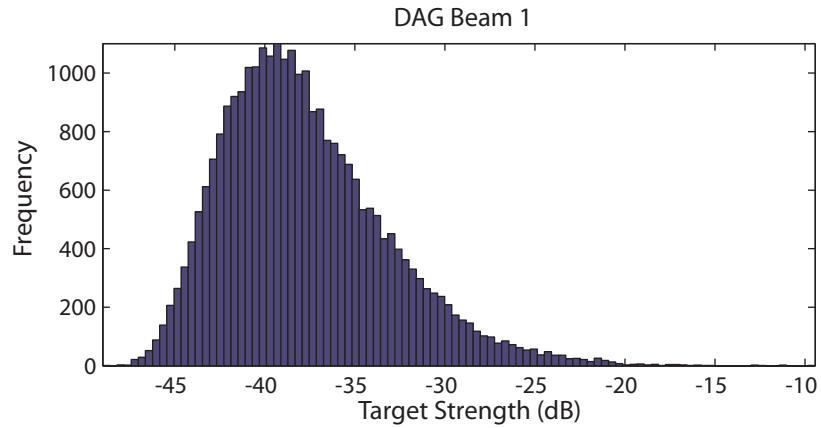


Figure 9. Binning pattern at the Dagmars Landing measurement site.

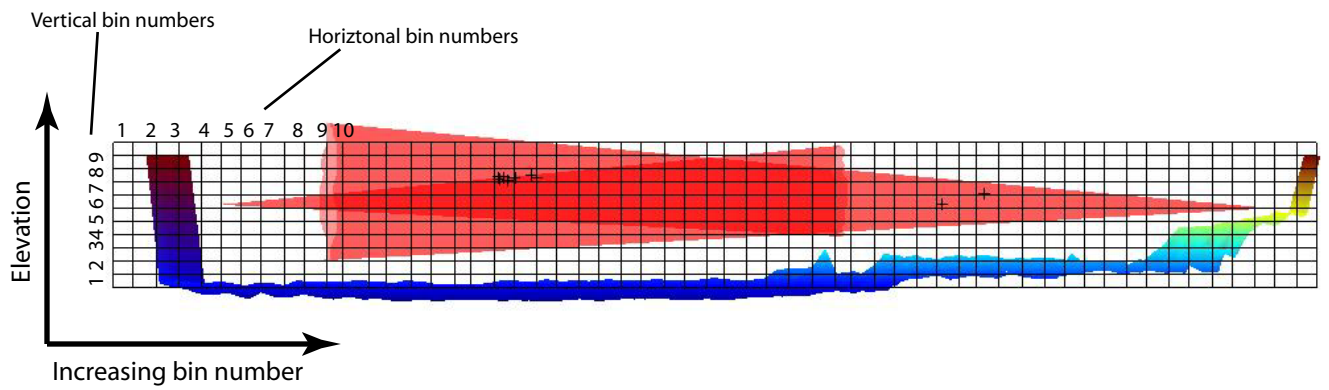
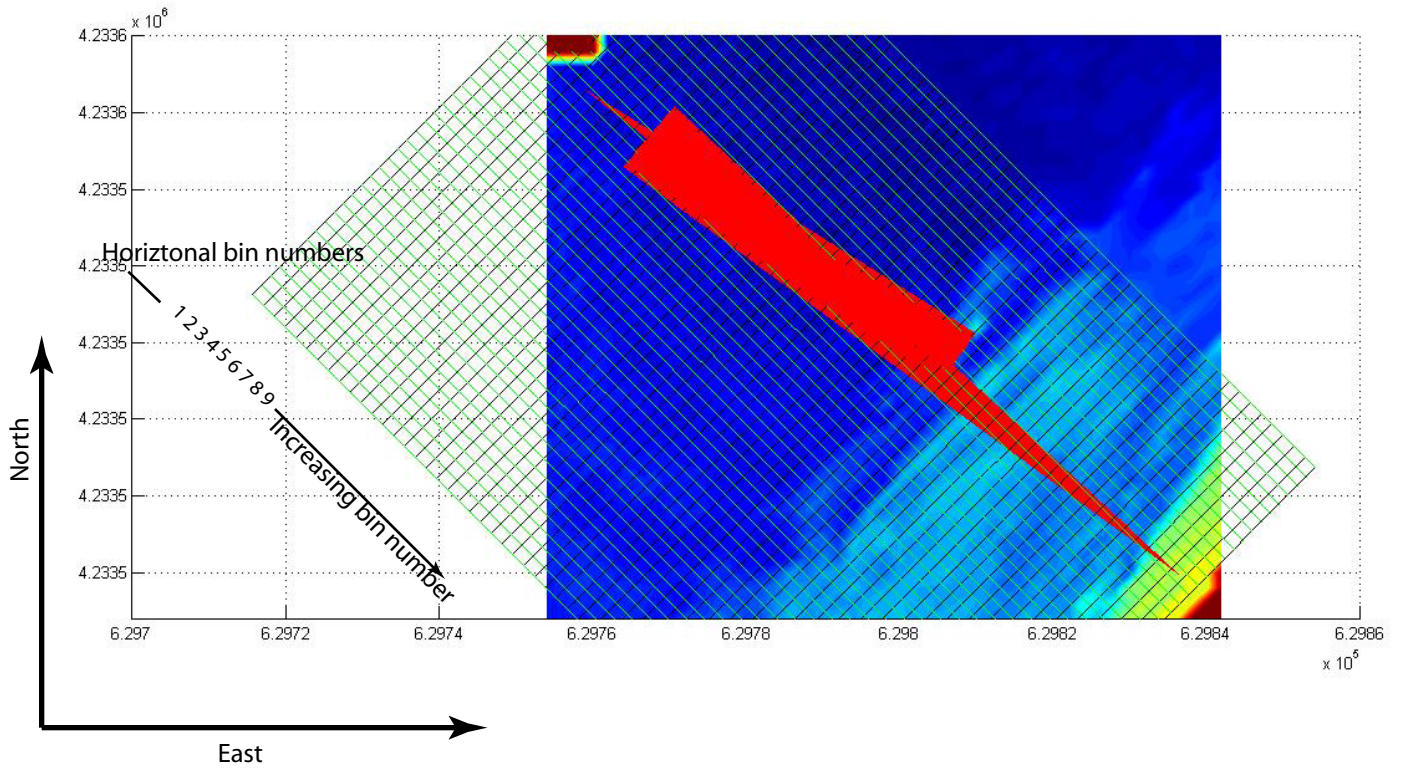


Figure 10. Binning pattern at the Sacramento River Downstream measurement site.

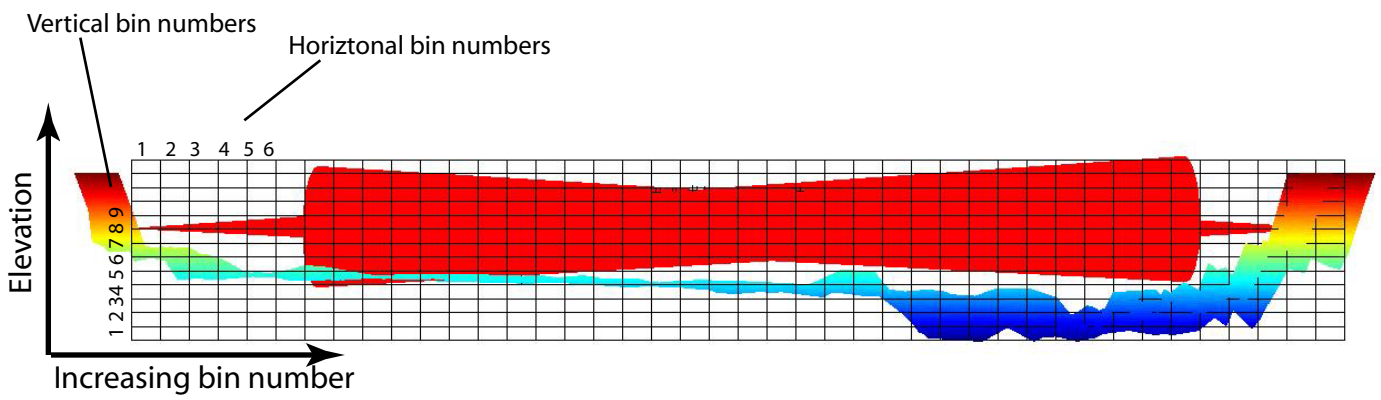
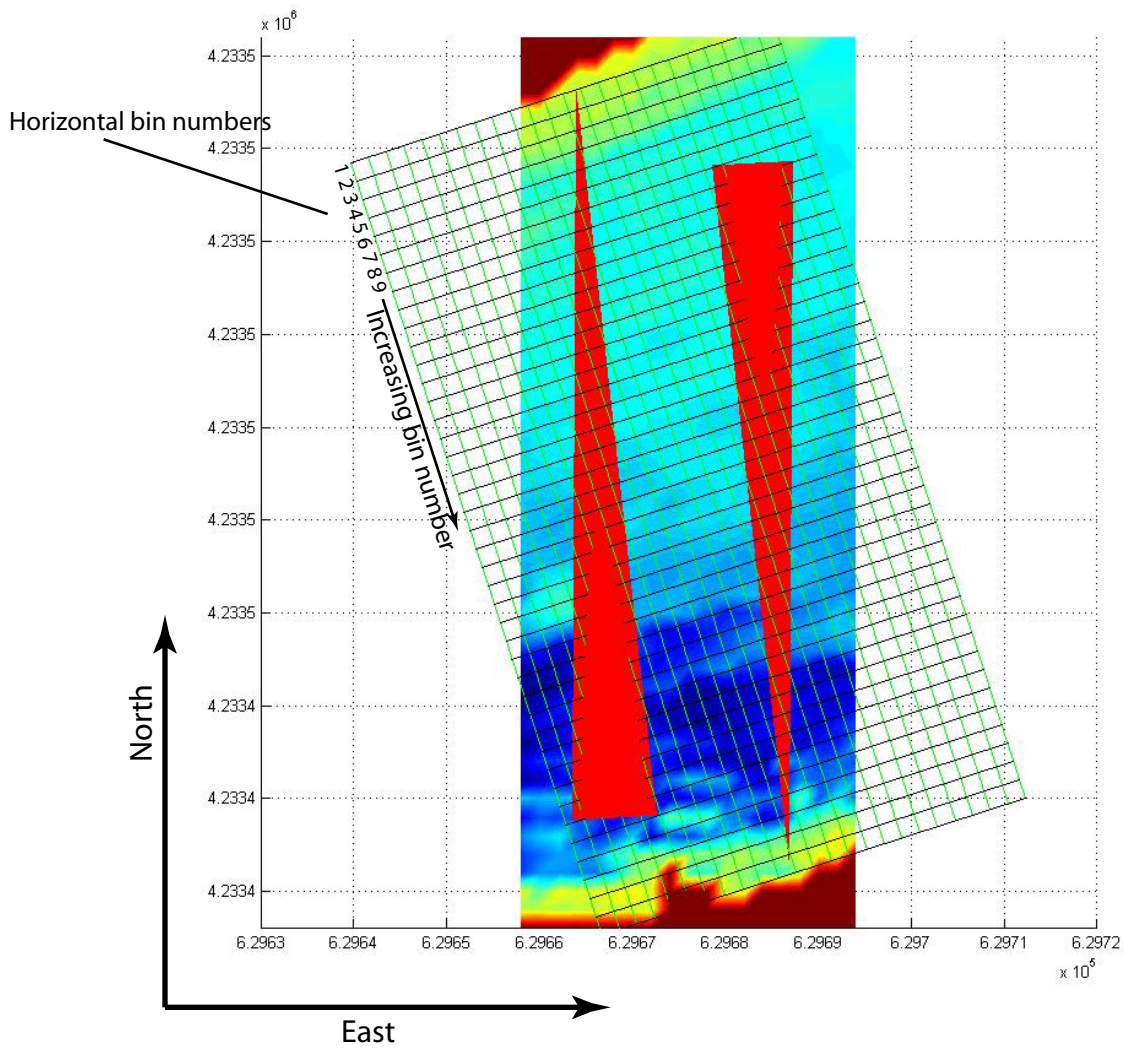


Figure 11. Binning pattern at the Georgiana Slough measurement site.

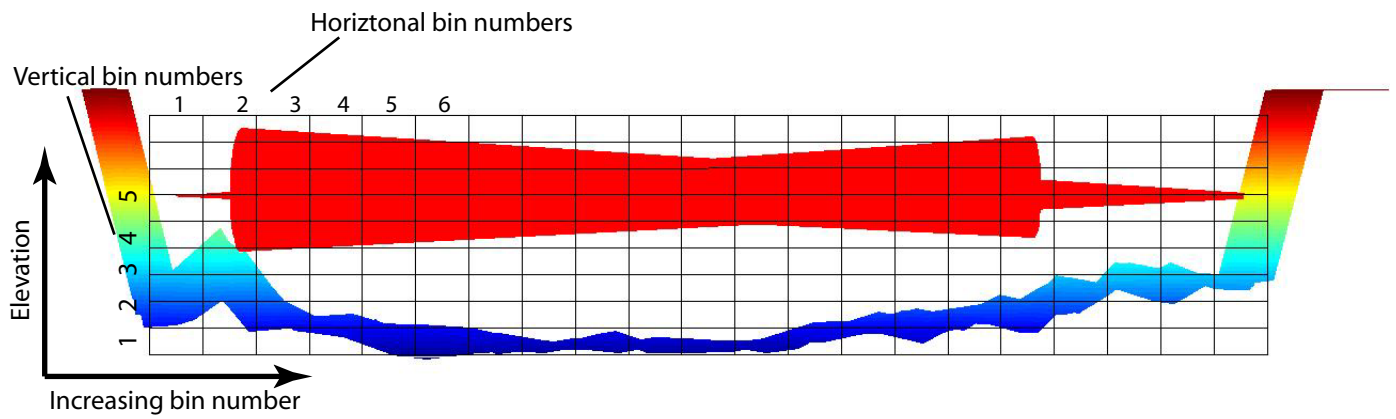
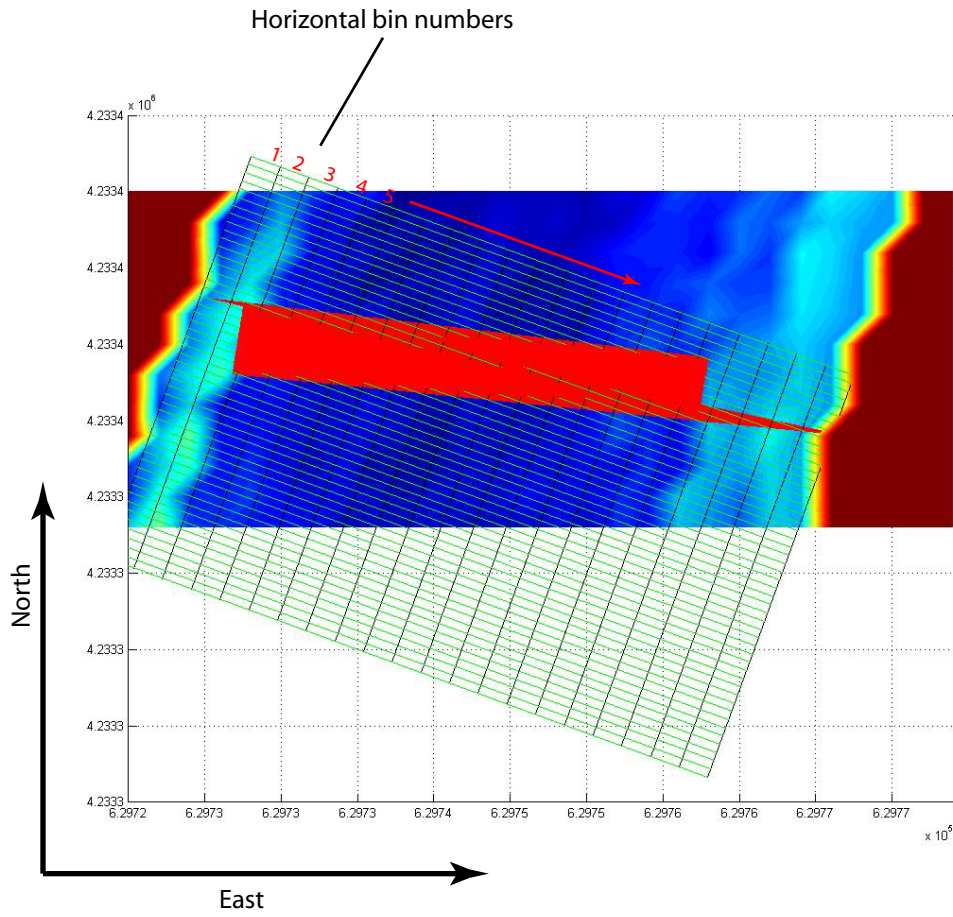


Figure 12. Average beam volume distributions for each measurement site. The height of each bar shows the total amount of beam volume in each horizontal bin, with the contributions of each vertical bin shown by color.

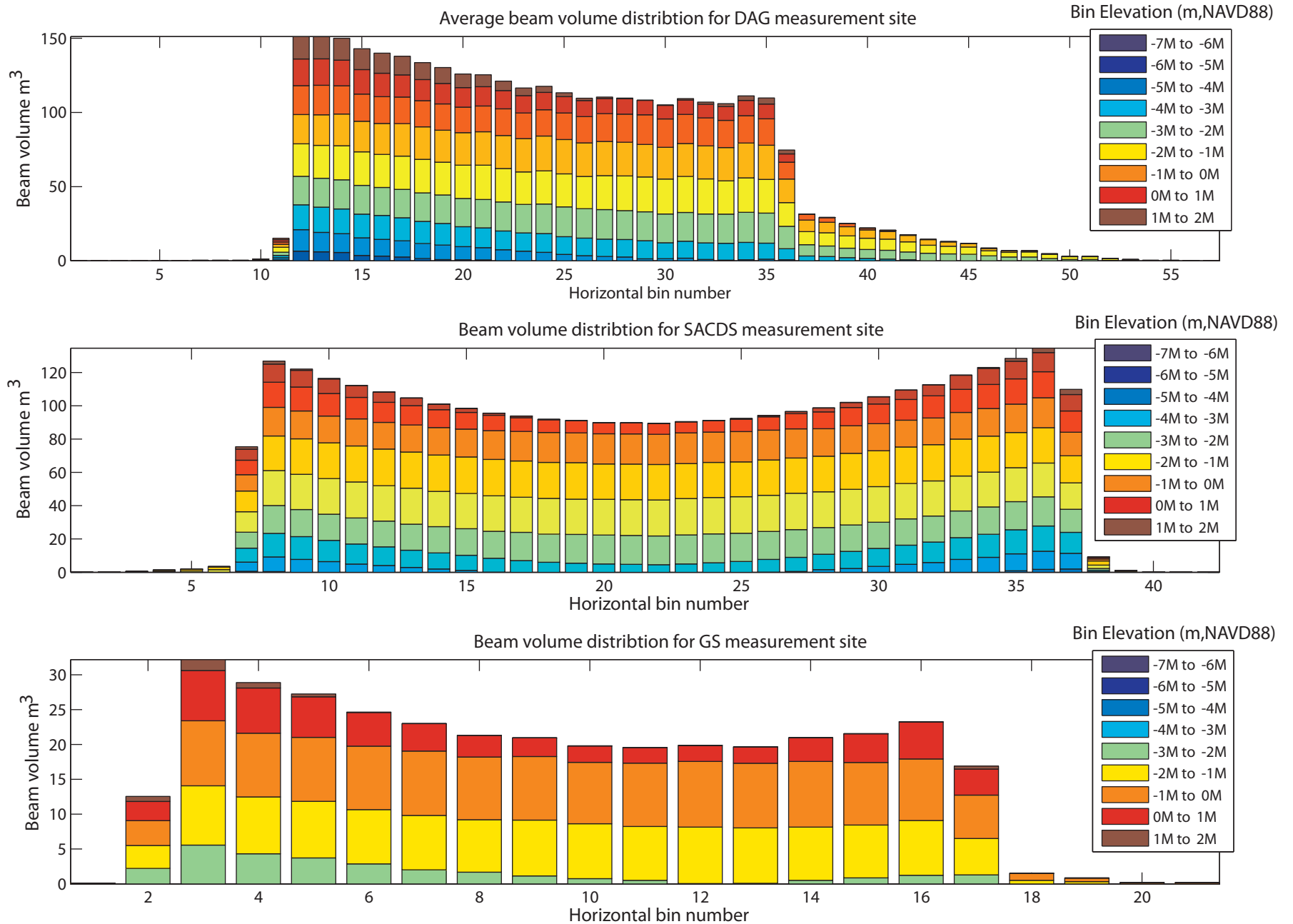
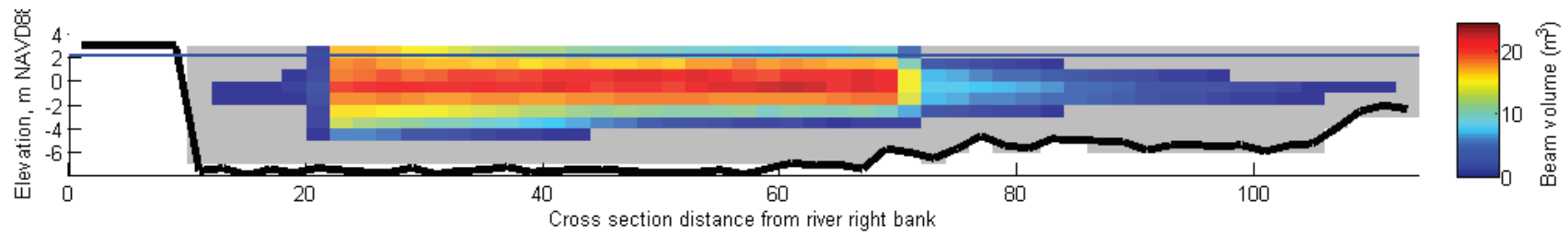
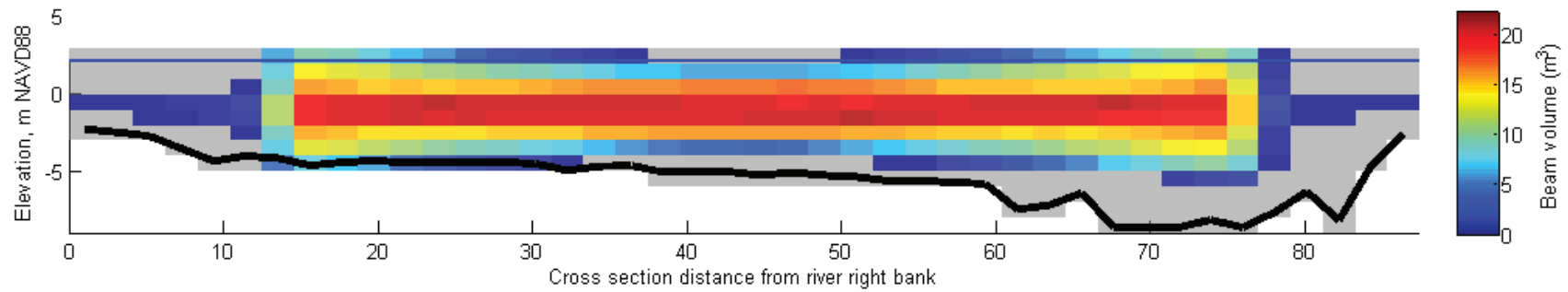


Figure 13. Beam volumes for each measurement site shown in the river cross-section, wet areas without any beam coverage are shown in grey



Cross sectional distribuion of beam volumes for the SACDS measurement site



Cross sectional distribuion of beam volumes for the GS measurement site

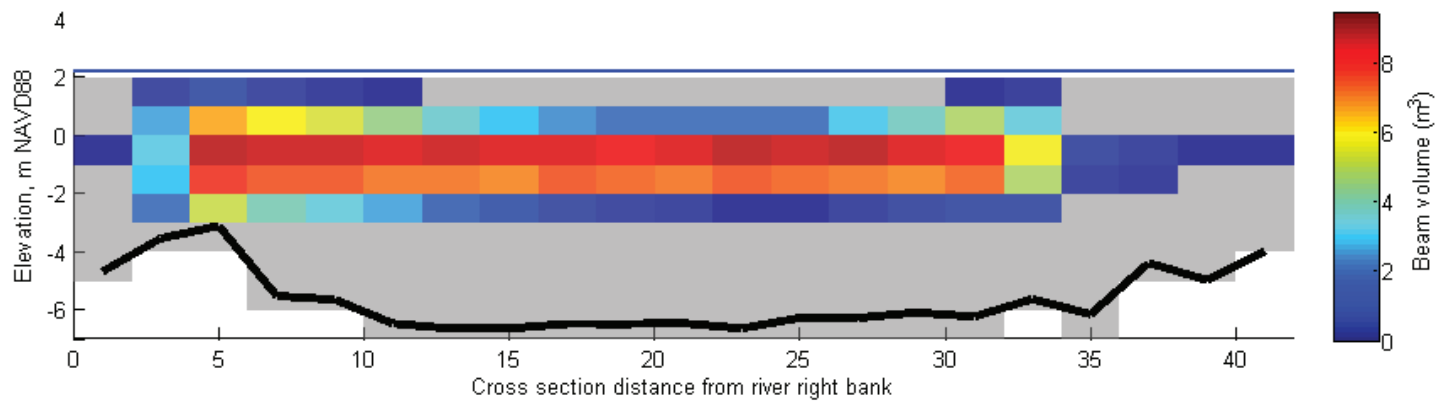
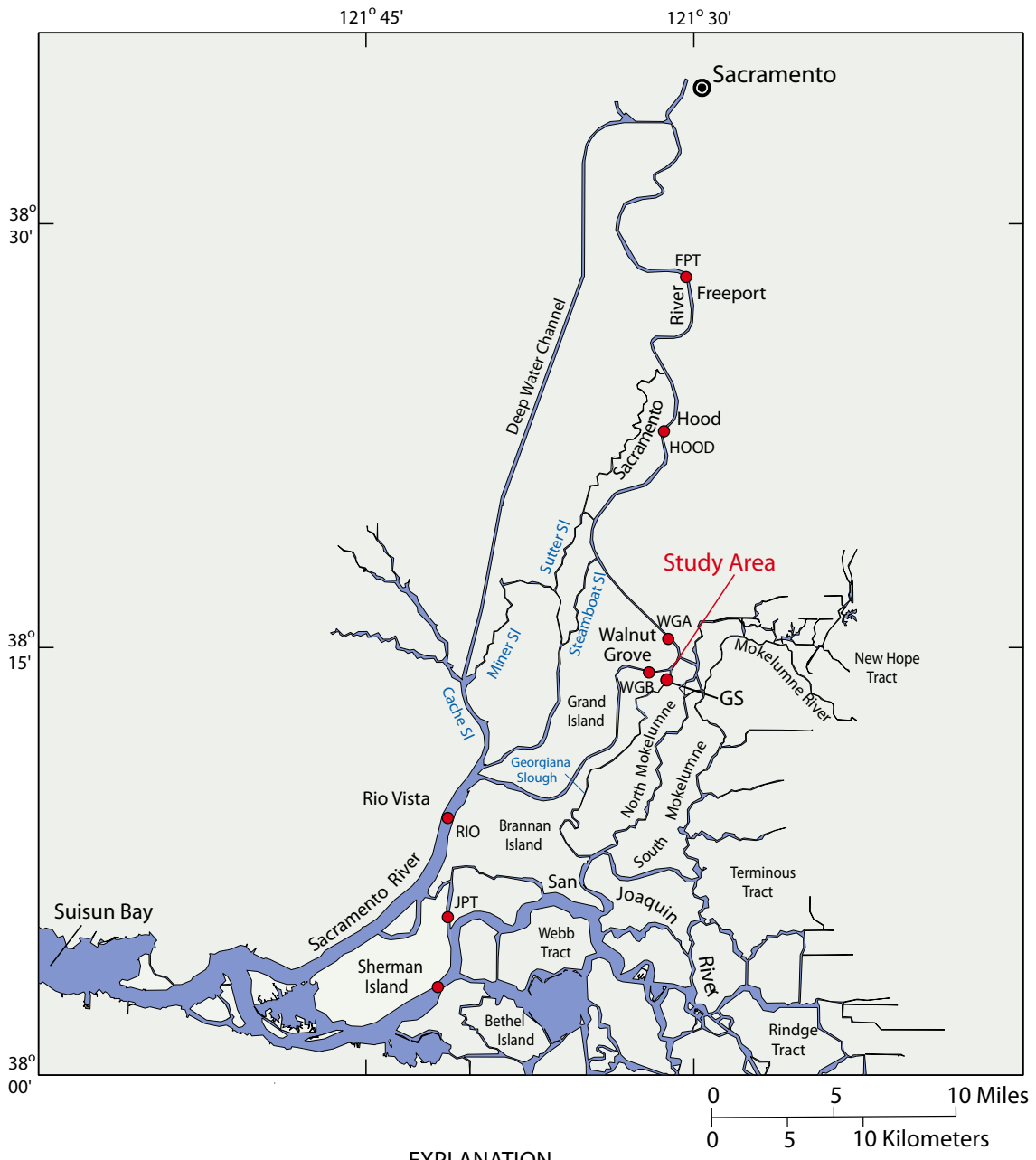


Figure 14. Map of North Delta region showing USGS flow gauging stations



EXPLANATION

North Delta Flow Sites

● Existing

FPT - Freeport

HOOD - Hood

WGA - Walnut Grove - above DCC

WGB - Walnut Grove - below DCC

GS - Gorgiana Slough

RIO - Rio Vista

JPT - Jersey Point

Figure 15. Various physical signals used in the analysis of fish density signals

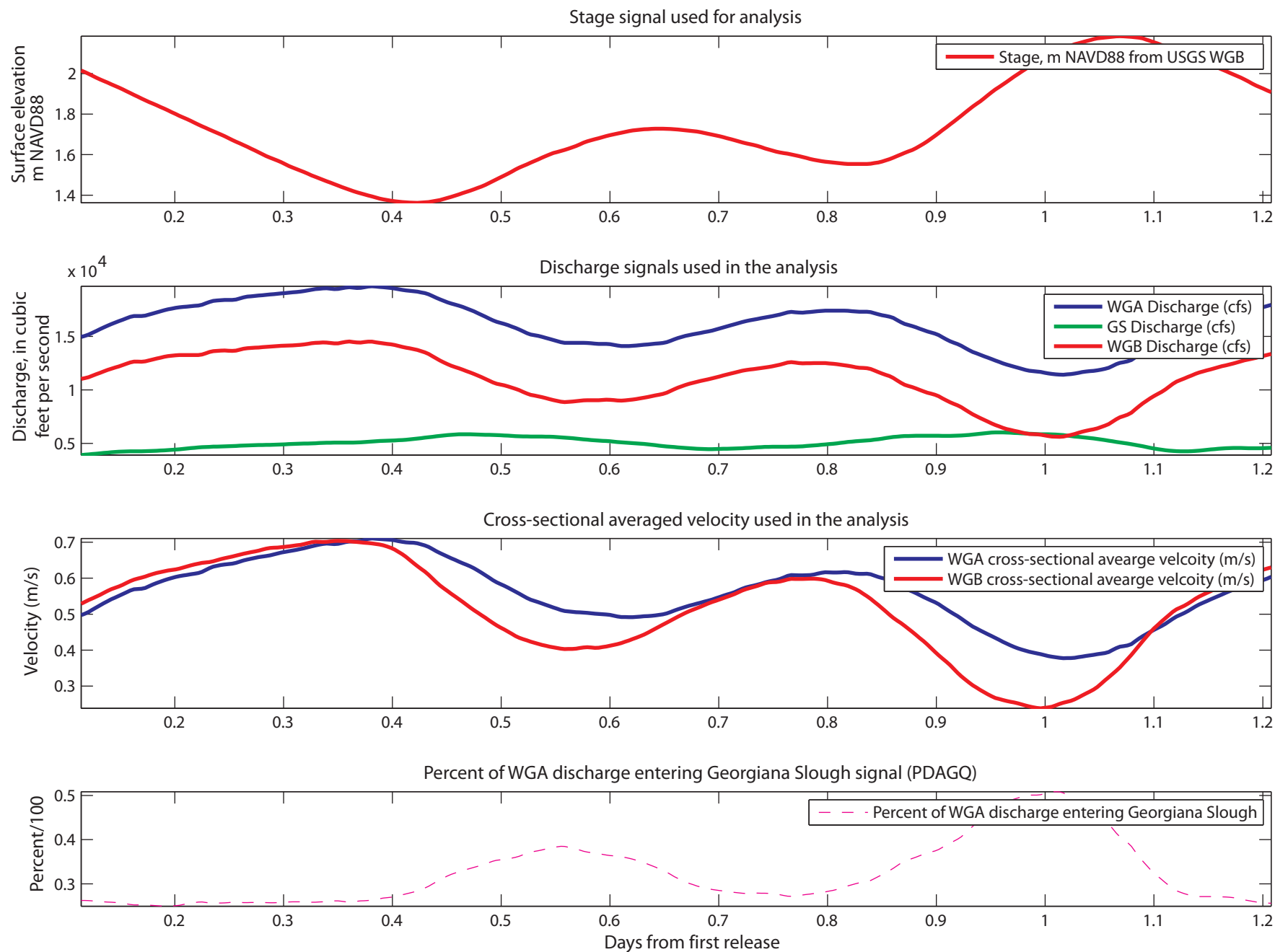


Figure 16. Artificial light and crepuscular signals used for analysis

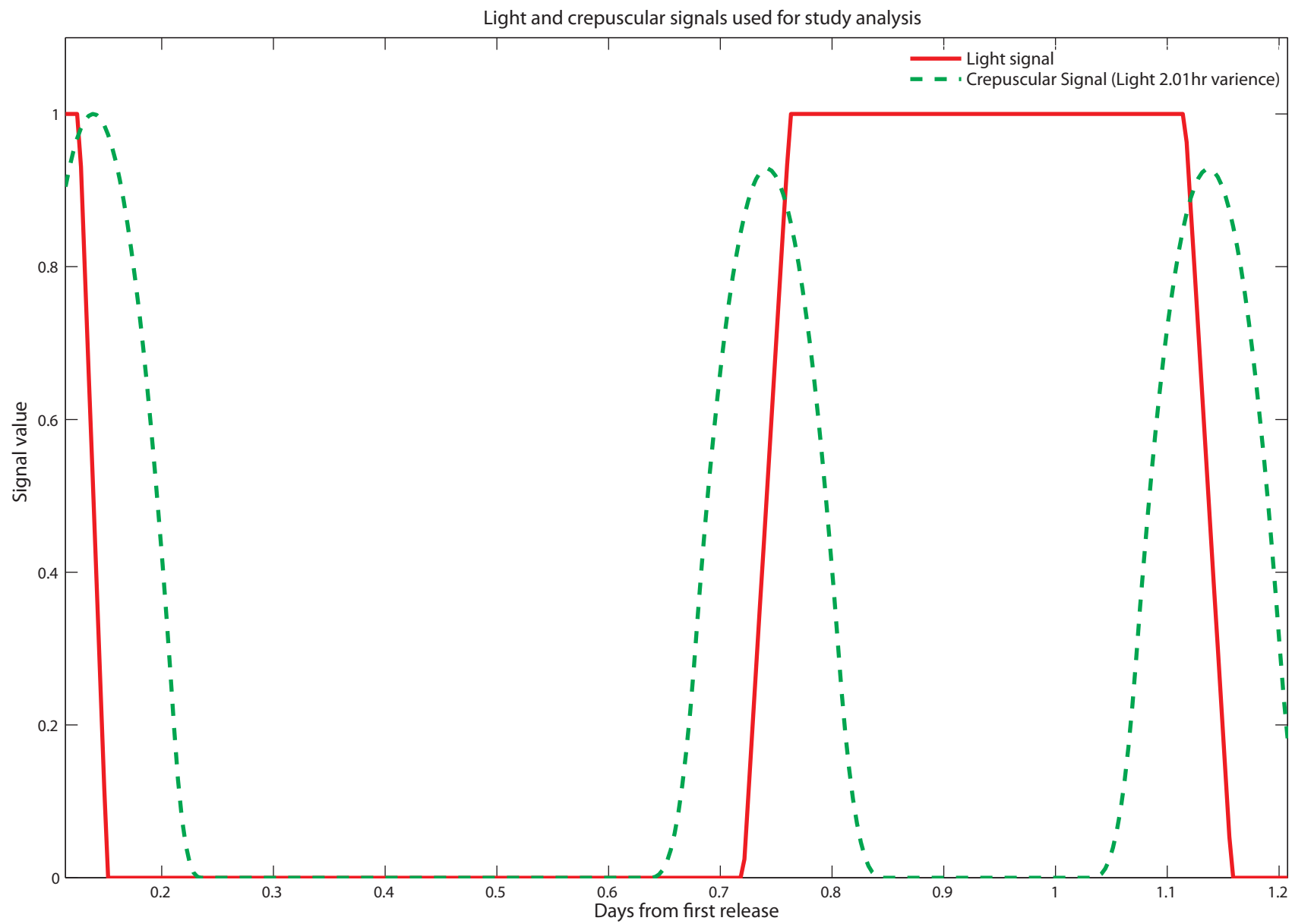


Figure 17. Signals used to determine the salmon analysis period

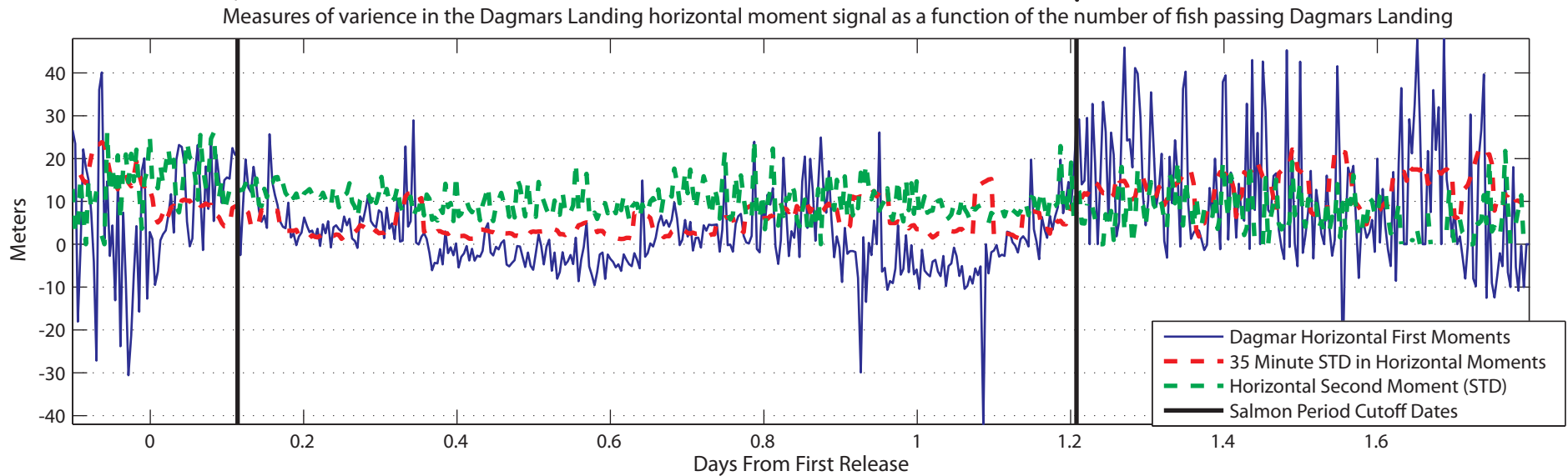
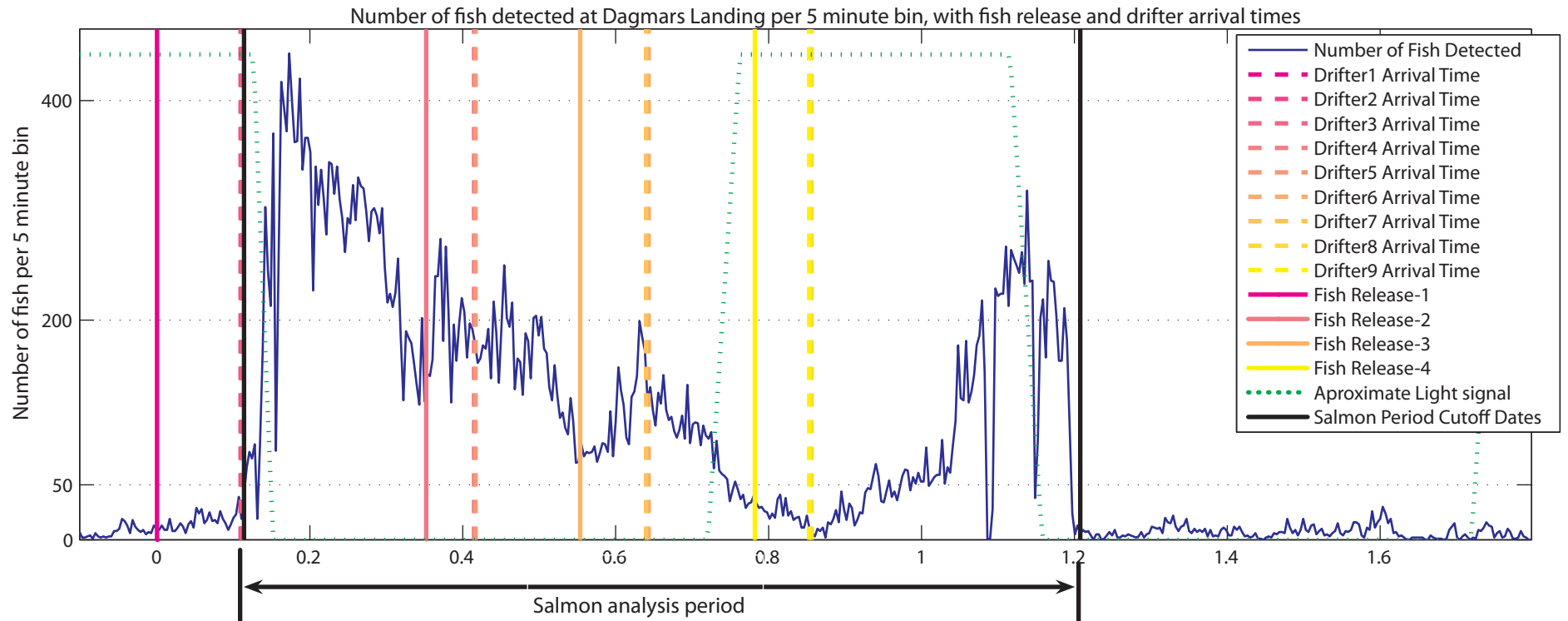


Figure 18. Temporal variance in the Dagmars Landing horizontal moment signal decreasing exponentially with the number of fish detected

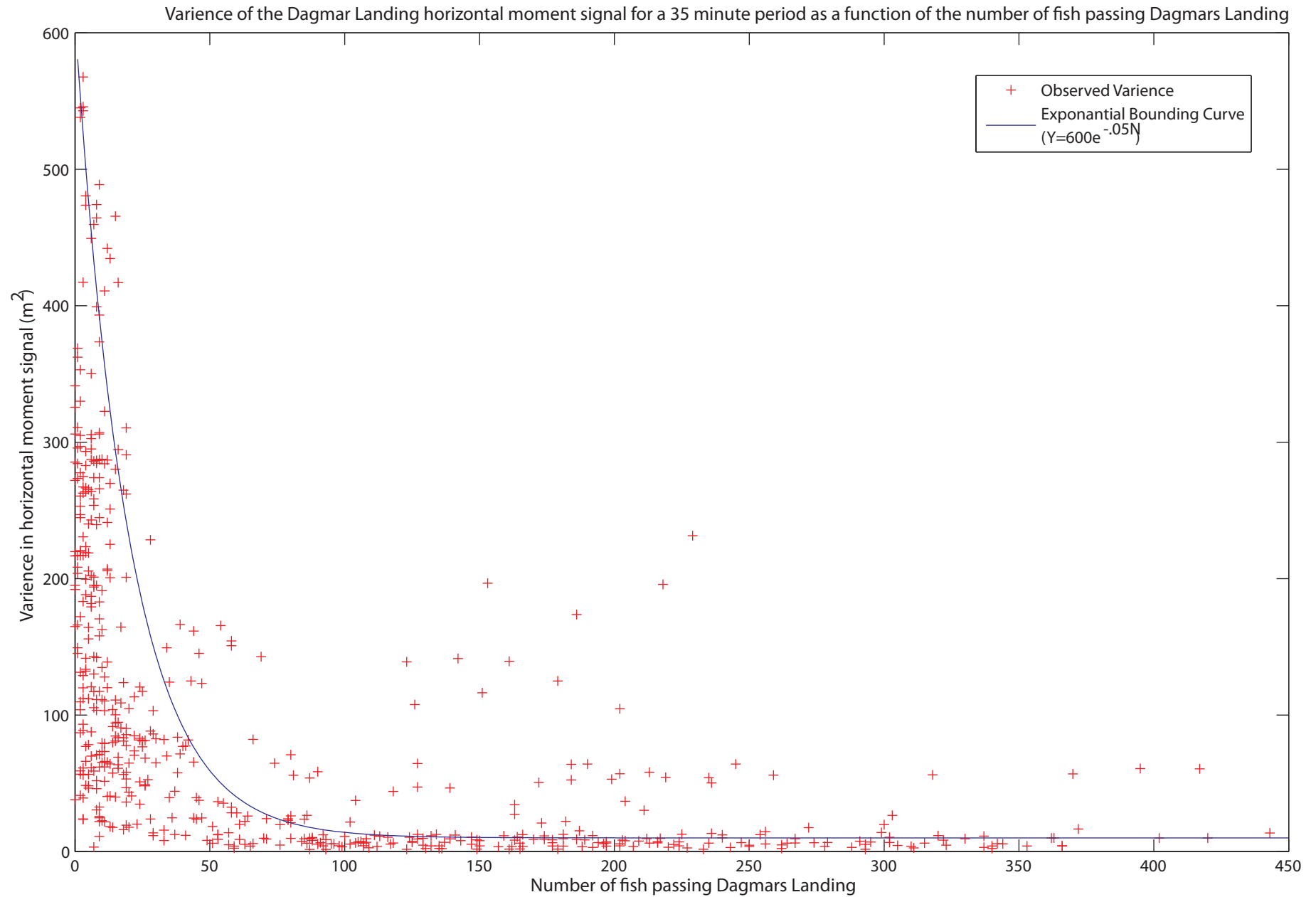


Figure 19. Dramatic decrease in the temporal standard deviation of Dagmars Landing horizontal first moment signal during analysis period

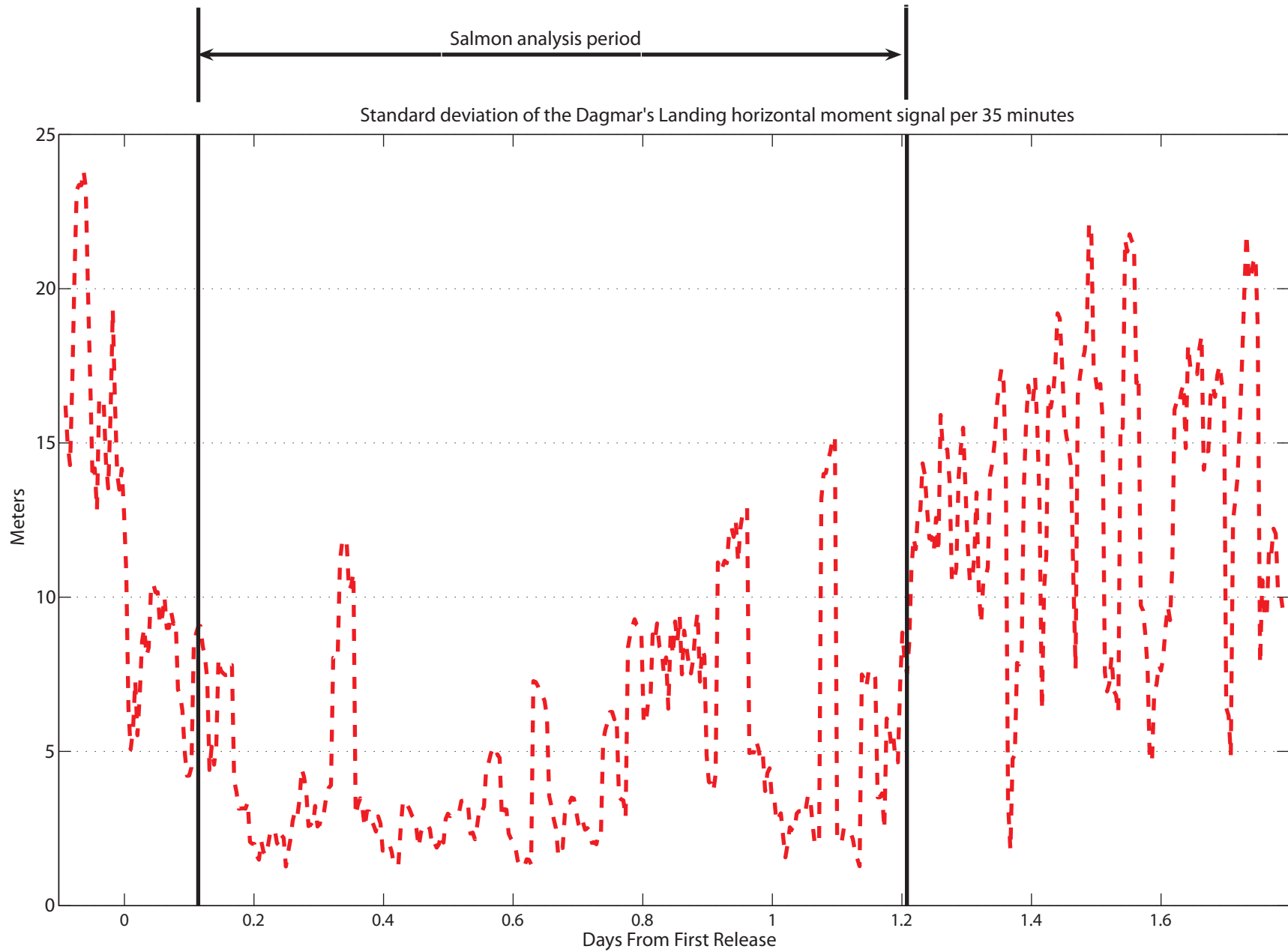


Figure 20. PSD for Georgiana Slough vertical first moments calculated by filling in missing data with zeros, introducing spurious frequency content. For illustrative purposes this PSD was calculated directly from the periods spectrogram without employing Welch's method.

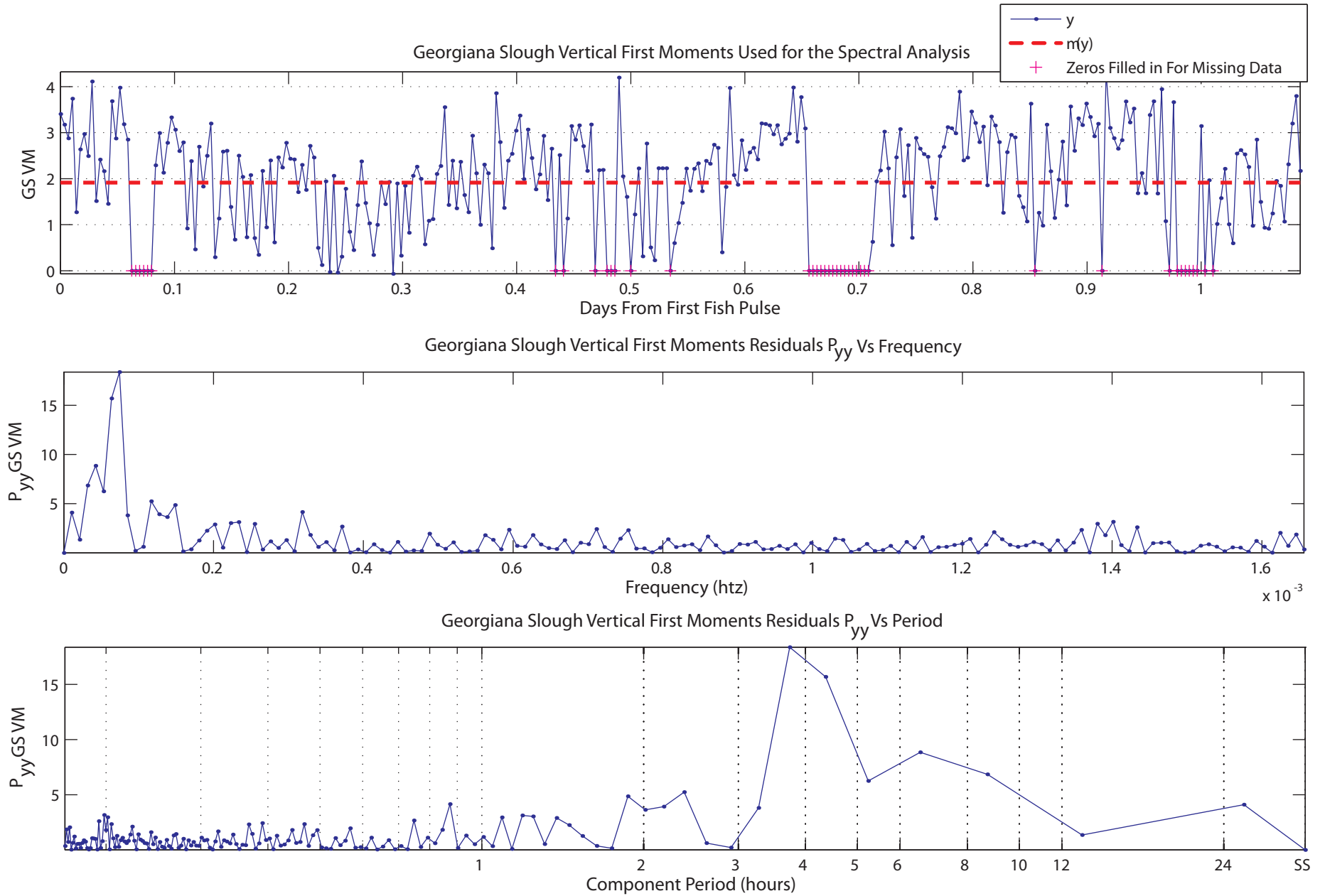


Figure 21. PSD of Georgiana Slough Vertical First Moments calculated using white noise to fill in missing data. For illustrative purposes this PSD was calculated directly from the periods spectrogram without employing Welch's method.

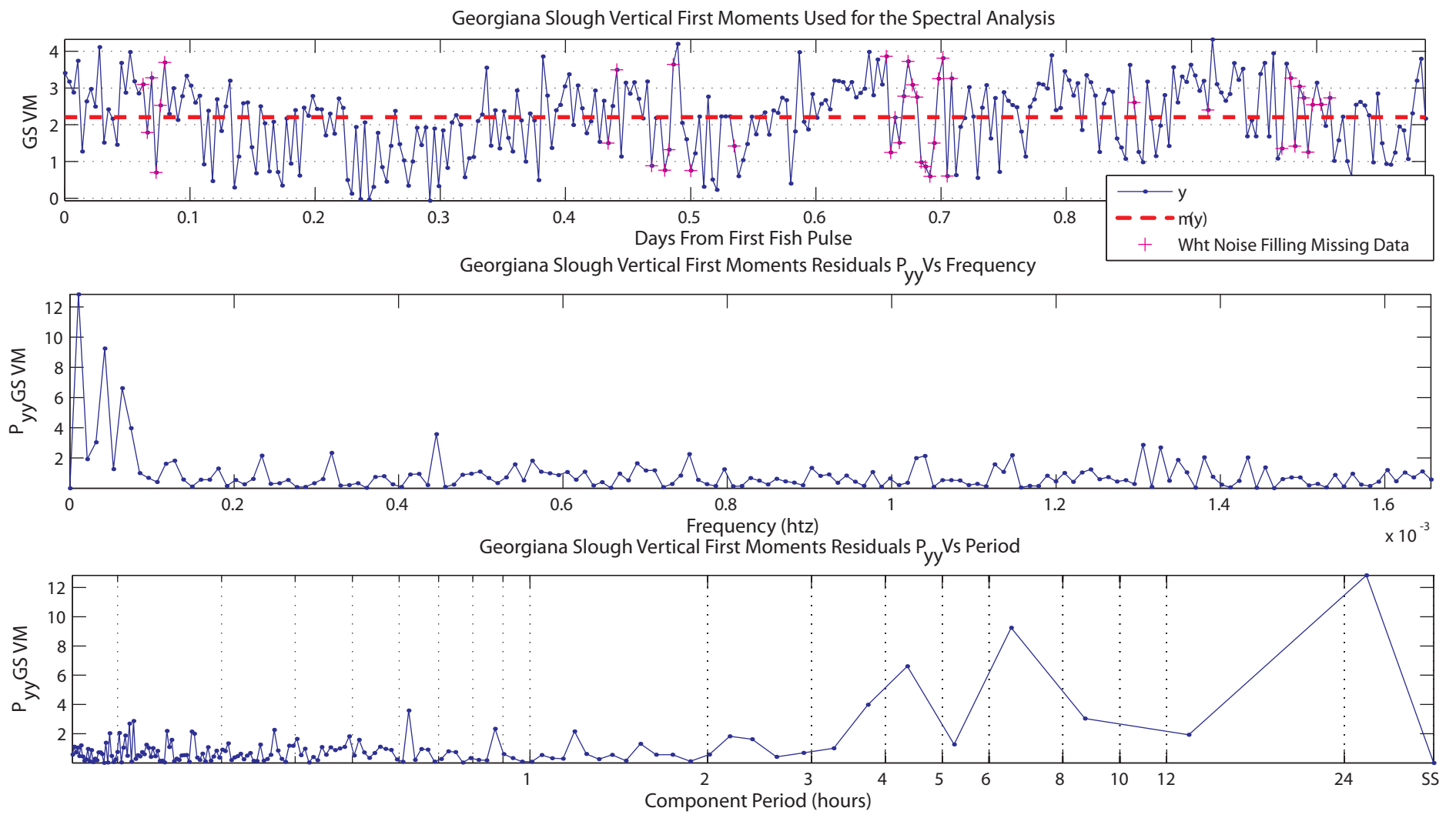


Figure 22. Fish detections per five minute bin over time at each measurement site

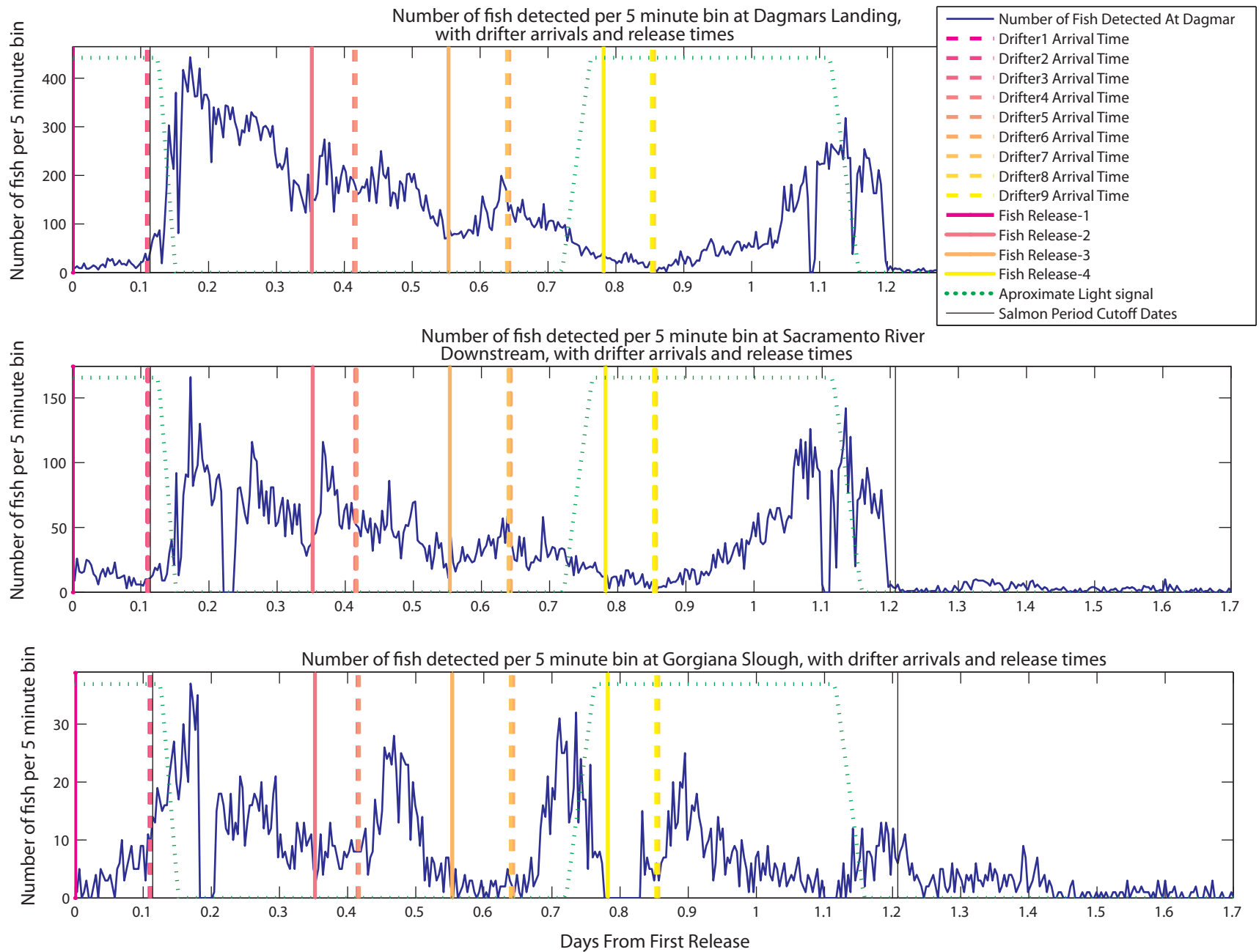
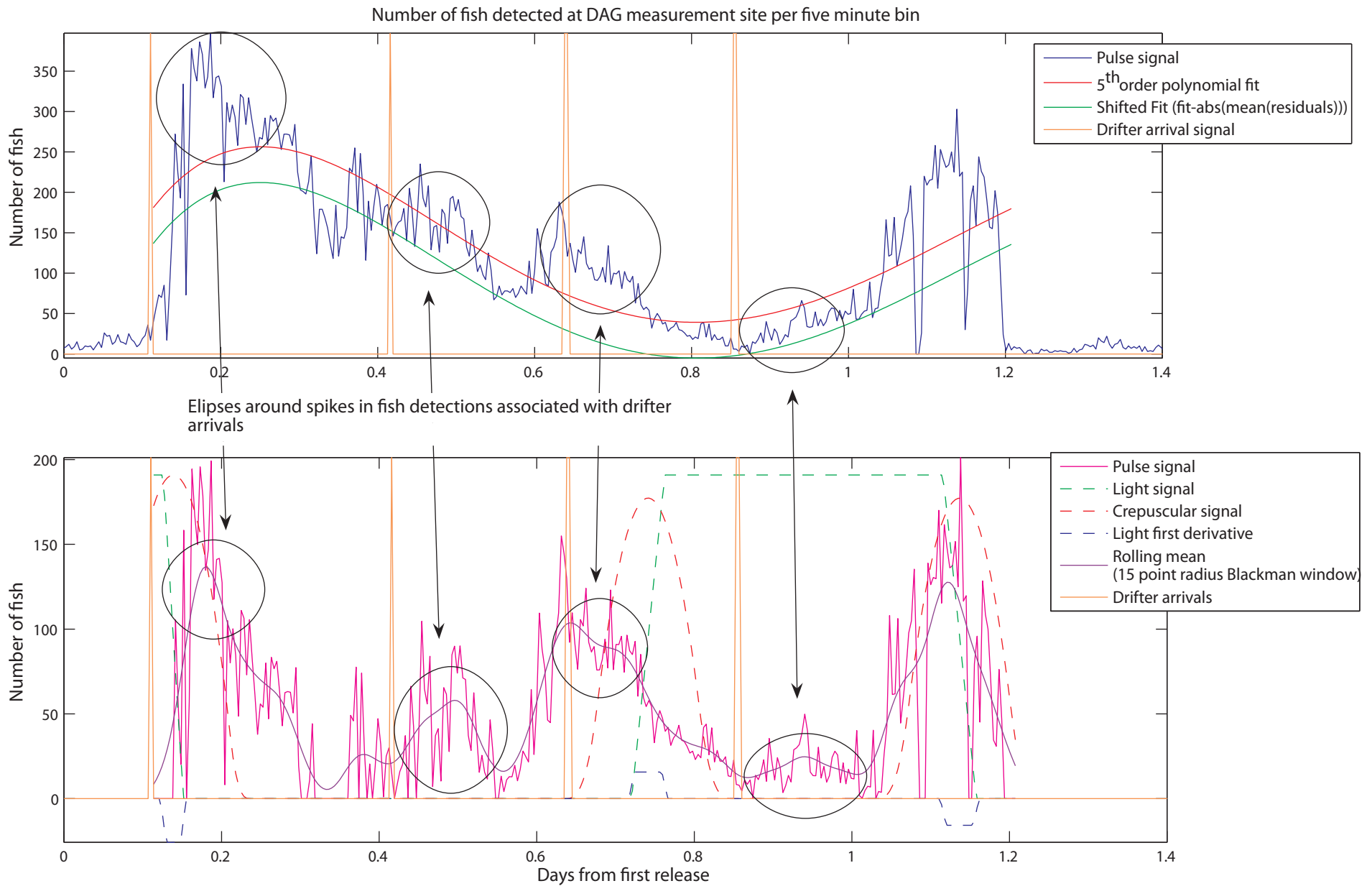
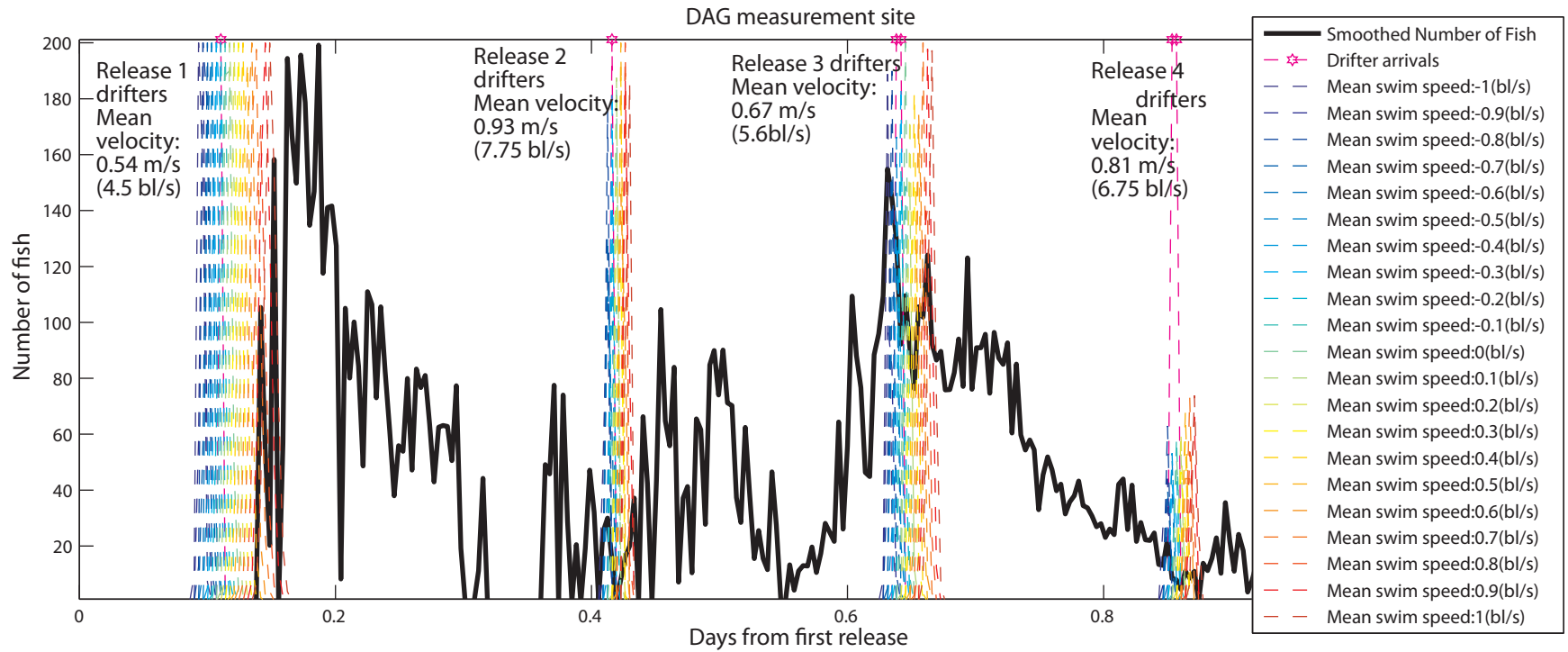


Figure 23. Creation of a pulse signal by subtracting a polynomial fit to the number of fish passing the DAG measurement site from the observed number of fish. This pulse signal is used in following figures.



Pulse signal calculated by subtracting the shifted polynomial fit from the DAG downstream fish detections signal, and setting negative values to 0.0

Figure 24. Arrival time pulses and distributions for various swim speed distributions superimposed on the DAG pulse signal. All pulses in the upper axes were generated with a swim speed distribution having a std of .1 bl/s, and the mean shown by line color.



Mean swim speed, .7 bl/s, std .1 bl/s

Mean swim speed, 2.4 bl/s, std .3 bl/s

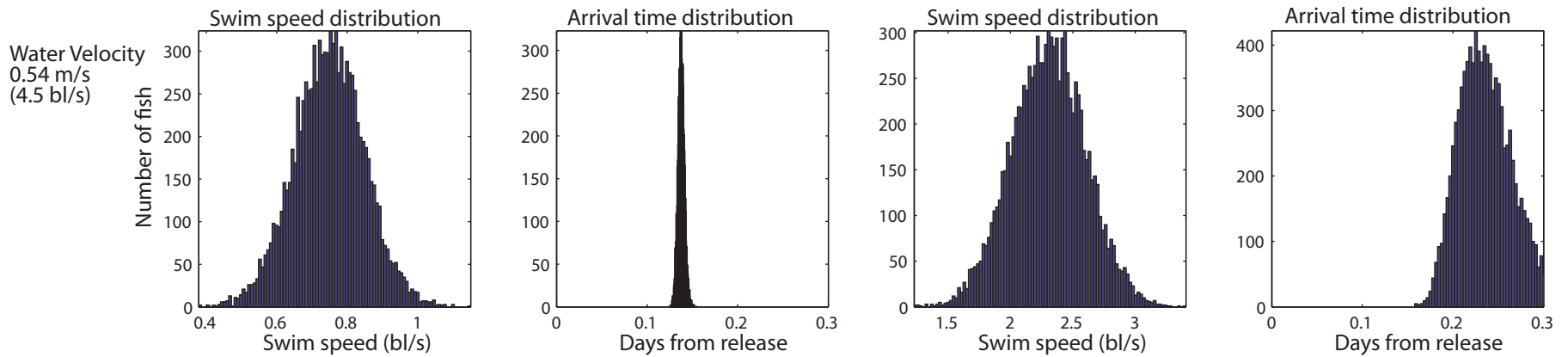


Figure 25. Pulse signals generated using a gamma holding time distribution ($a=3, b=.025$), and a normal swim speed distribution ($\text{std}=.1 \text{ bl/s}$, mean shown by color). Swim speeds do not significantly influence the shape or spread of the arrival times, but act as a delay, with a more significant effect during times of lower Lagrangian mean water velocity.

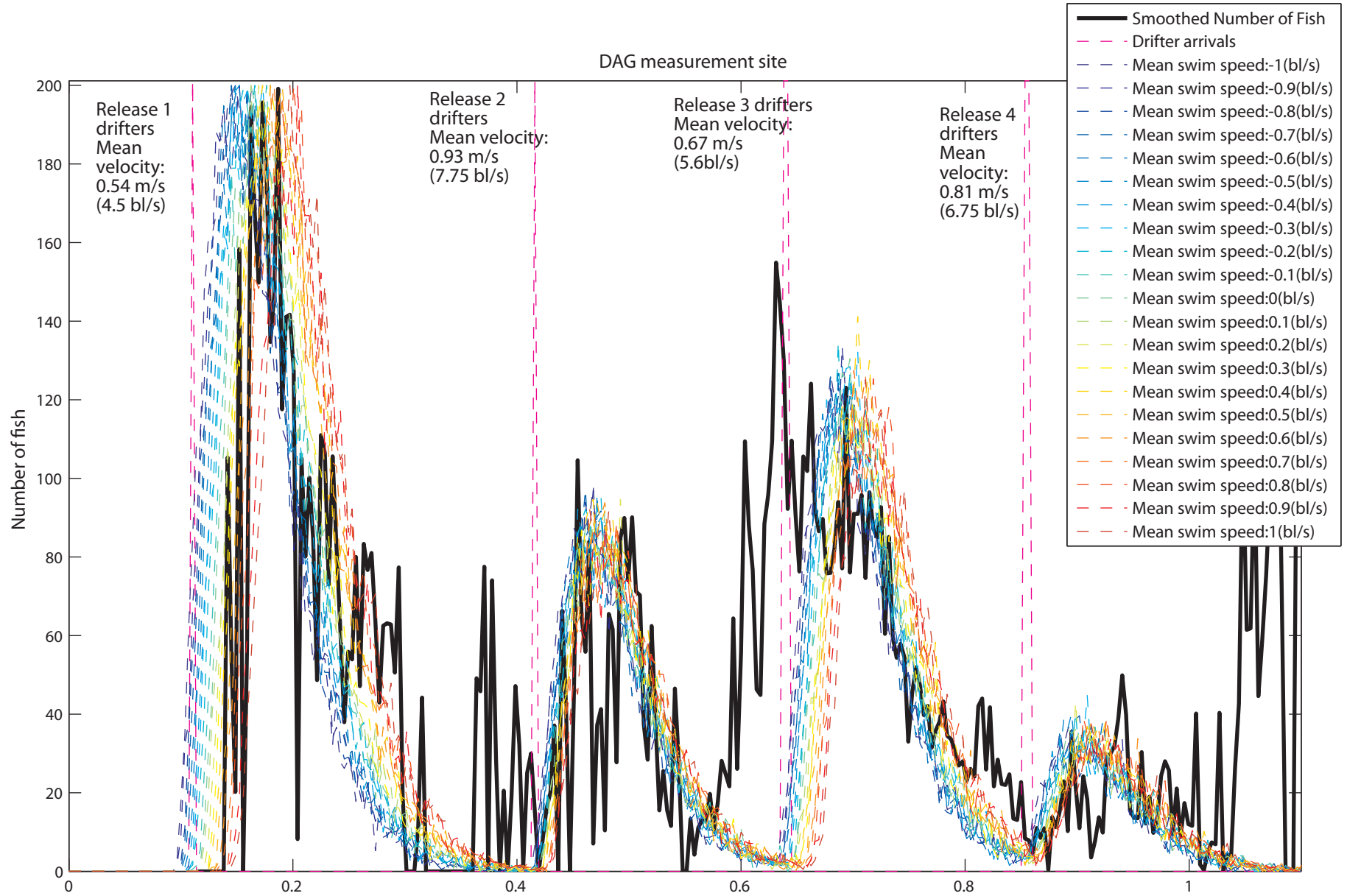


Figure 26. Hypothetical swim speed, holding time, and arrival time distributions for fish released at Vorden, CA for a range of Lagrangian mean water velocities

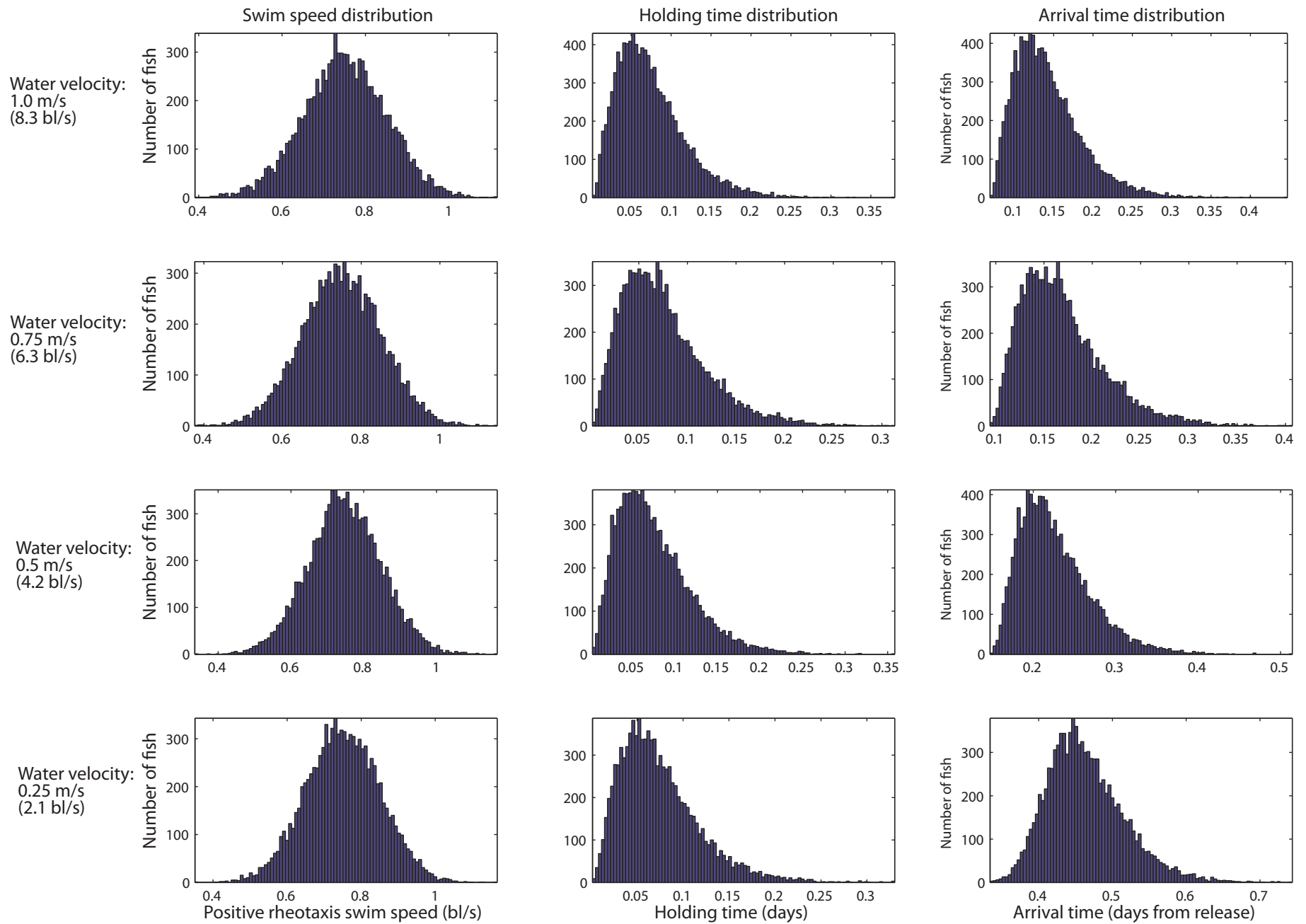


Figure 27. Time series of fish entering and leaving the control volume

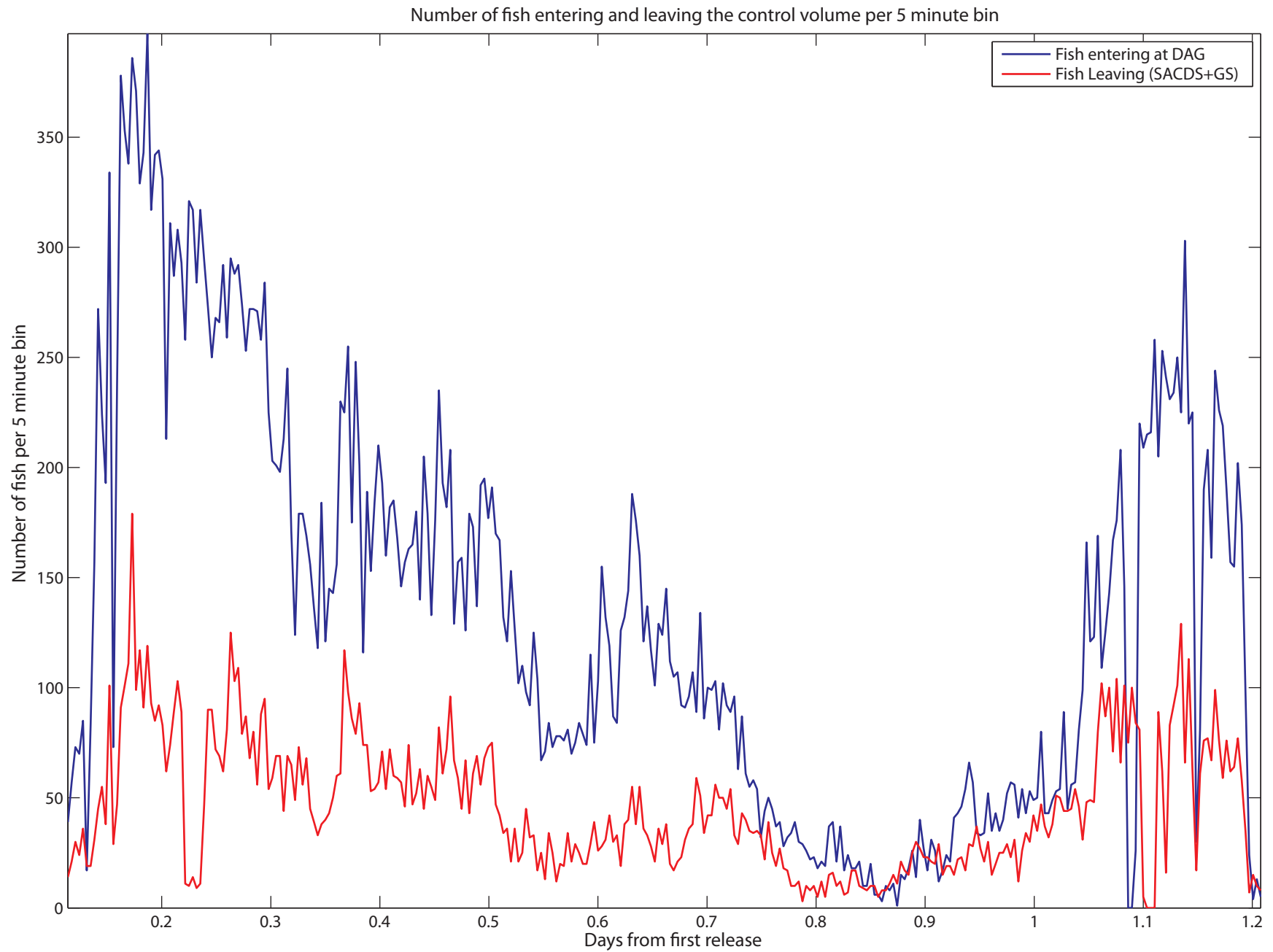


Figure 28. CCCF functions comparing the correlations between the total number of fish entering and leaving the control volume. A negative shift indicates that fish leaving the control volume are correlated with fish entering at an earlier time, and a positive shift indicates that fish leaving the control volume are correlated with fish entering at a latter date.

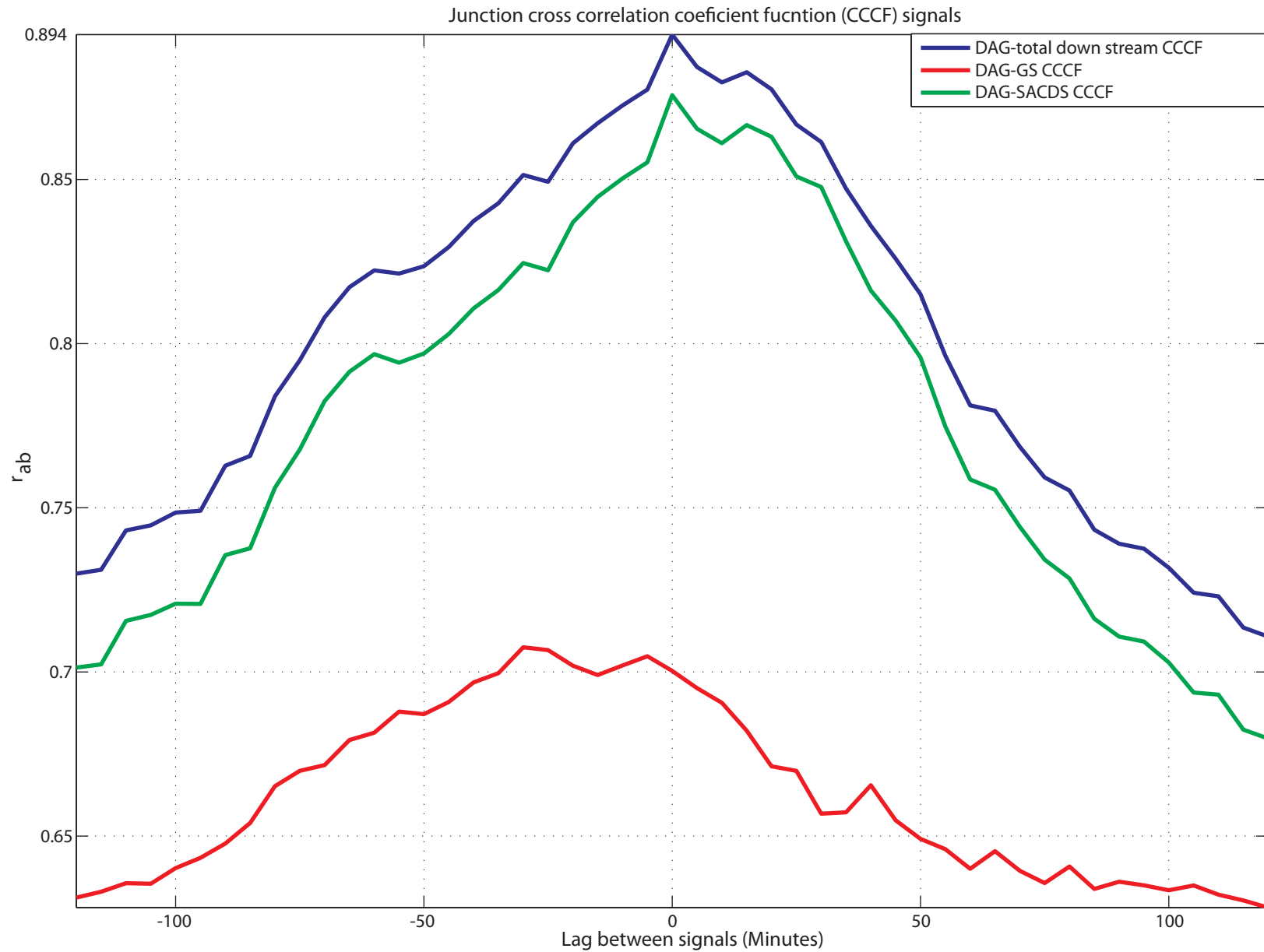


Figure 29. Histograms of the number of fish detected in a 5 minute period for each of the measurement sites, and for the total number of fish leaving the control volume

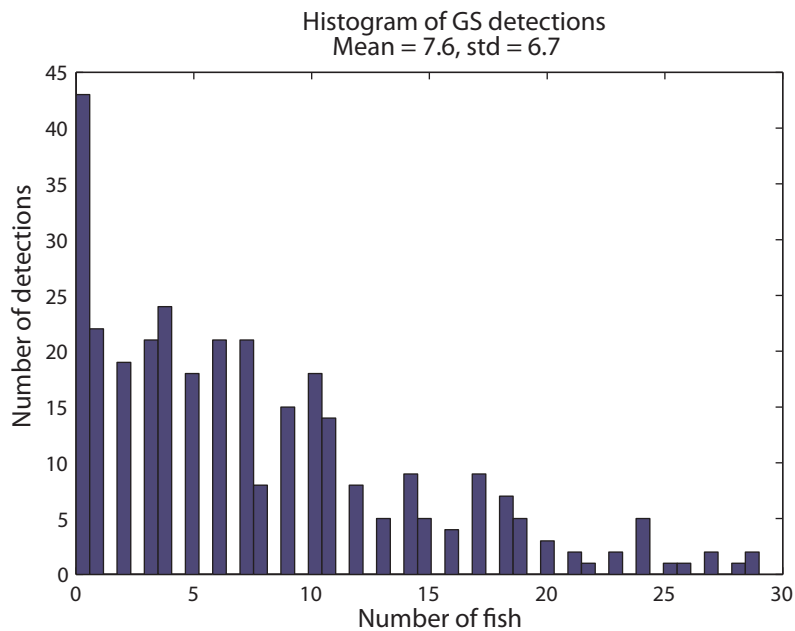
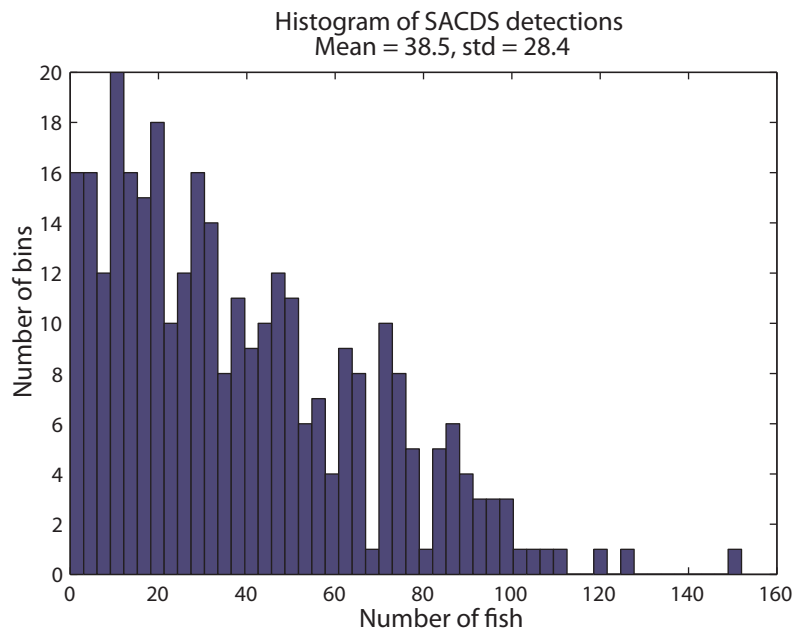
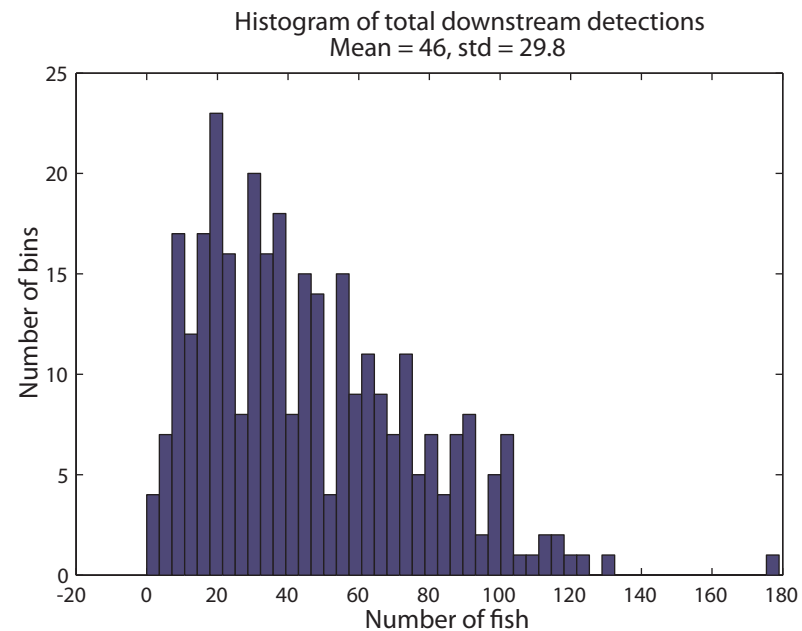
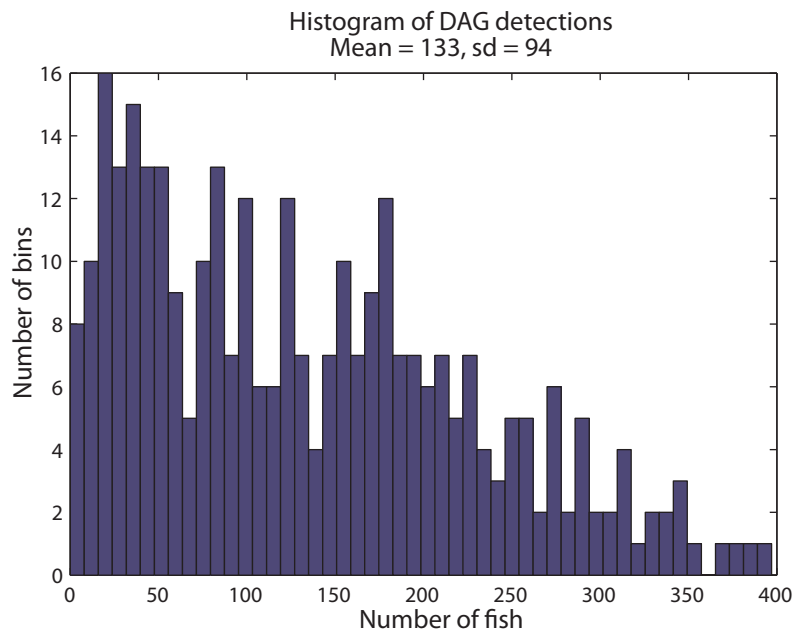


Figure 30 Relationship between the number of fish detected at DAG and the number of fish detected downstream. Regression equation and rsquared value are from regression with the labeled outliers removed. Outliers are labeled with their observation number.

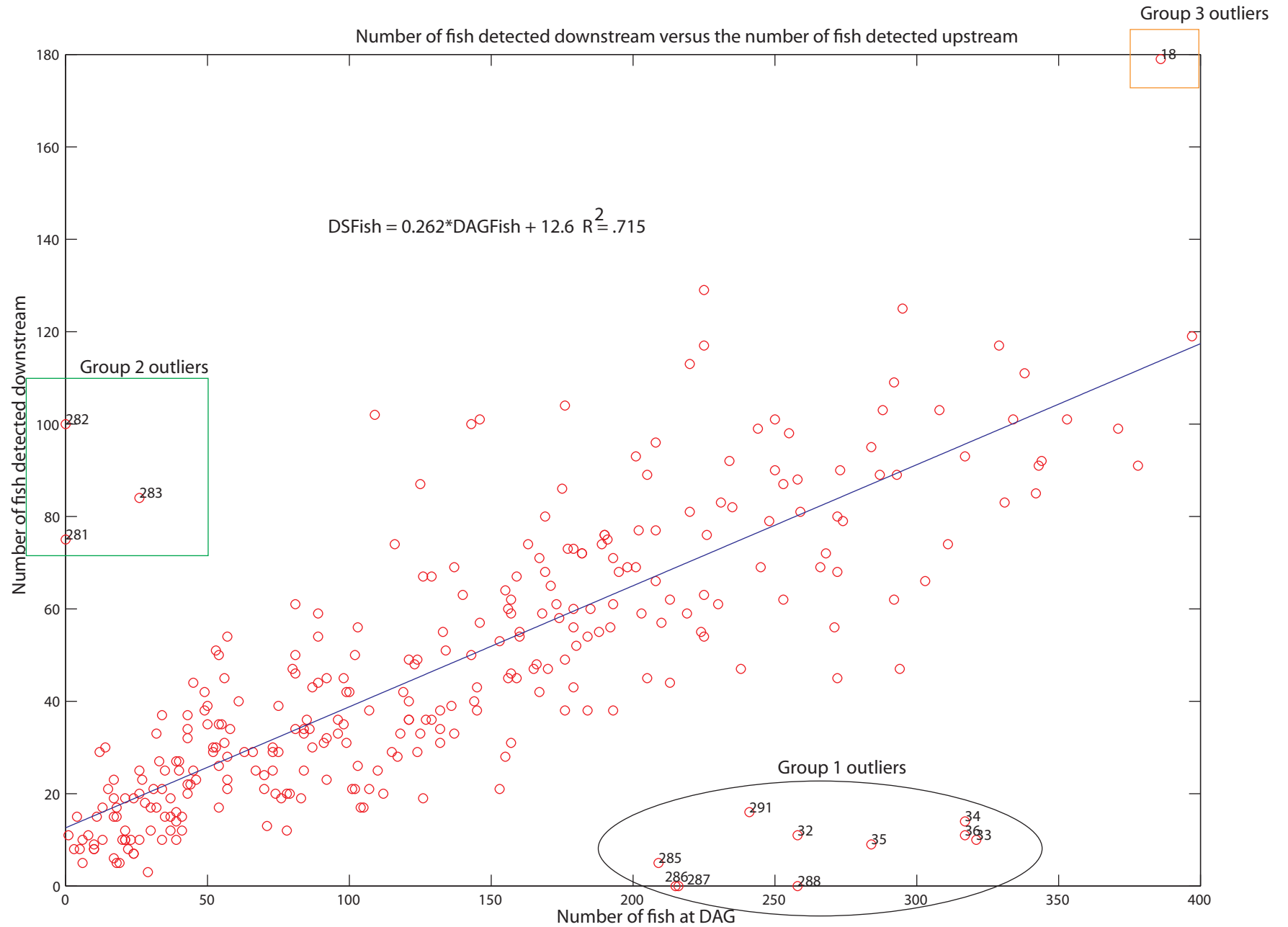


Figure 31. Outliers in the control volume regression plotted with physical signals and the number of fish passing the DAG measurement site. Note that all outliers fall within a narrow band of GS discharge

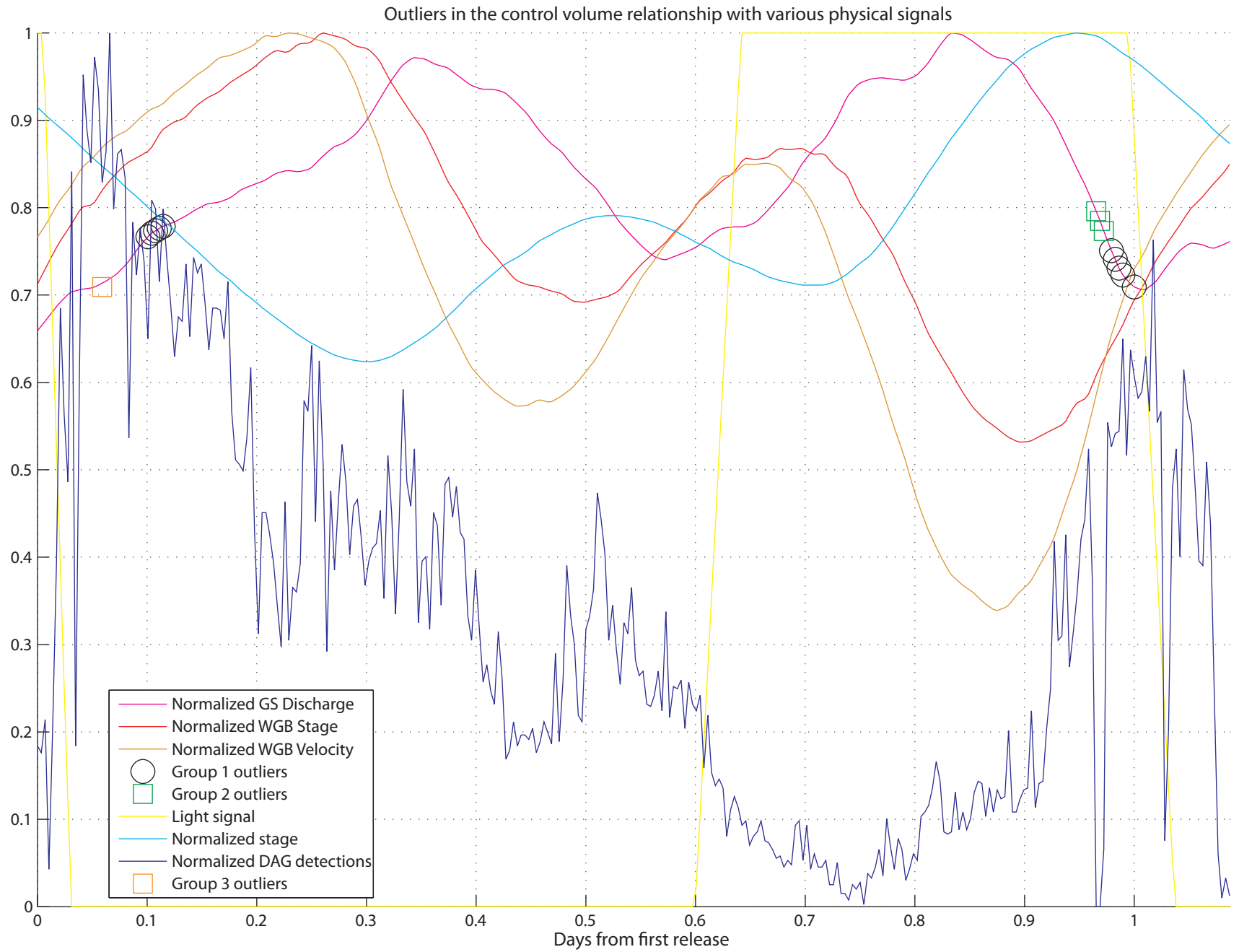
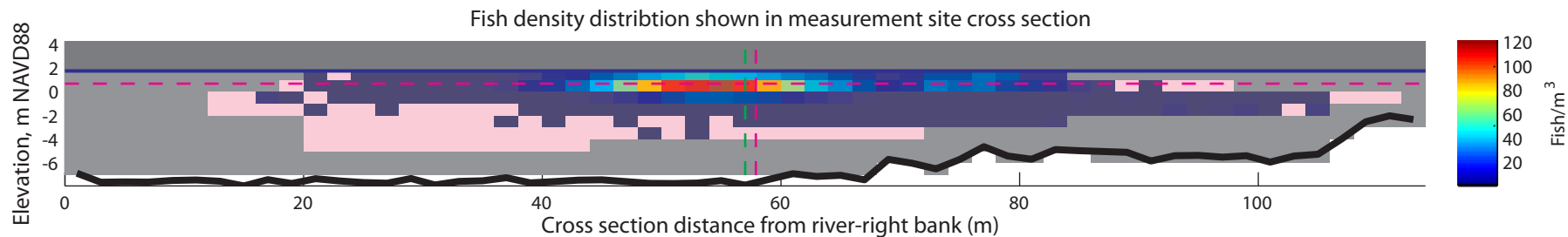


Figure 32. Overall fish density distribution for Dagmar's Landing measurement site. In the upper axis fish density in each bin is depicted by color, pink areas are bins with beam coverage, but no fish detections, grey areas are wet bins with no beam coverage. The bottom elevation profile is drawn in dark black, and the mean surface stage is drawn in dark blue. The area above the surface is shaded to represent mean sunlight levels for the period. Horizontal and vertical first moments are shown with dashed pink lines, and the horizontal cross section center point is shown with a dashed green line.



Fish density distribution shown as two dimensional histograms, with each bar showing the fish density detected in each bin.

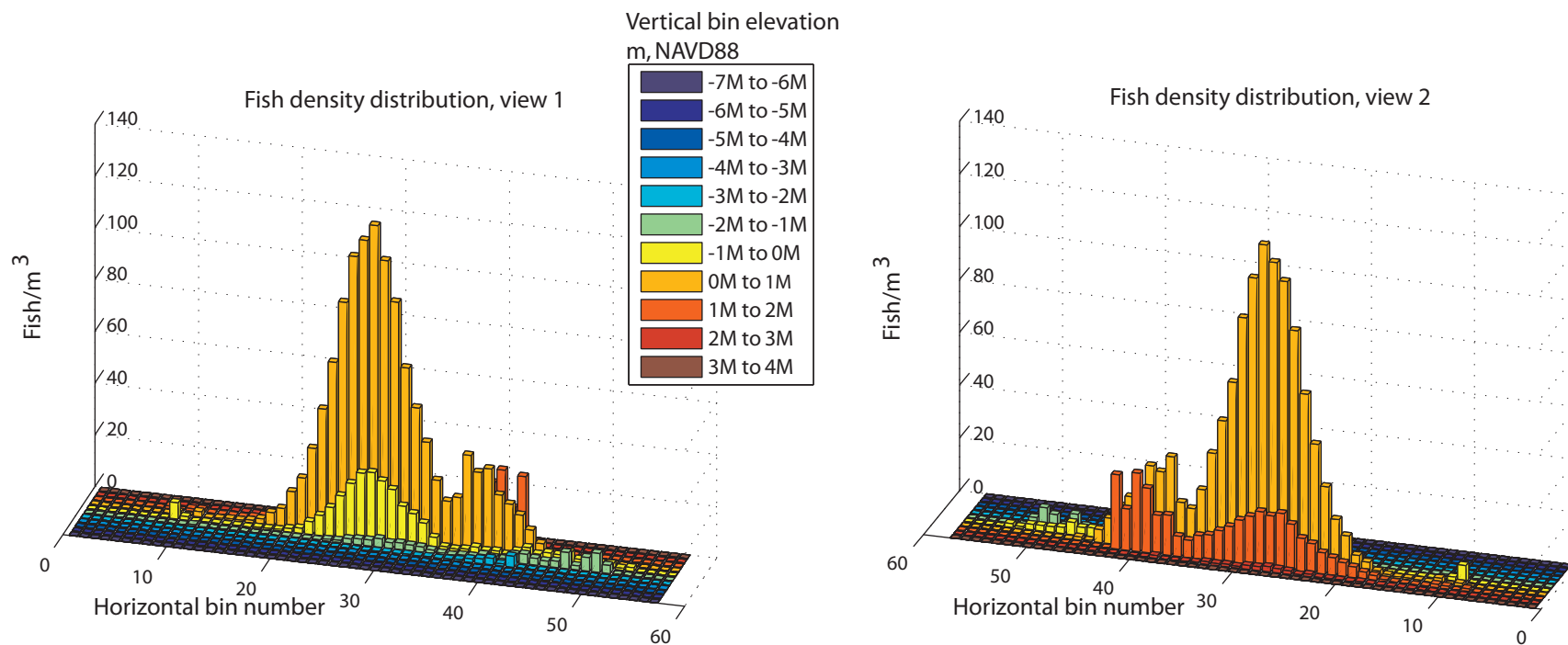


Figure 33. Time series of Dagmar's Landing measurement site fish density distribution statistics

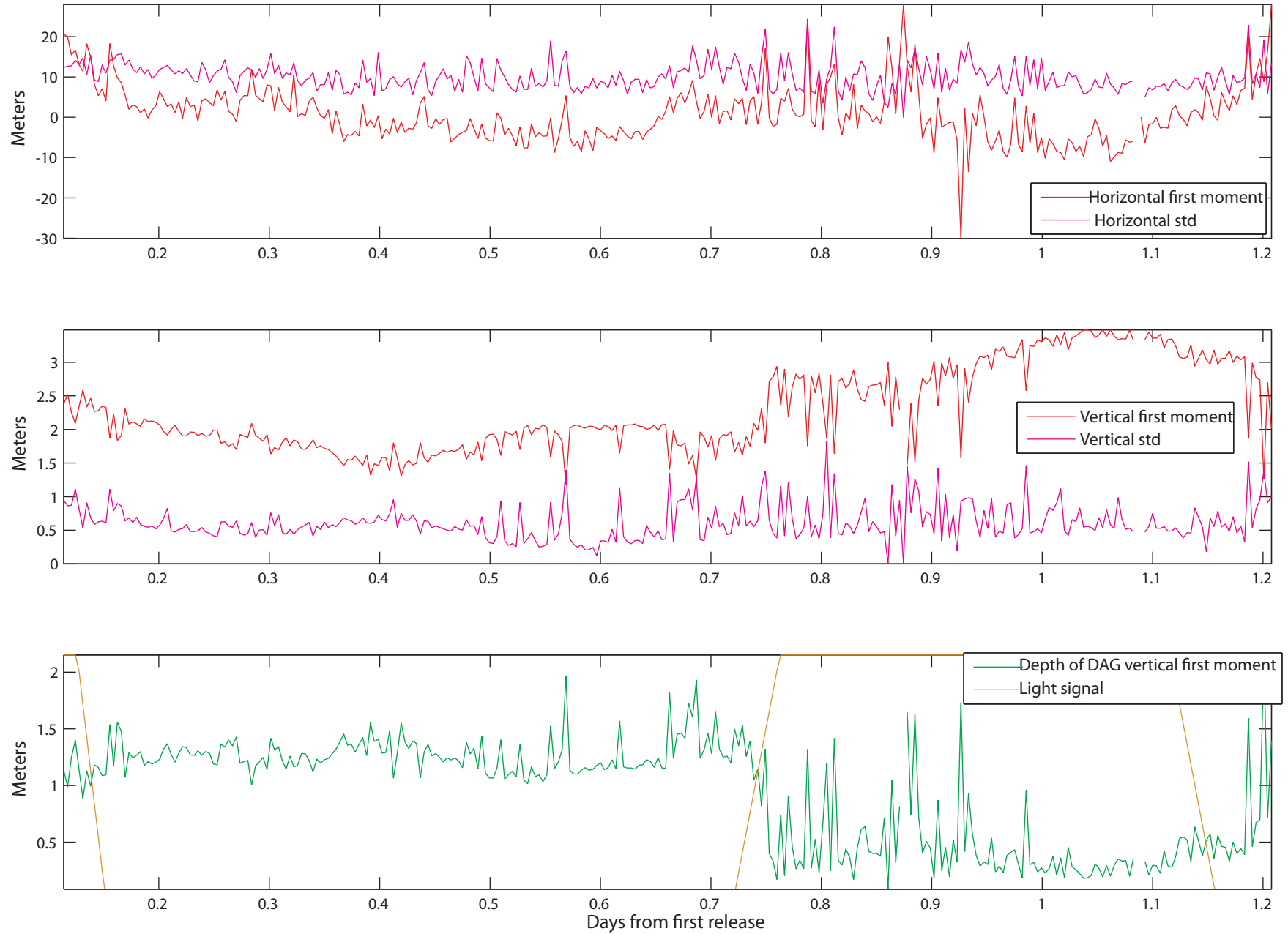


Figure 34. Distributions of time series statistics for each measurement site's fish density distributions. IM = horizontal first moment in meters, std(IM) = square root of the horizontal second moment in meters KMDepth = depth of the vertical first moment in meters, std(KM) = square root of the vertical second moment in meters.

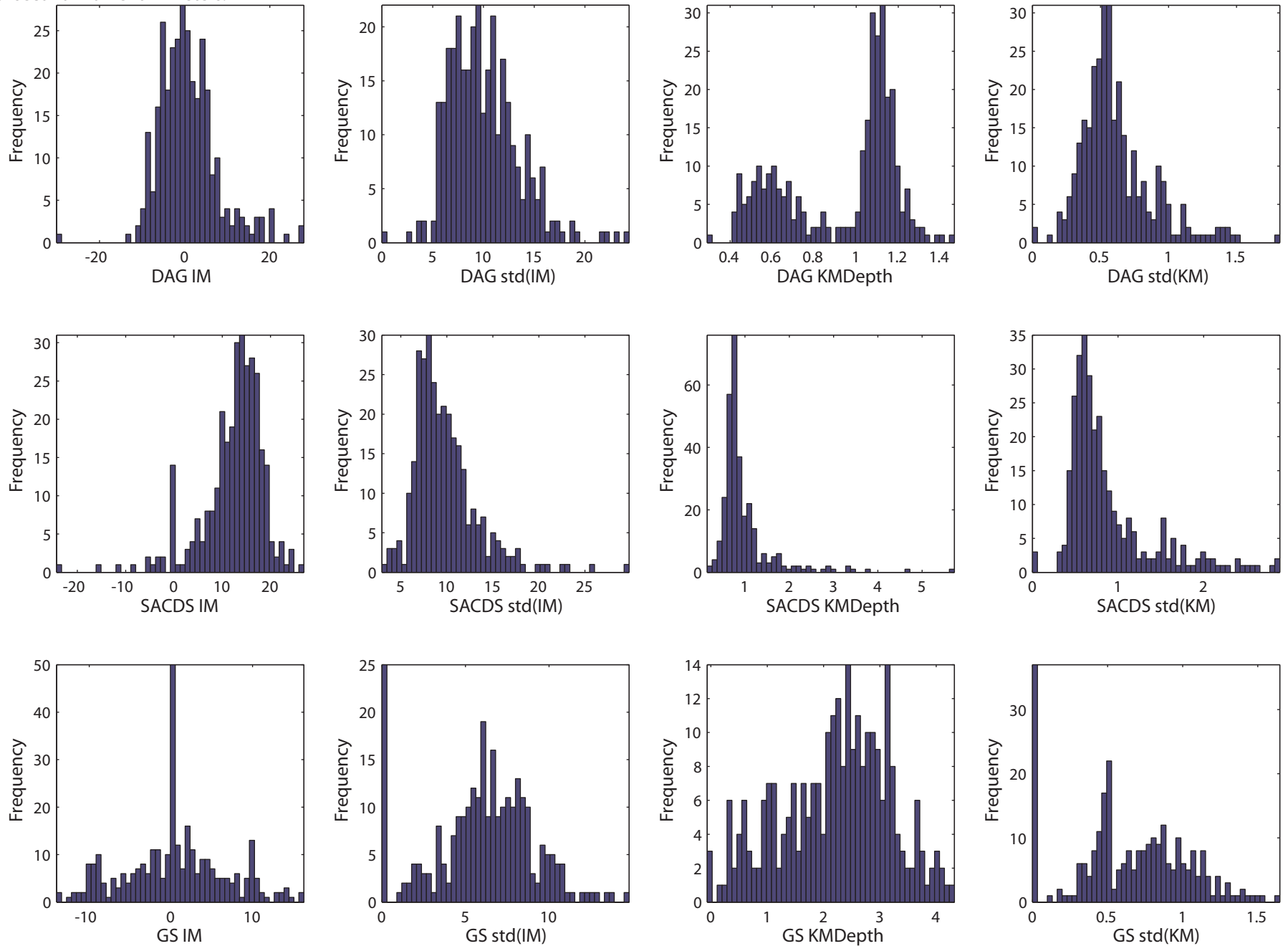


Figure 35. Daytime and nighttime distributions of Dagmar's Landing vertical first moment depth. Night time depths were chosen as periods with light = 0, and the crepuscular signal < 0.1. Day time periods were chosen as periods with light = 1, and the crepuscular signal < 0.1.

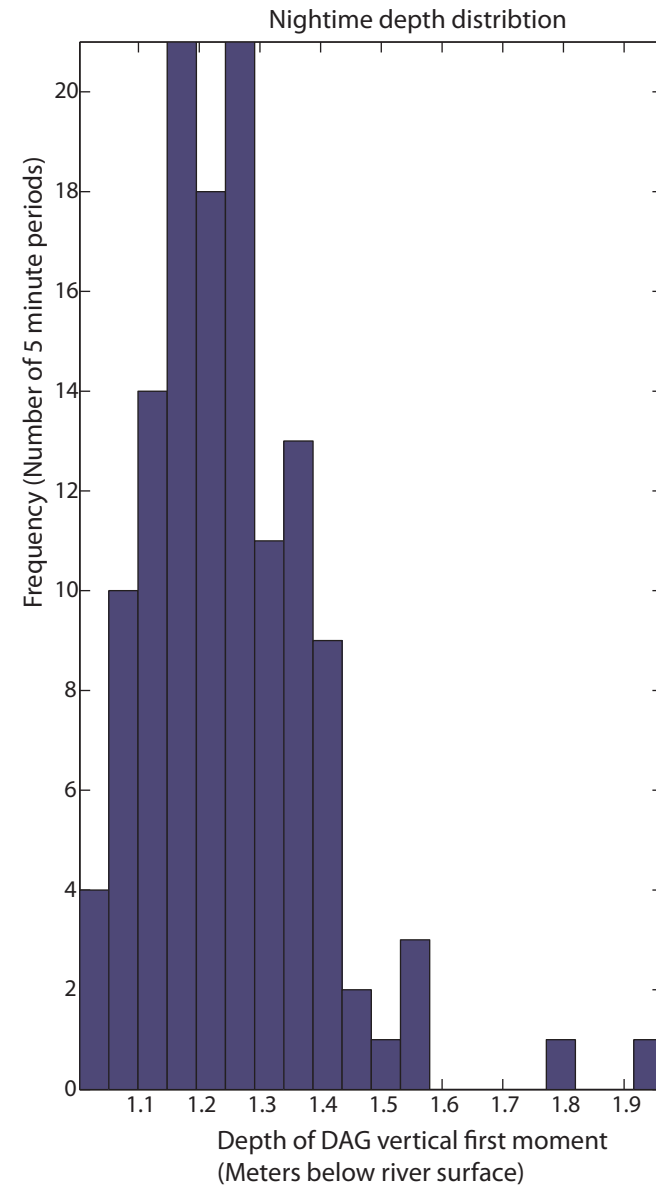
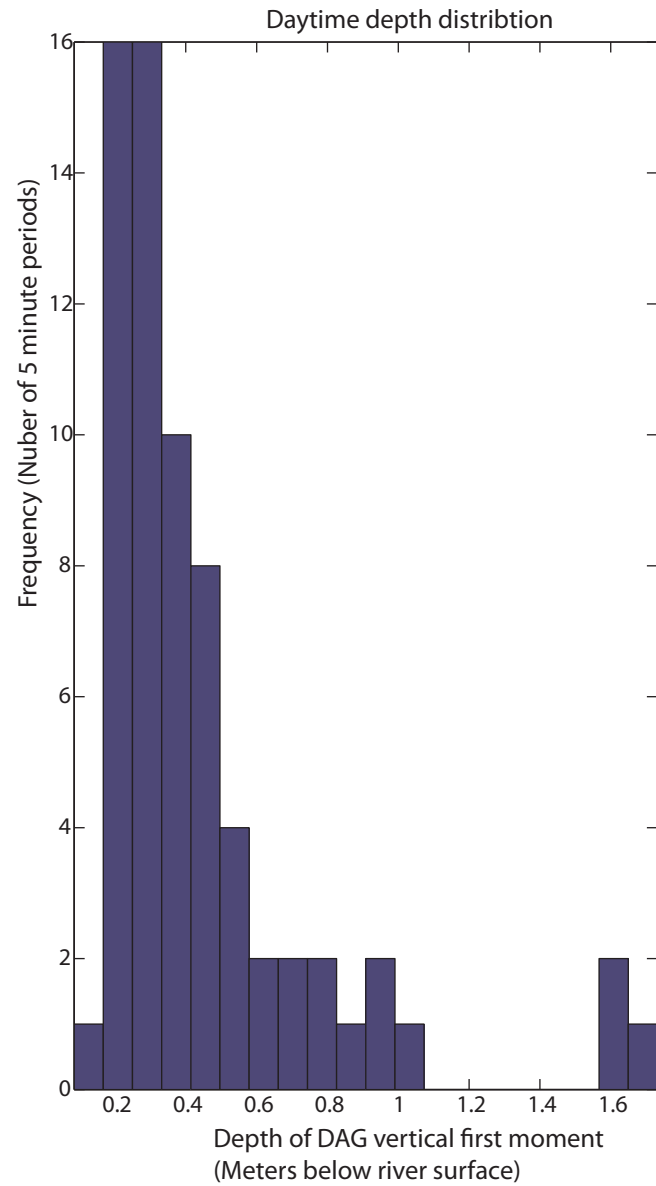
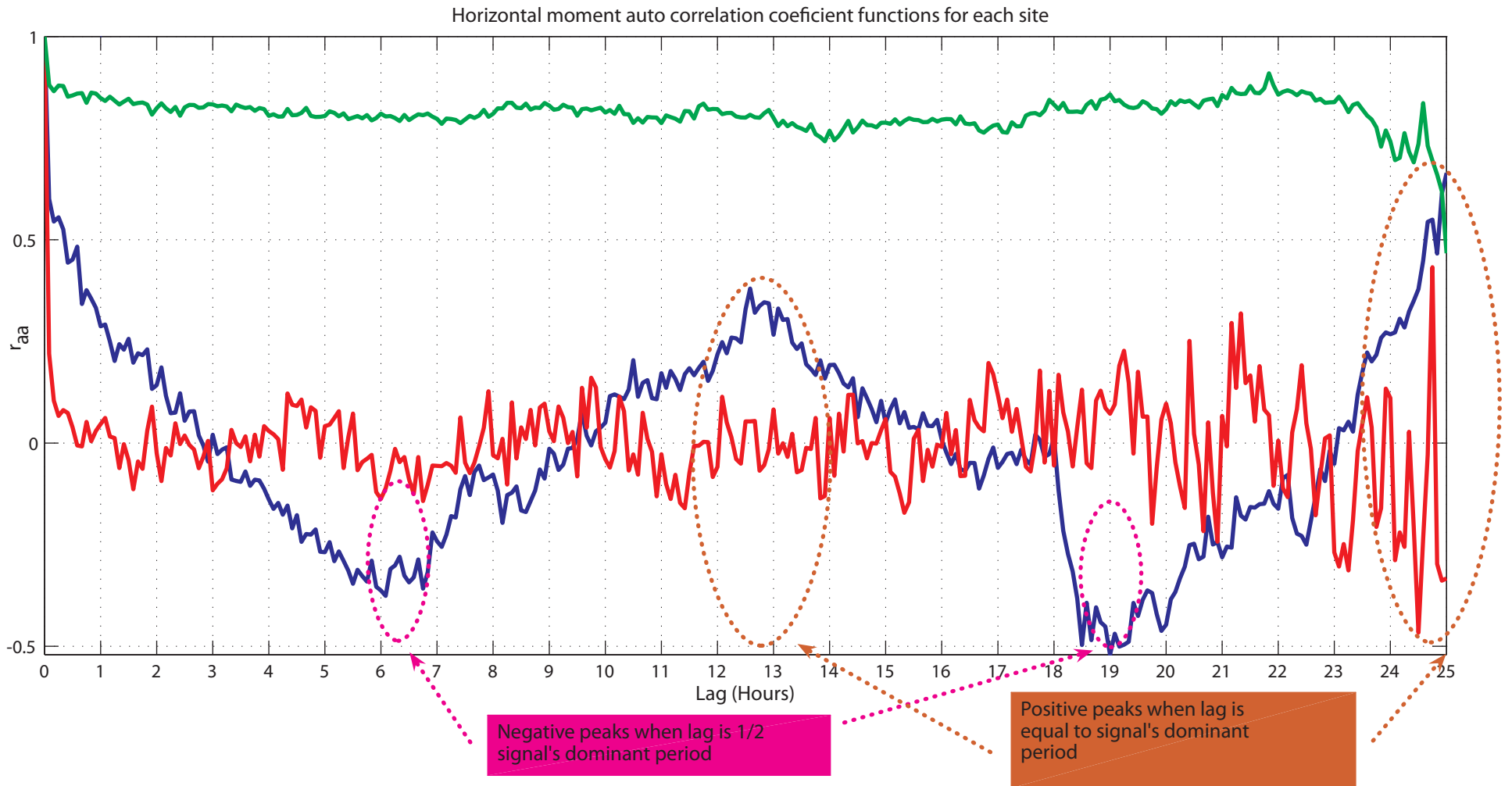


Figure 36. Auto correlation functions for each sites horizontal first moment signals



- Dagmar r_{aa} (Indicates fish distribution influenced by 12.5hr tide)
- Georgiana r_{aa} (Indicates fish that are randomly distributed)
- Sacramento Downstream r_{aa} (Indicates fish that are consistently distributed independent of tidal effects)

Figure 37. Spectral analysis of Dagmar's Landing horizontal first moment signal

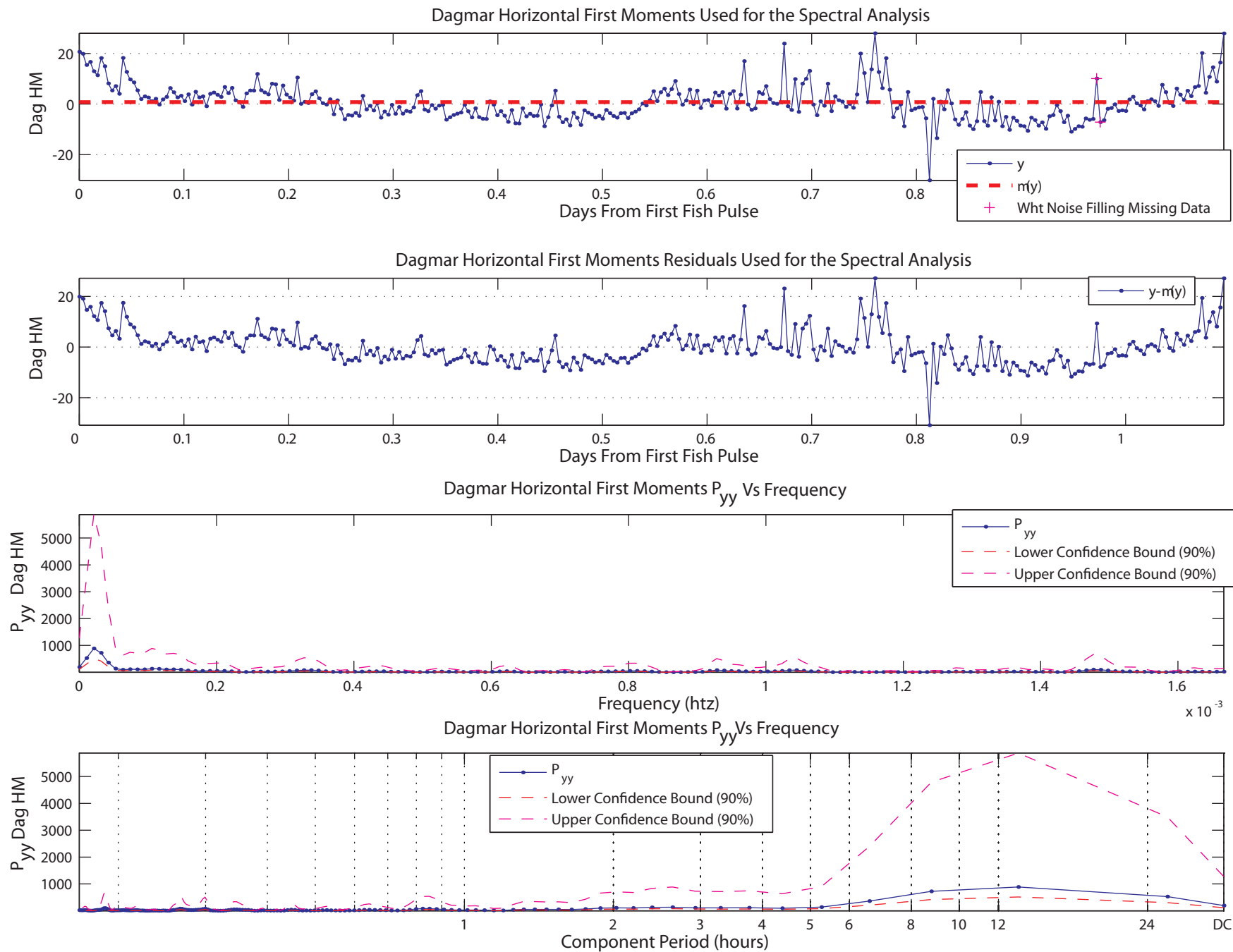


Figure 38. Spectral analysis of WGA cross sectional average velocity signal.

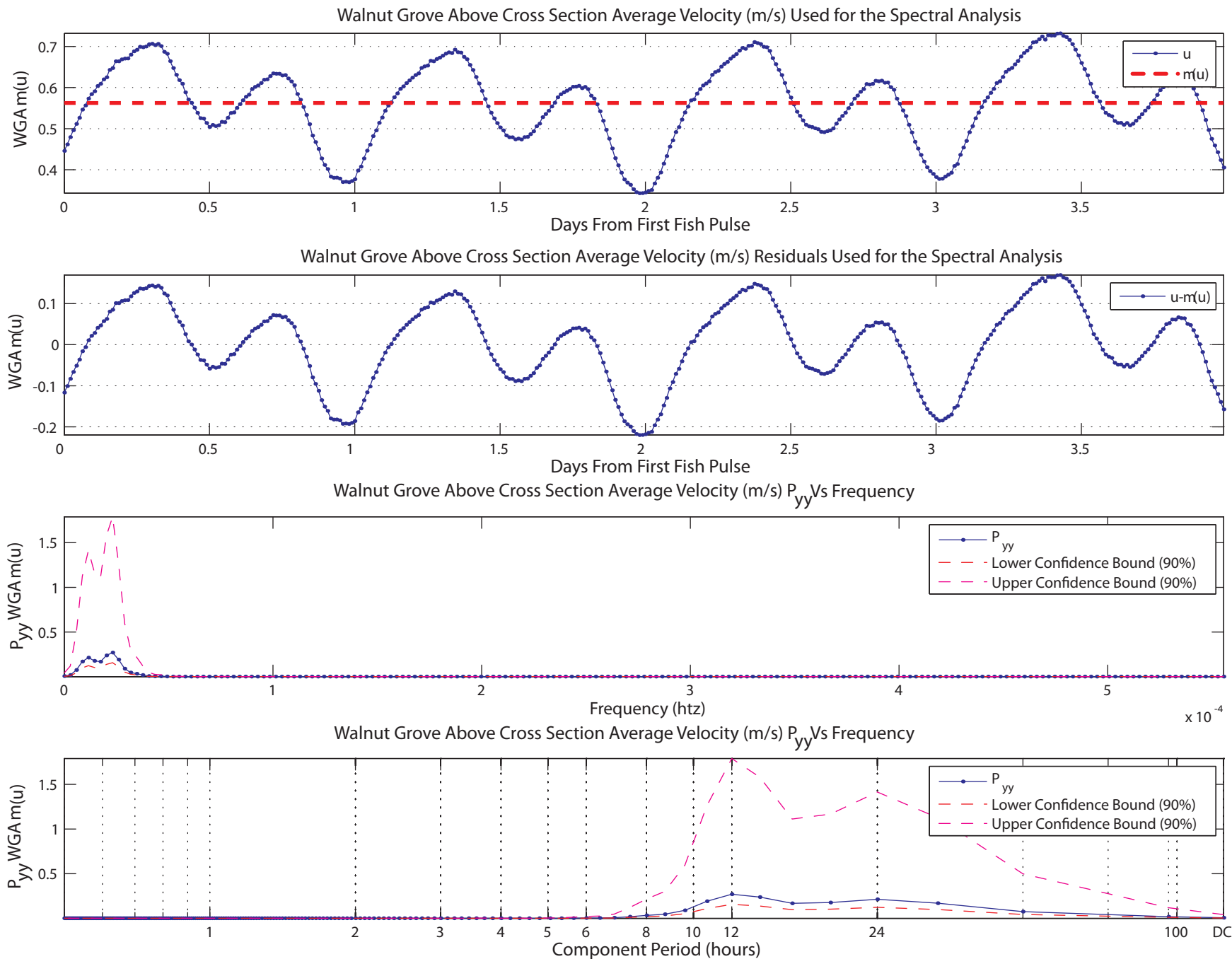


Figure 39. Spectral analysis of the Dagmar's Landing depth of vertical first moment signal

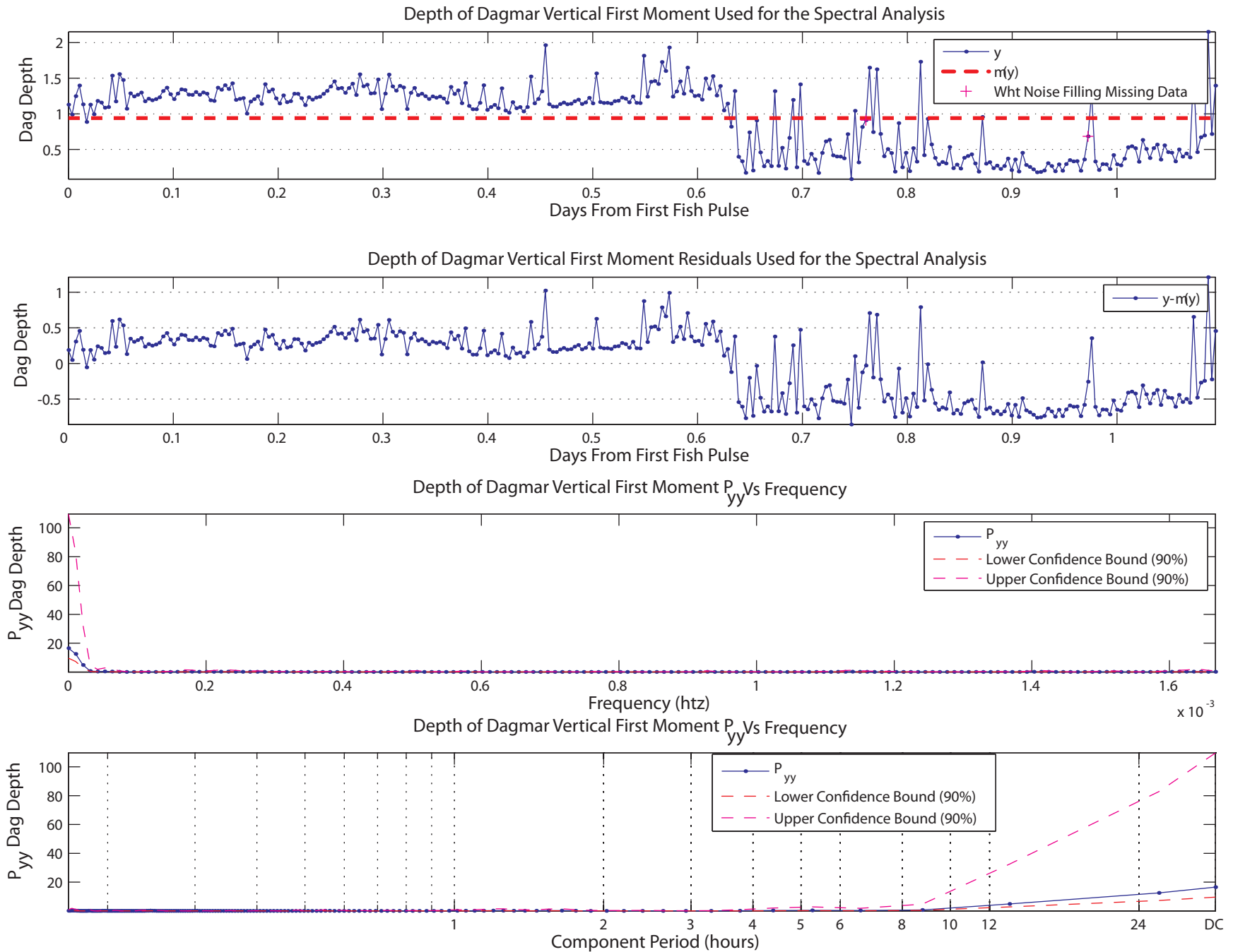


Figure 40. Dagmar's Landing horizontal first moments as a function of the cross sectional average water velocity upstream. Points are colored by their crepuscular value, and sized relative to the number of fish passing Dagmar's Landing. Most outliers are from periods of crepuscular activity, or periods when very few fish were detected.

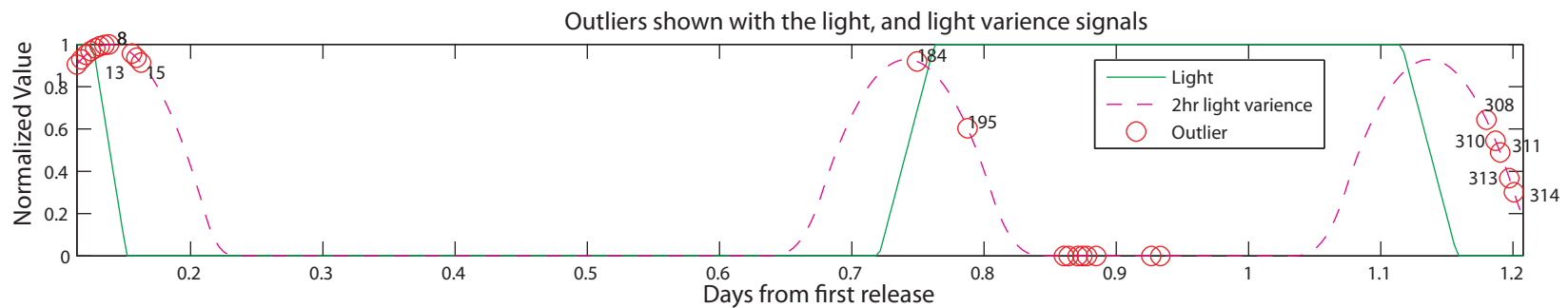
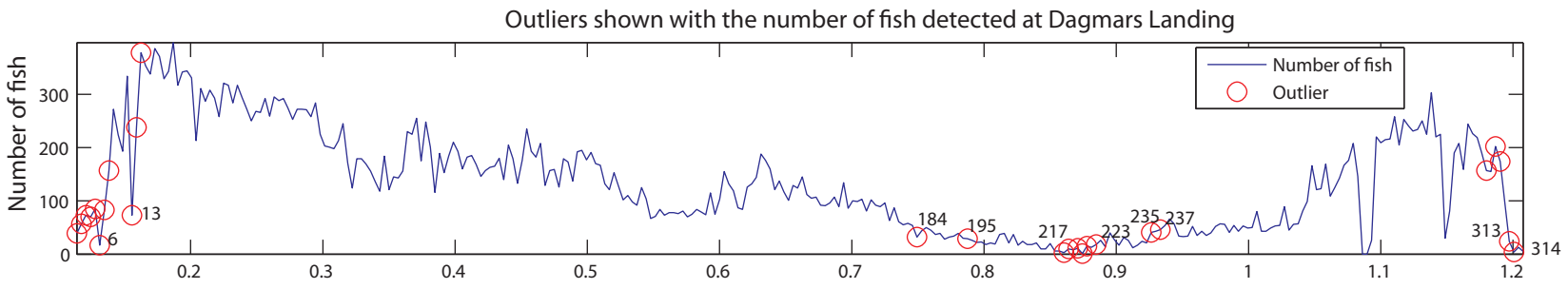
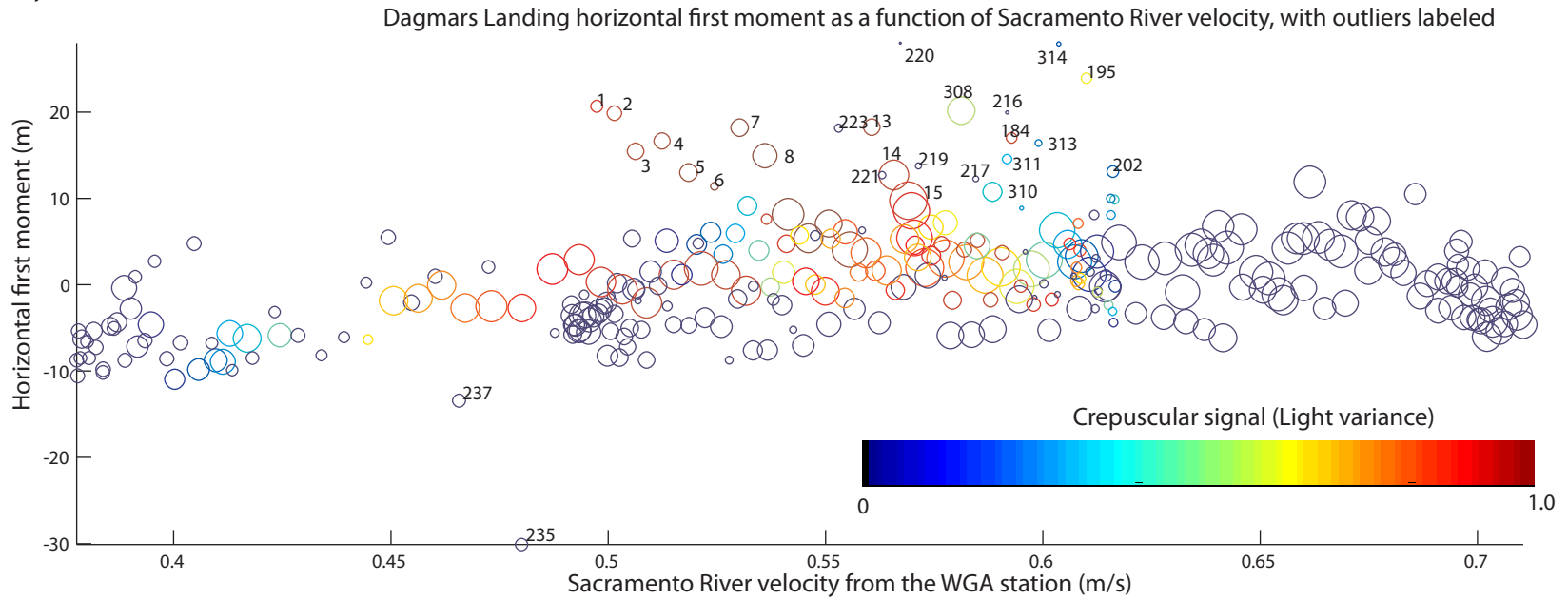


Figure 41. Relationship between the horizontal first moment at Dagmar's Landing and WGA cross sectional averaged velocity. Note that the largest residuals are smaller than the mean standard deviation in the horizontal first moment signal calculated from the horizontal second moment signal

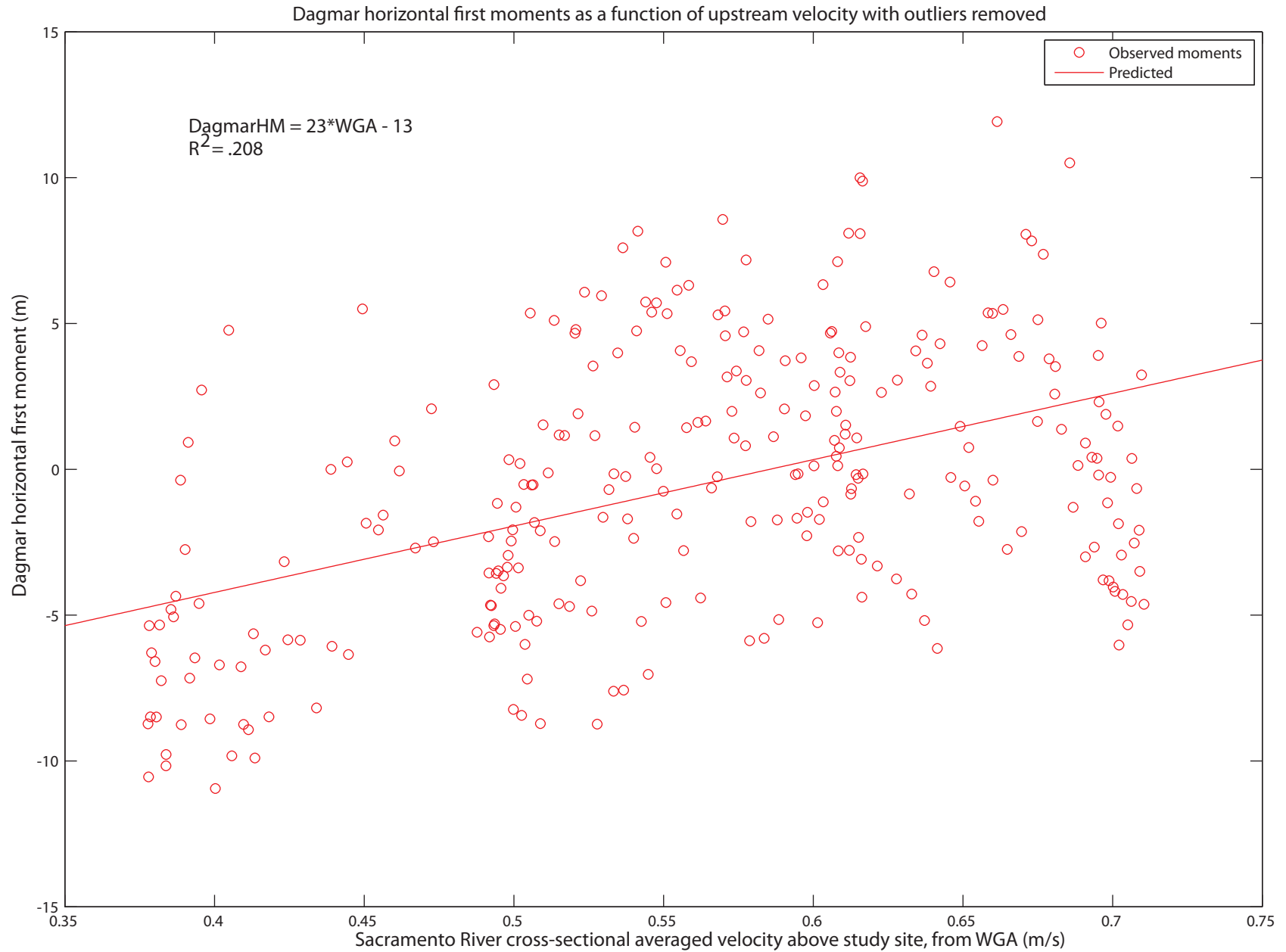


Figure 42. Signals used to predict Dagmars Landing horizontal first moment signal

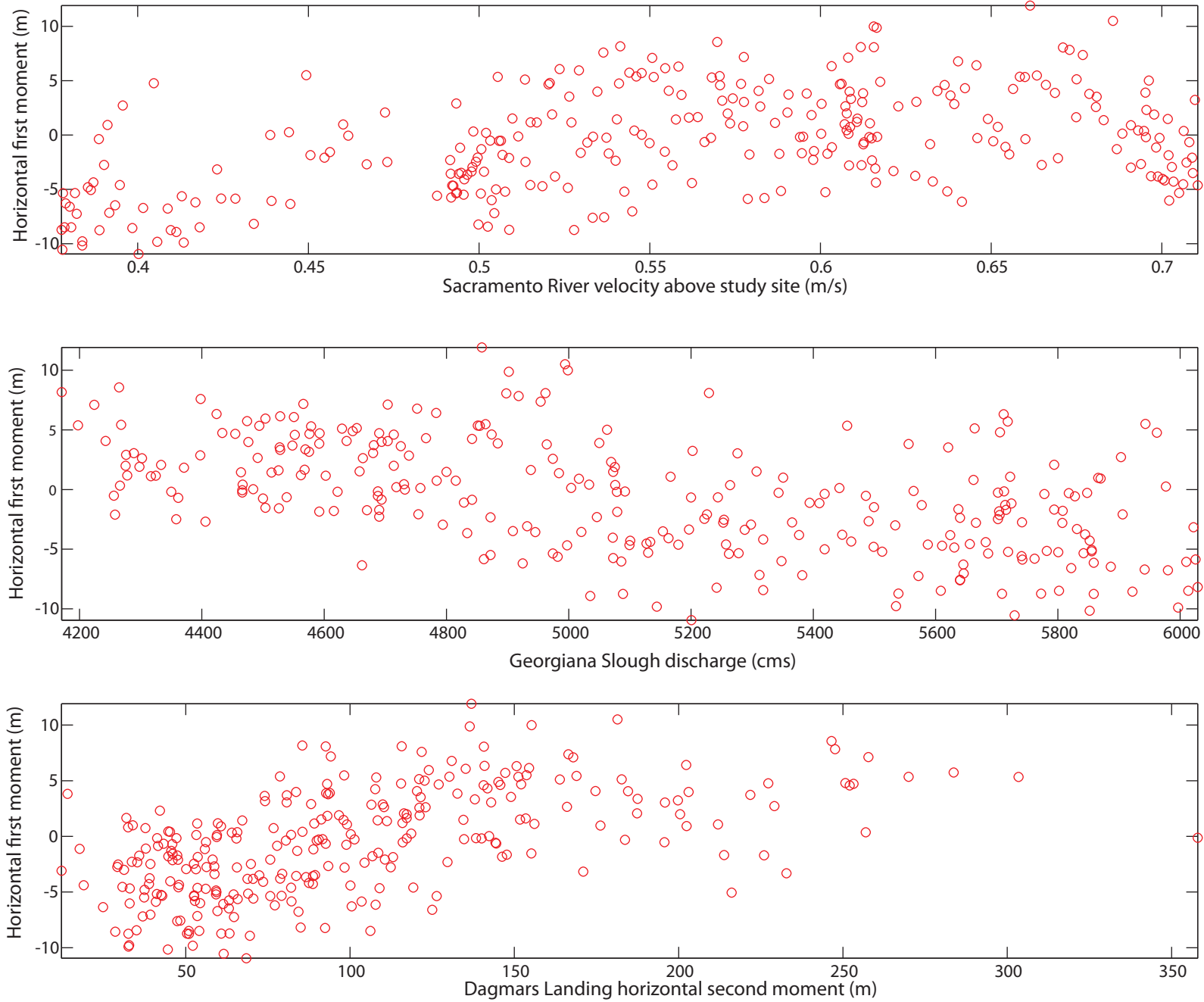


Figure 43. Weak relationship between residuals in the initial fit and depth of fish at Dagmars Landing

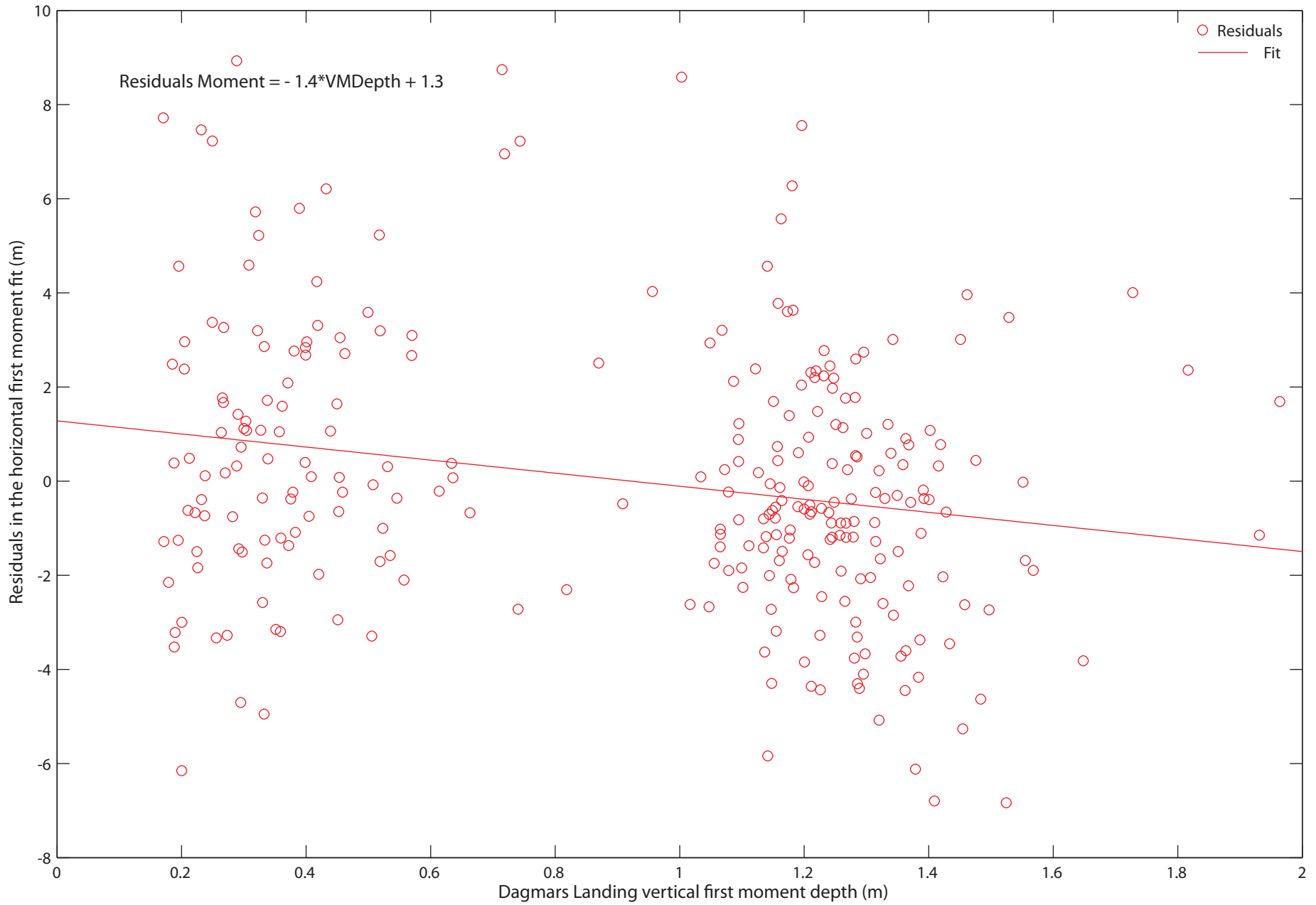


Figure 44. Evaluation of regression model for Dagmar's Landing horizontal first moment signal

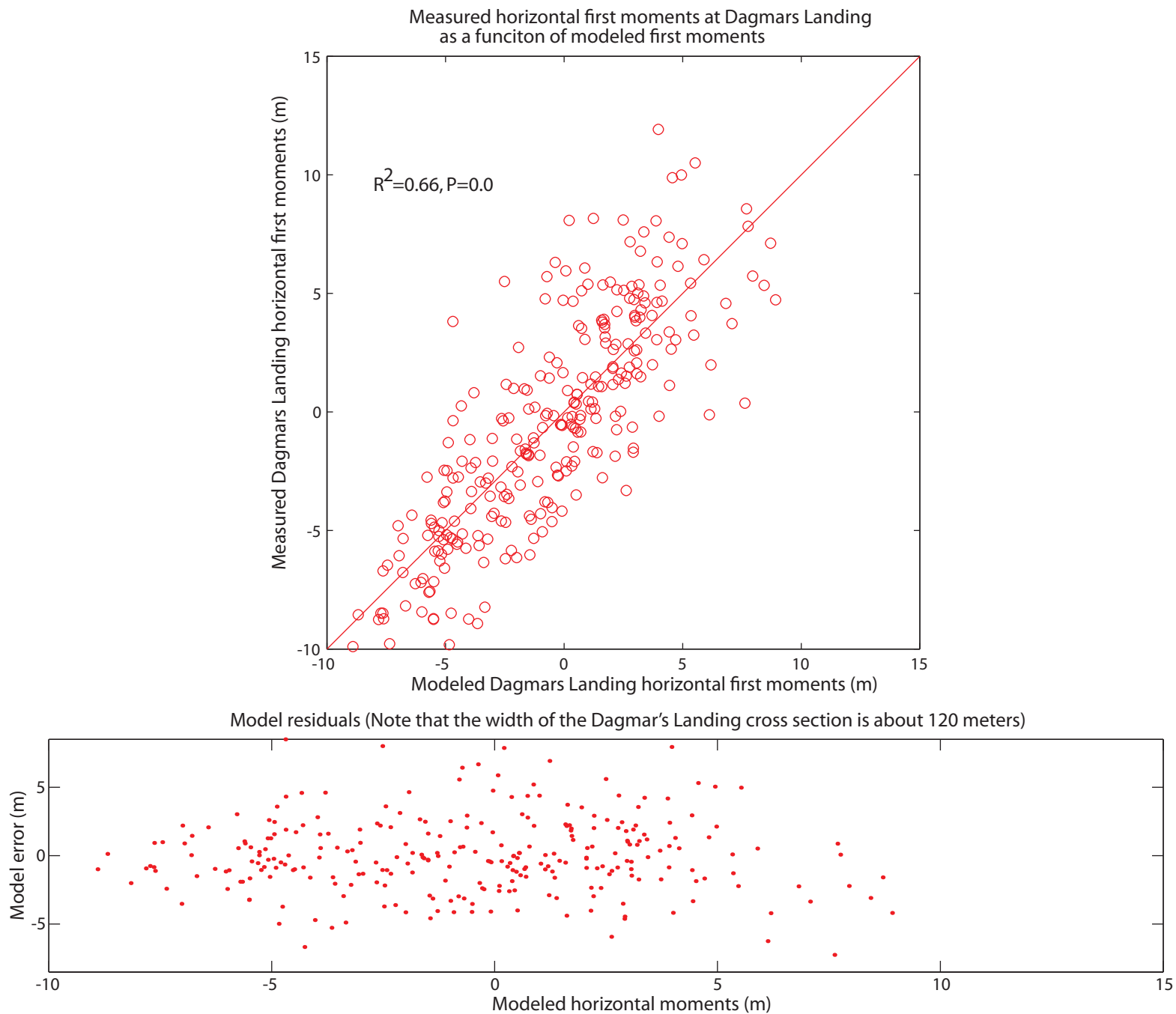
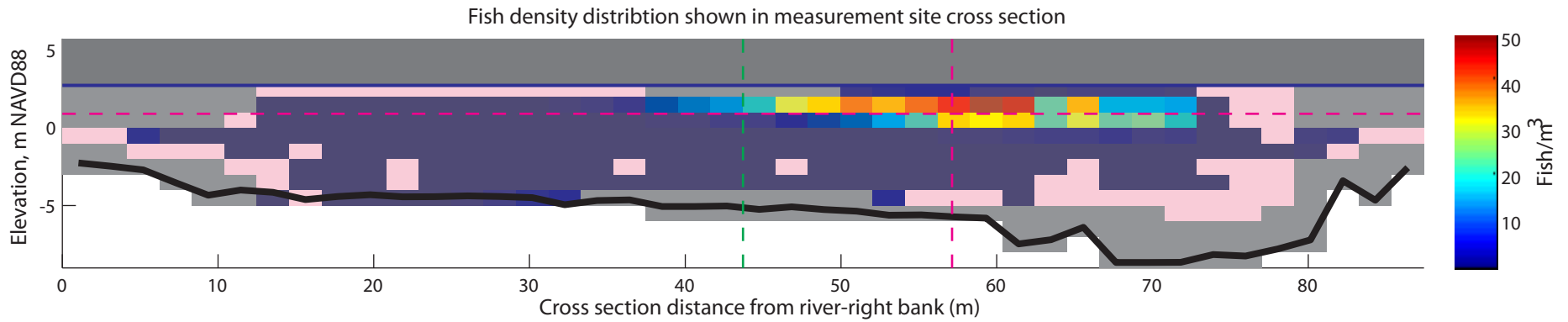


Figure 45. Overall fish density distribution for Sacramento River downstream measurement site. In the upper axis fish density in each bin is depicted by color, pink areas are bins with beam coverage, but no fish detections, grey areas are wet bins with no beam coverage. The bottom elevation profile is drawn in dark black, and the mean surface stage is drawn in dark blue. The area above the surface is shaded to represent mean sunlight levels for the period. Horizontal and vertical first moments are shown with dashed pink lines, and the horizontal cross section center point is shown with a dashed green line.



Fish density distribution shown as two dimensional histogram, with each bar showing the fish density detected in each bin.

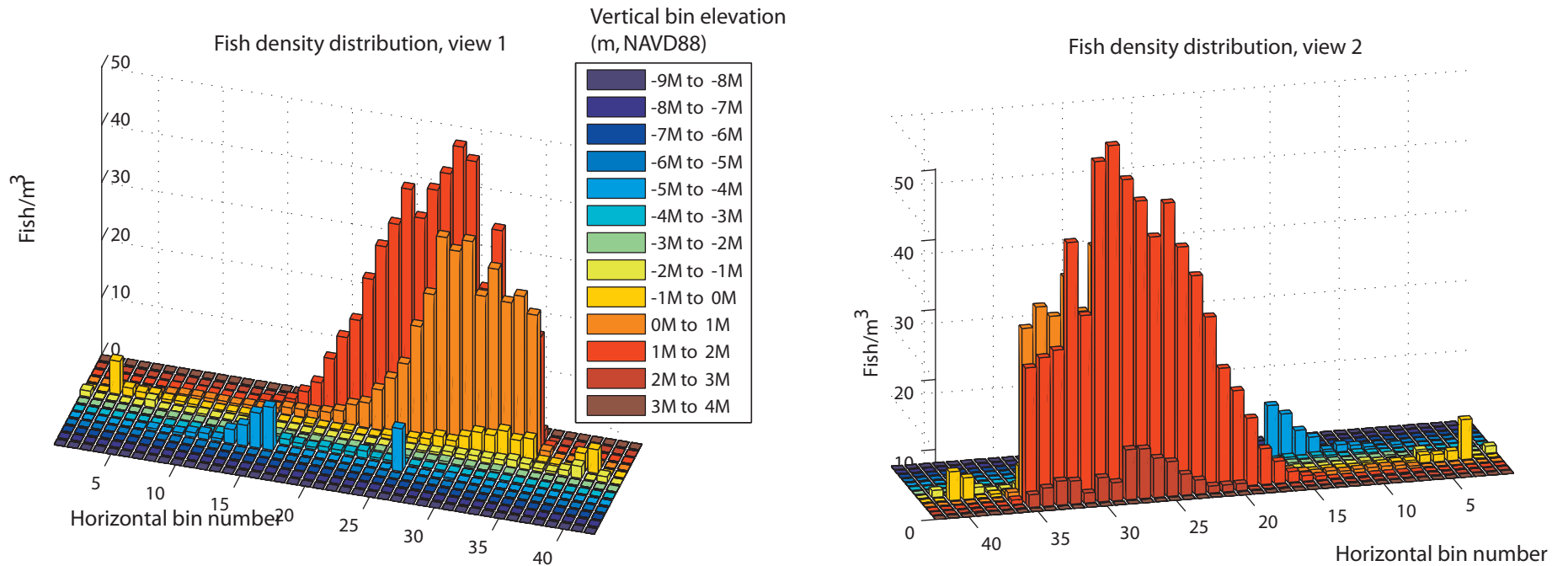
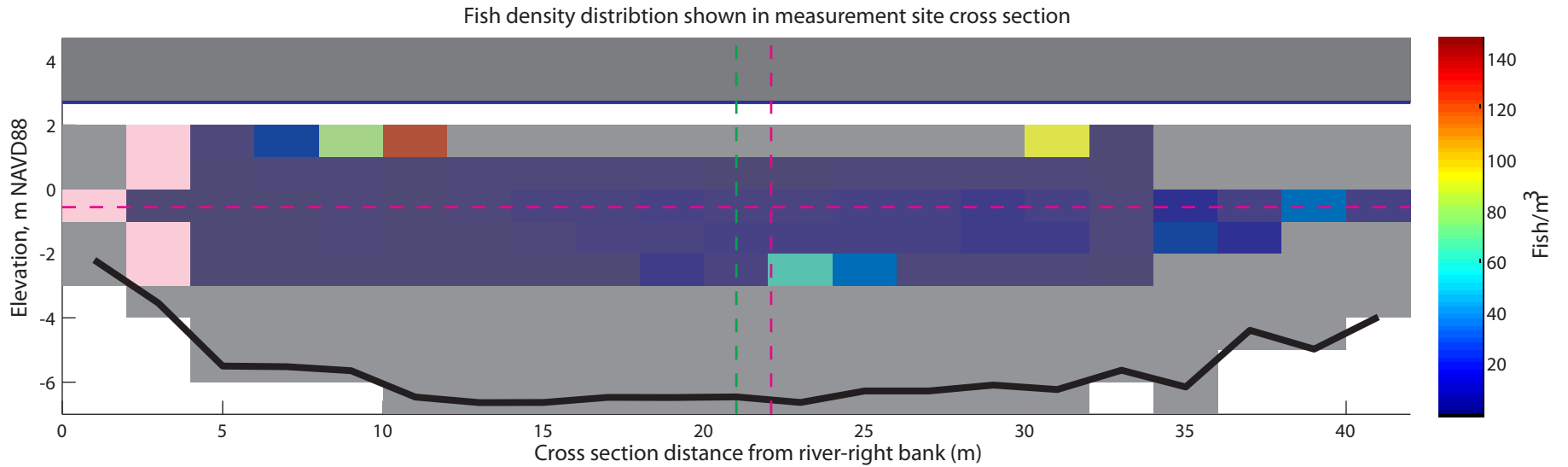


Figure 46. Overall fish density distribution for Georgiana Slough measurement site. In the upper axis fish density in each bin is depicted by color, pink areas are bins with beam coverage, but no fish detections, grey areas are wet bins with no beam coverage. The bottom elevation profile is drawn in dark black, and the mean surface stage is drawn in dark blue. The area above the surface is shaded to represent mean sunlight levels for the period. Horizontal and vertical first moments are shown with dashed pink lines, and the horizontal cross section center point is shown with a dashed green line.



Fish density distribution shown as two dimensional histogram, with each bar showing the fish density detected in each bin.

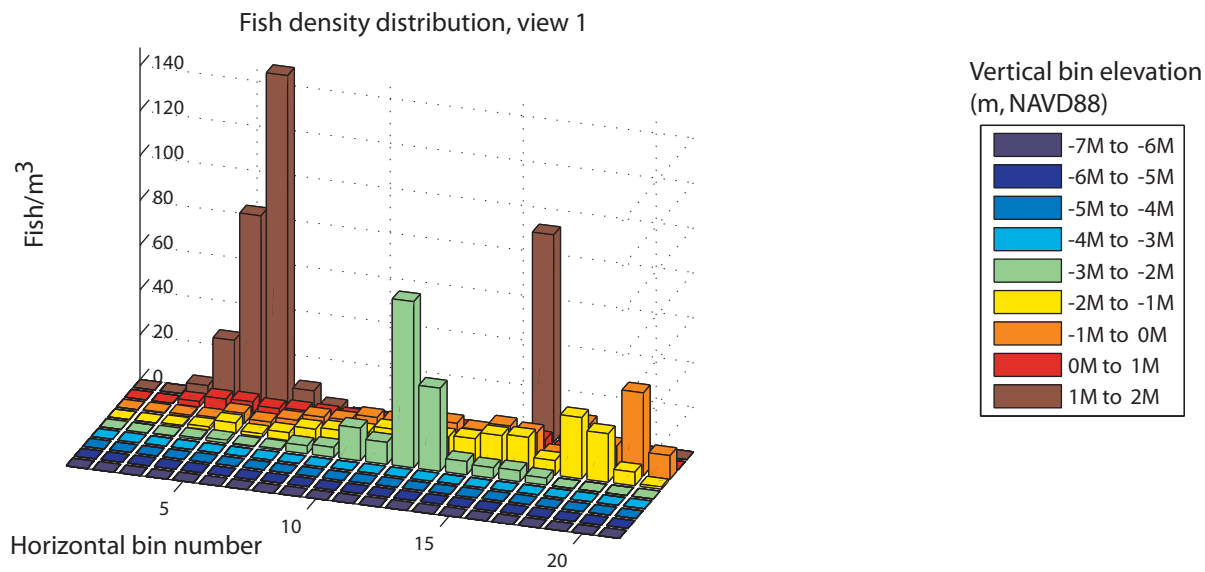


Figure 47. Time series of Sacramento River downstream measurement site fish density distribution statistics

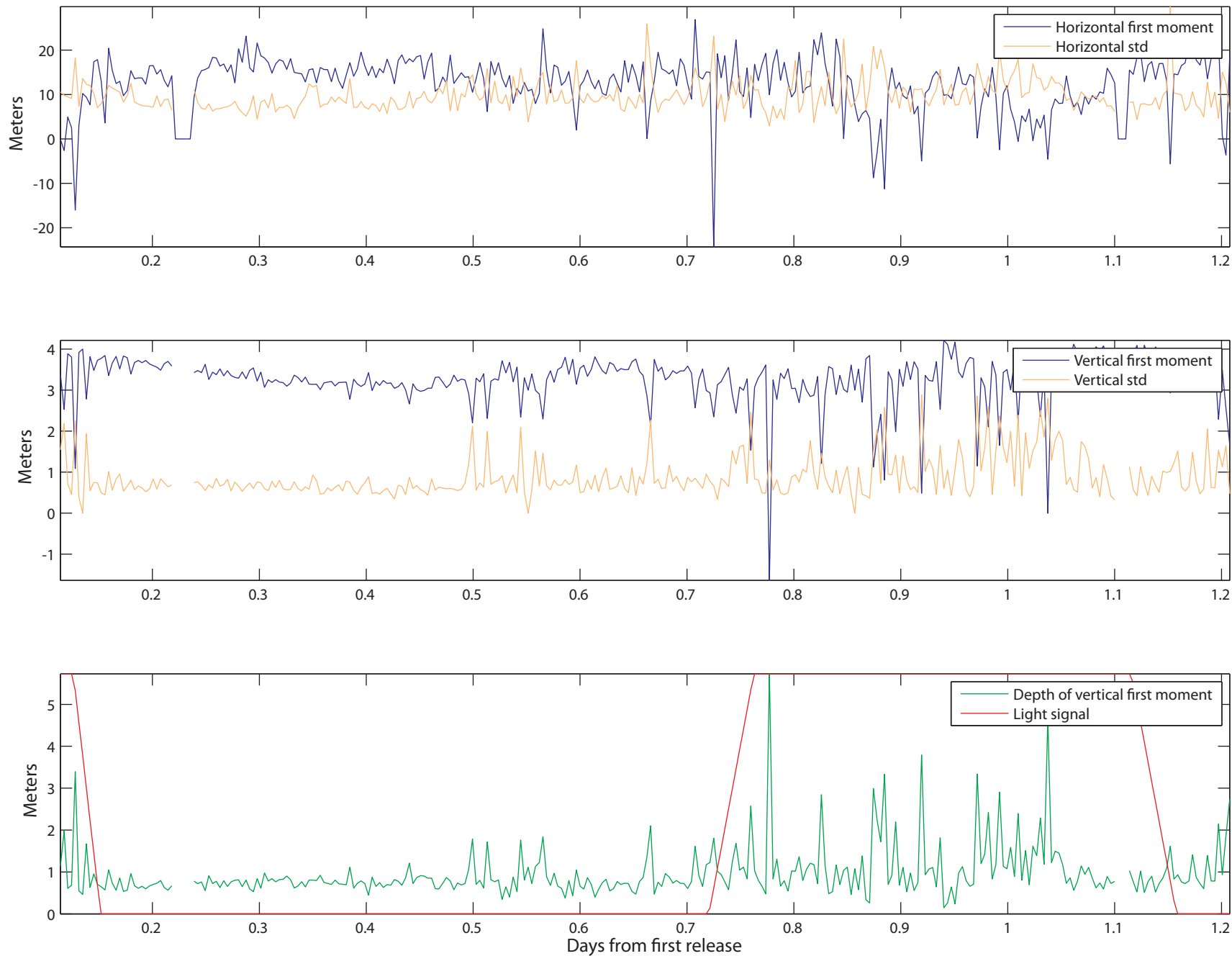


Figure 48. Time series of Sacramento River downstream measurement site fish density distribution statistics

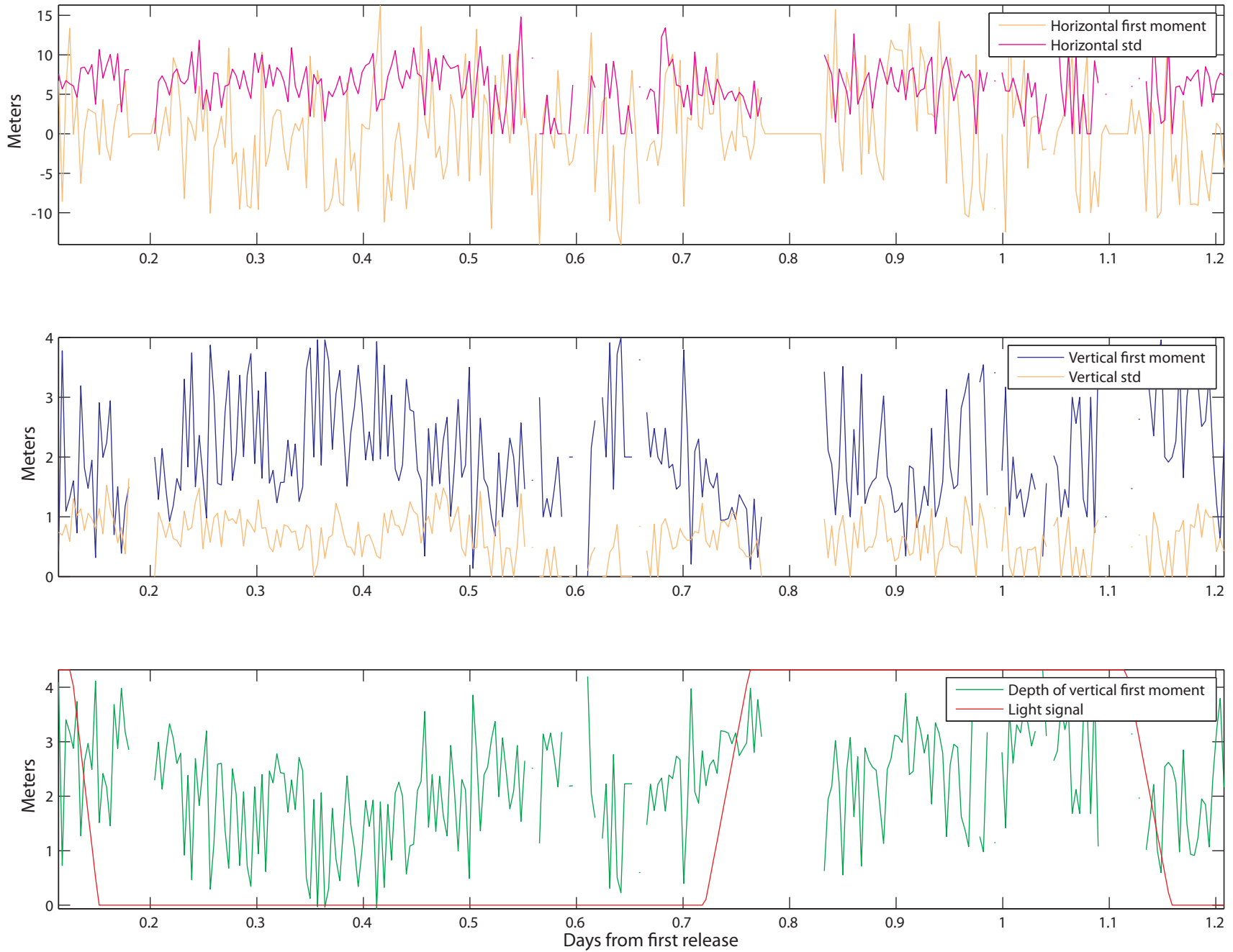


Figure 49. Daytime and nighttime distributions of SACDS and GS depth of vertical first moment signals. Night time depths were chosen as periods with light = 0, and the crepuscular signal < 0.1. Day time periods were chosen as periods with light = 1, and the crepuscular signal < 0.1.

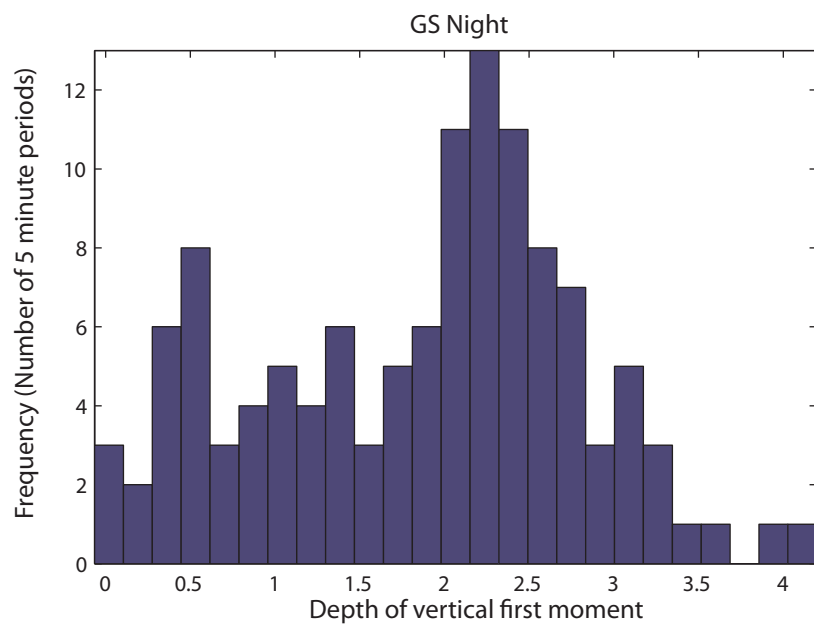
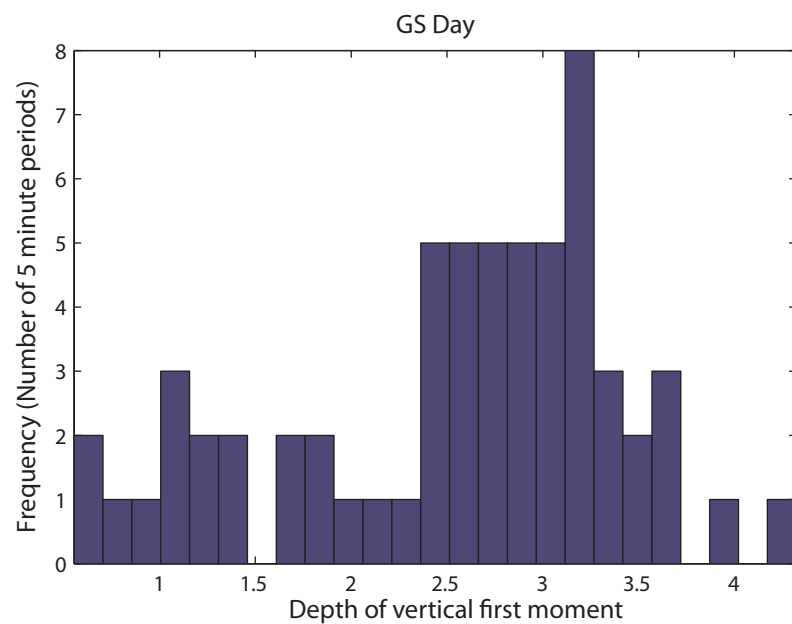
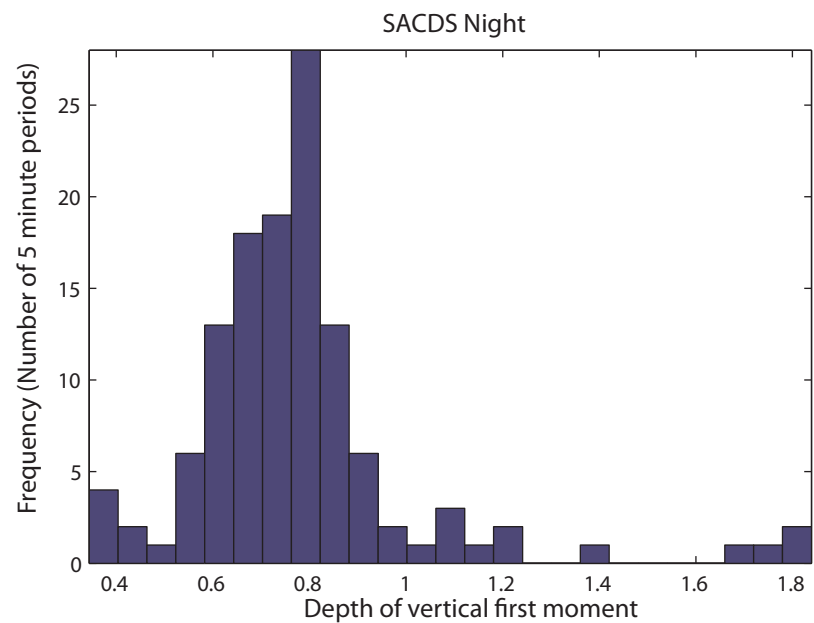
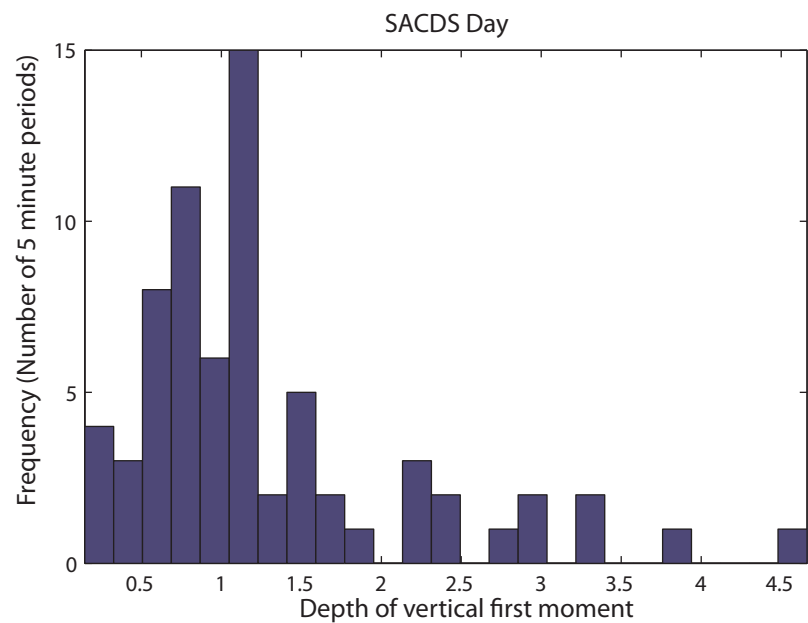


Figure 50. Spectral analysis of SACDS horizontal first moment signal

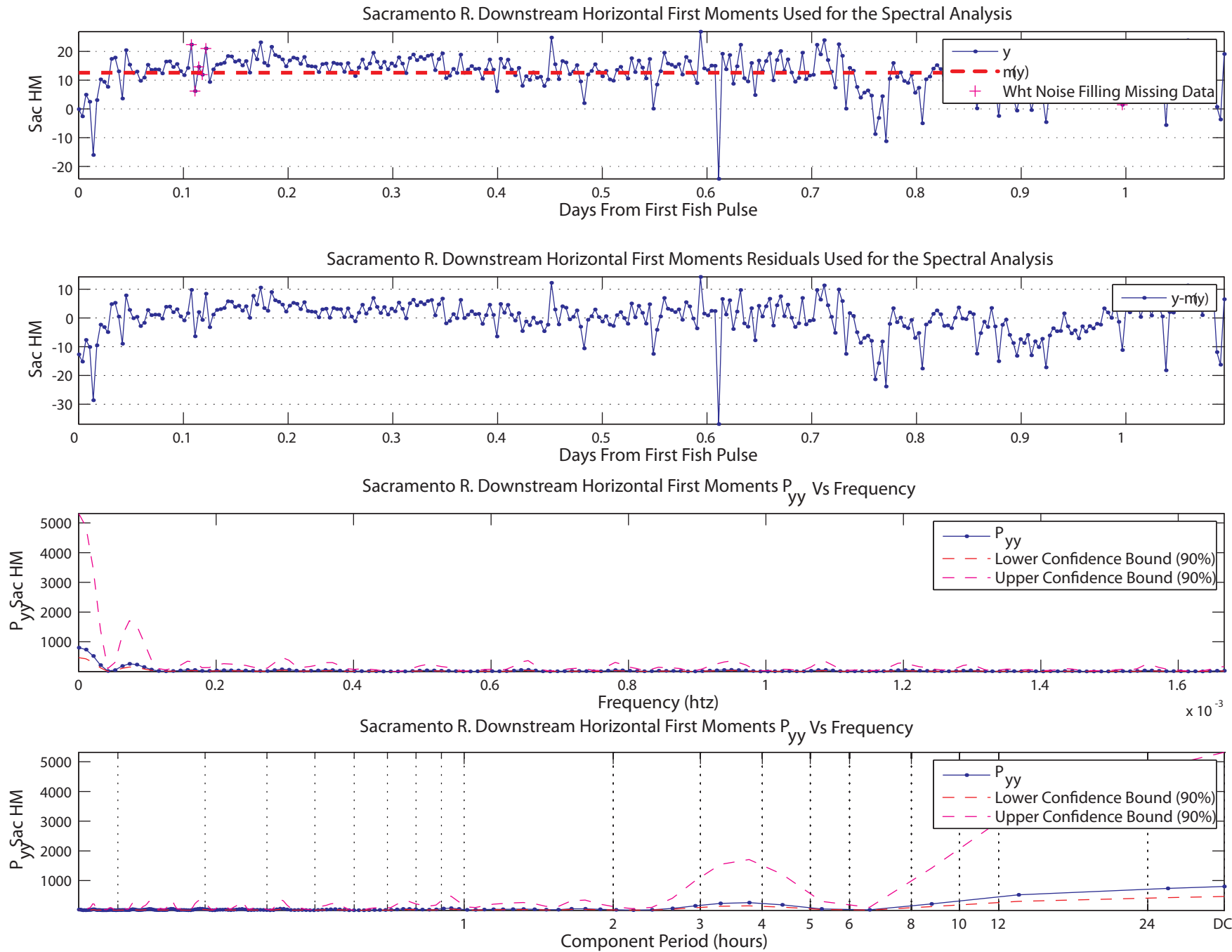


Figure 51. Spectral analysis of the GS horizontal first moment signal

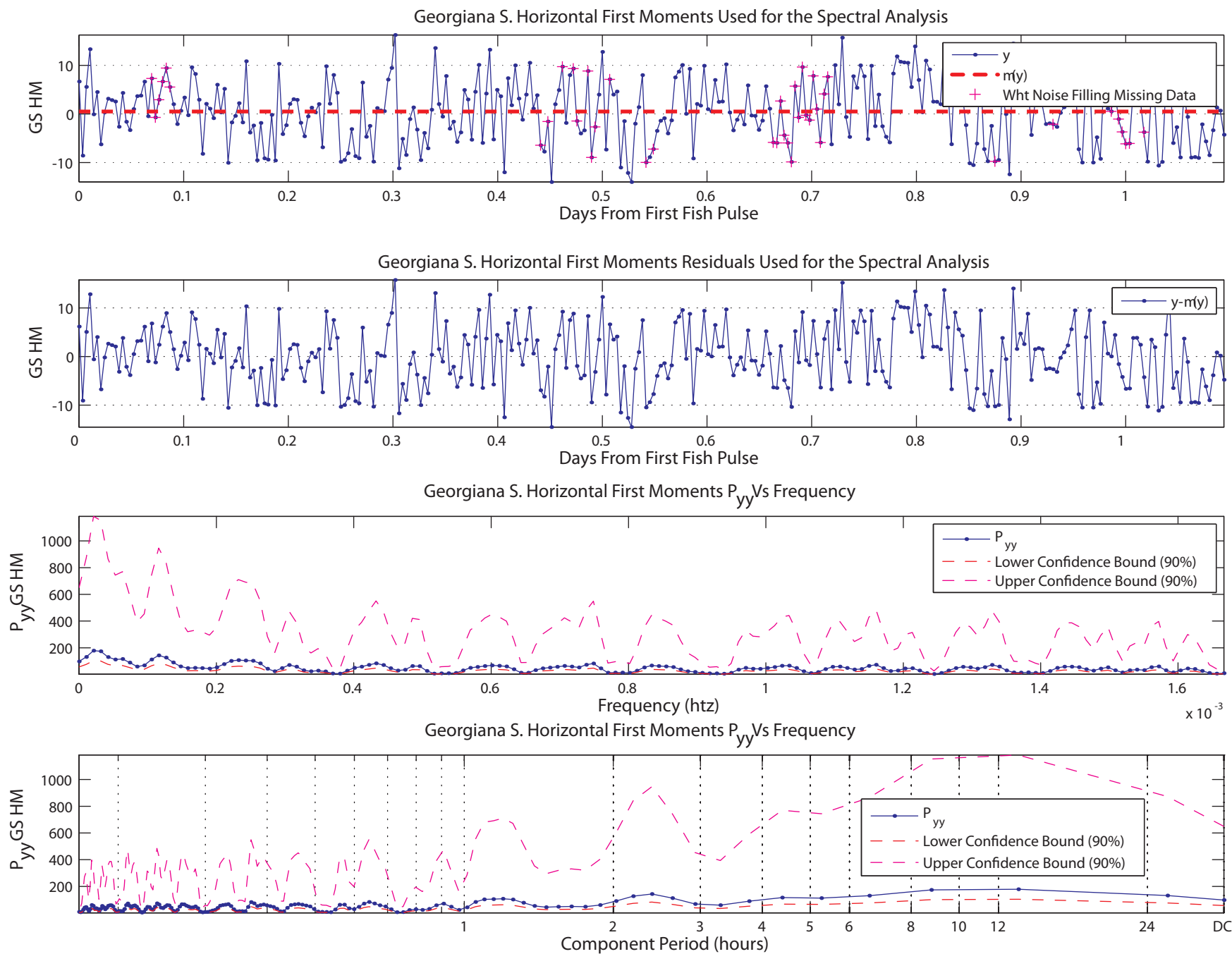


Figure 52. Plots the null entrainment hypothesis of fish entrainment proportional to flow entrainment.

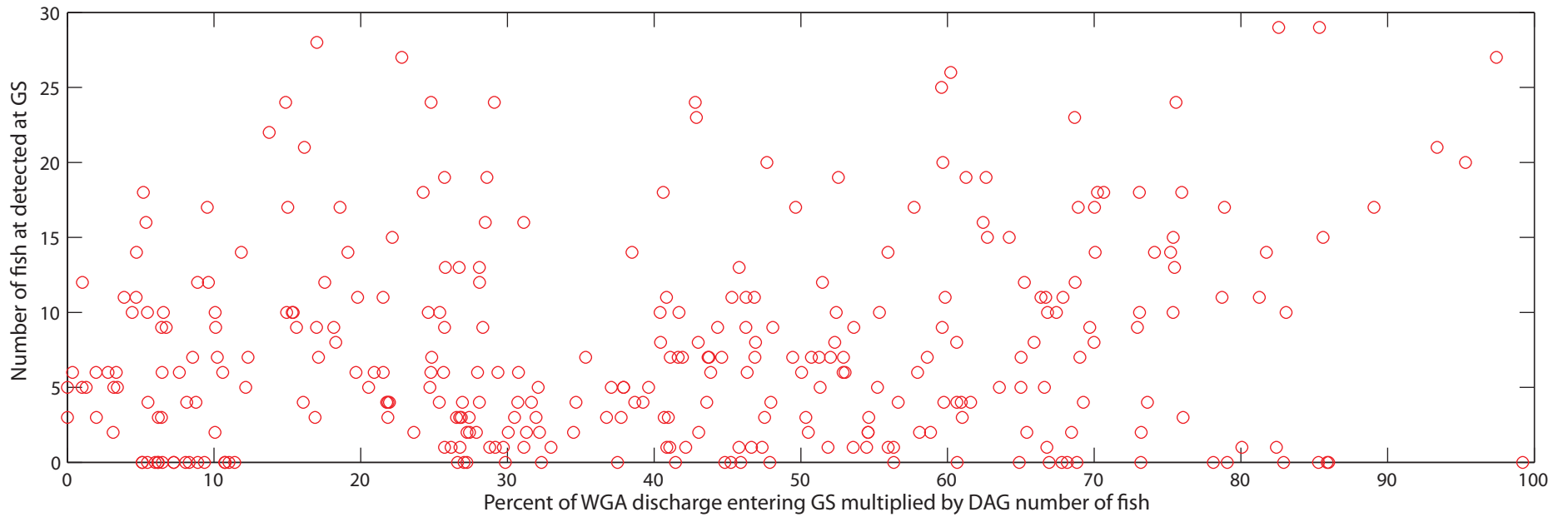
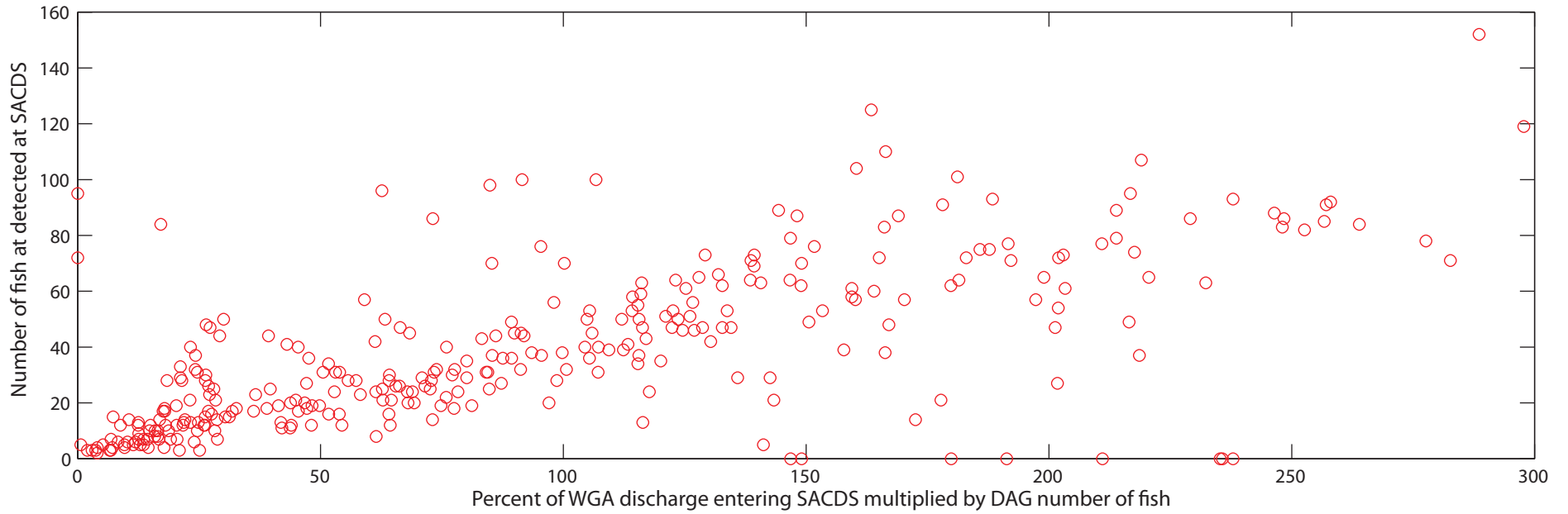


Figure 53. Histogram of the percentage of WGA discharge bypassing Georgiana Slough

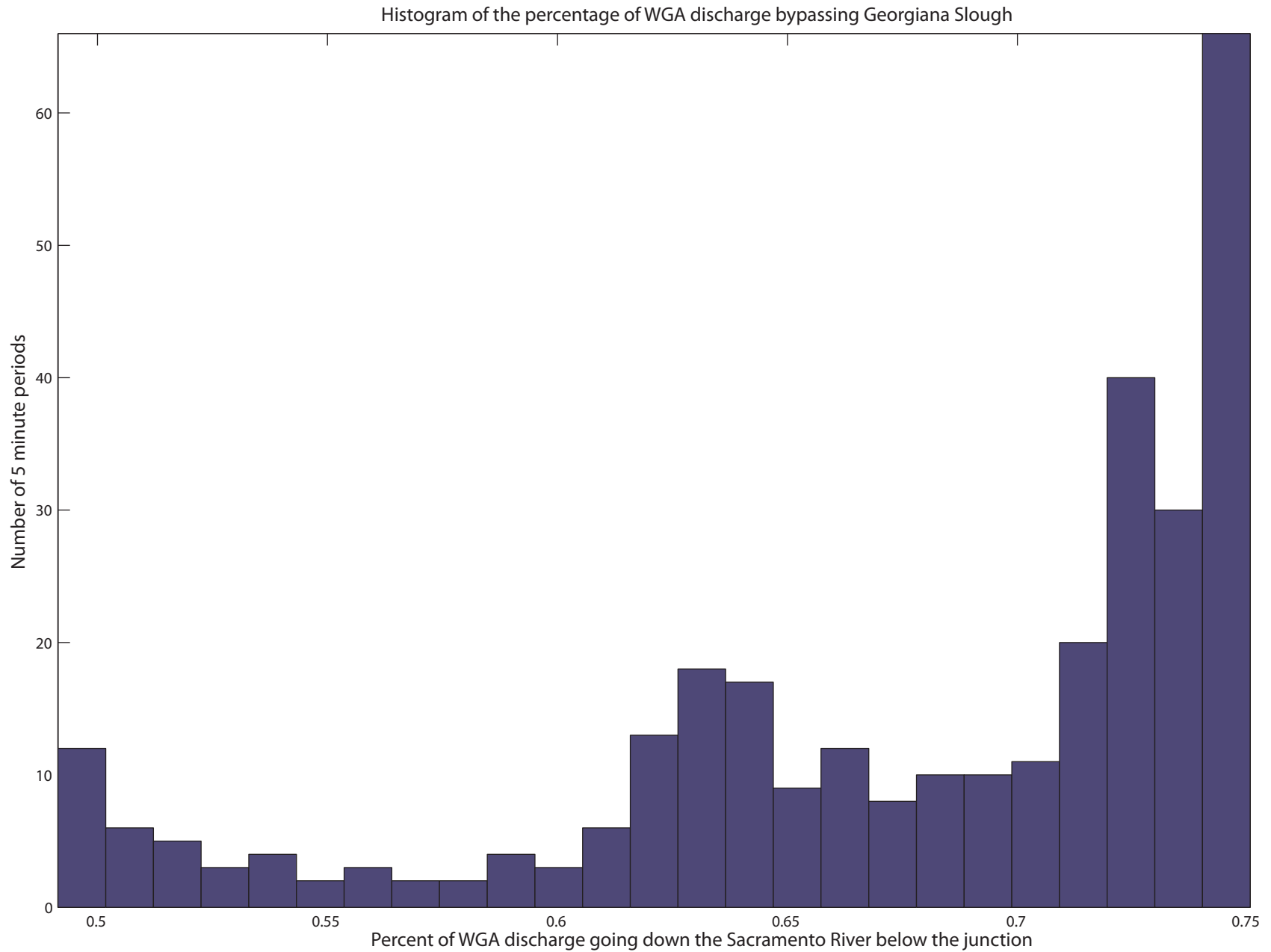


Figure 54. Relationship between various signals and SACDS detections

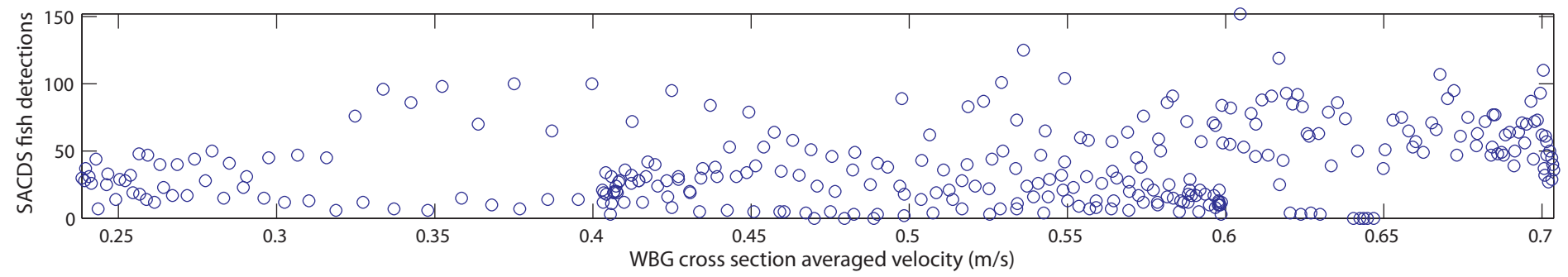
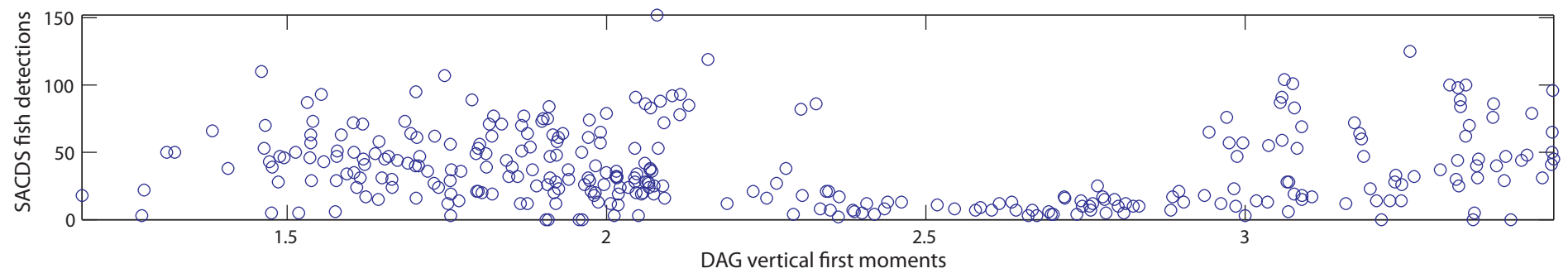
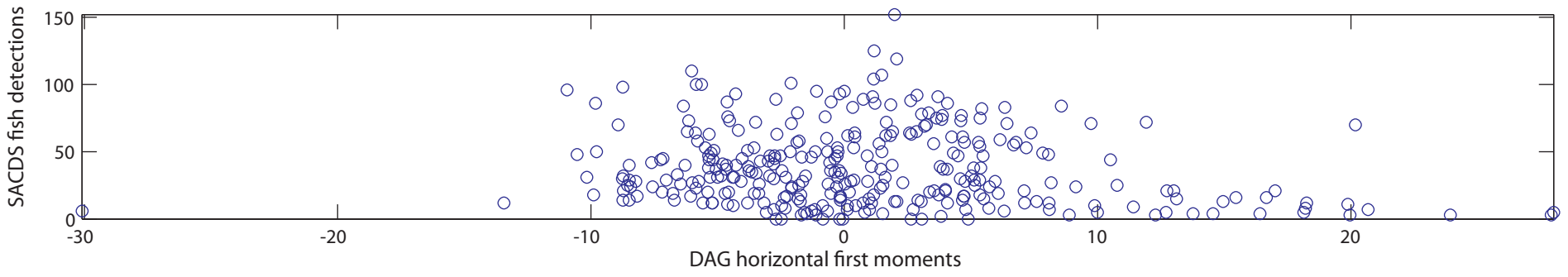
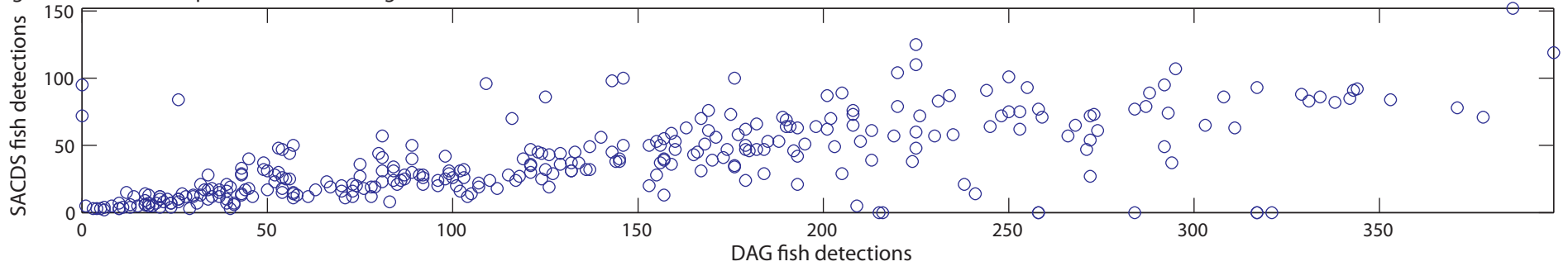


Figure 55. Sample of signals considered in the Georgiana Slough entrainment regression analyses

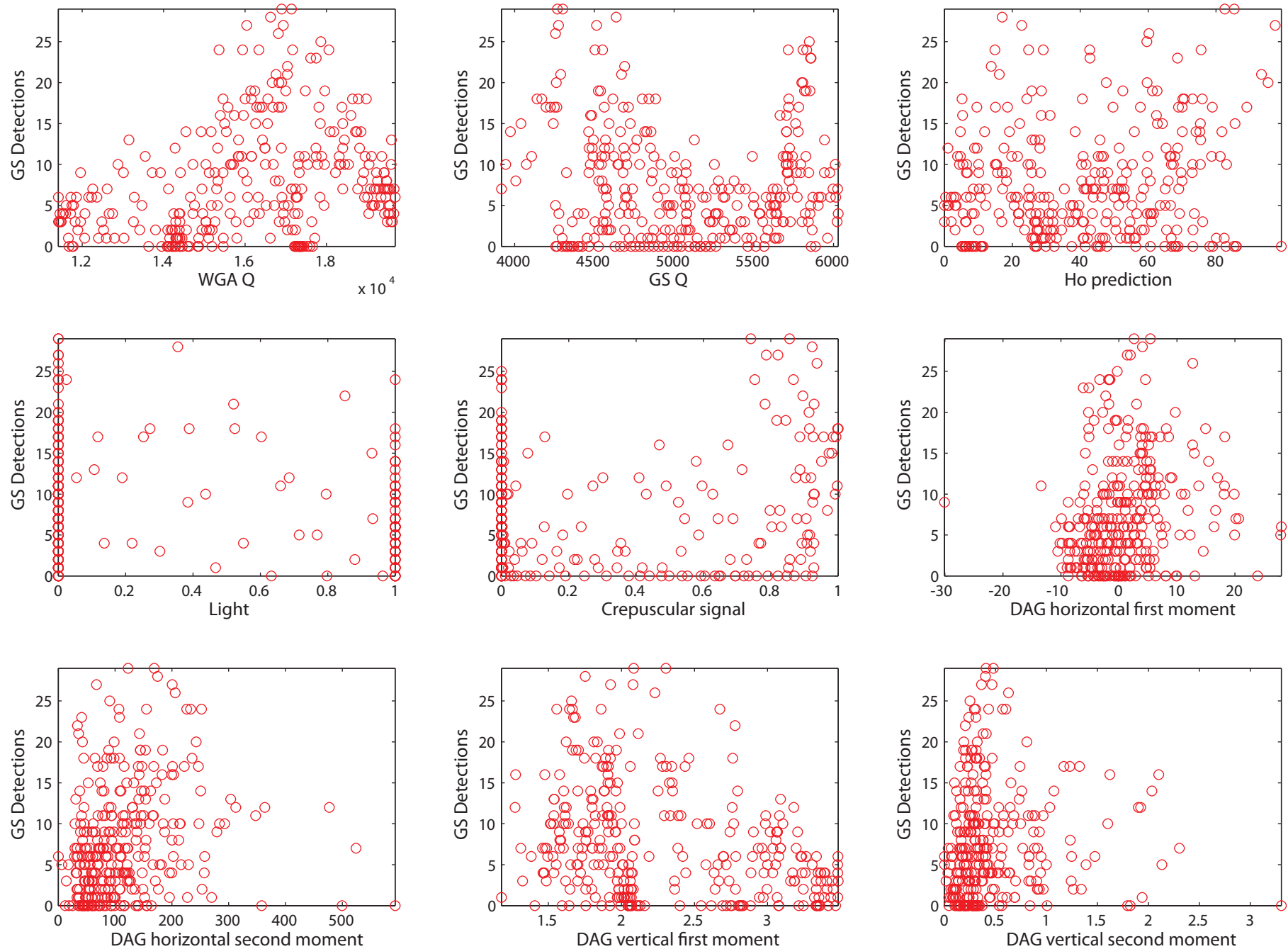


Figure 56. Bins used in the Georgiana Slough binwise number of fish regression (total $r^2 = .420$)

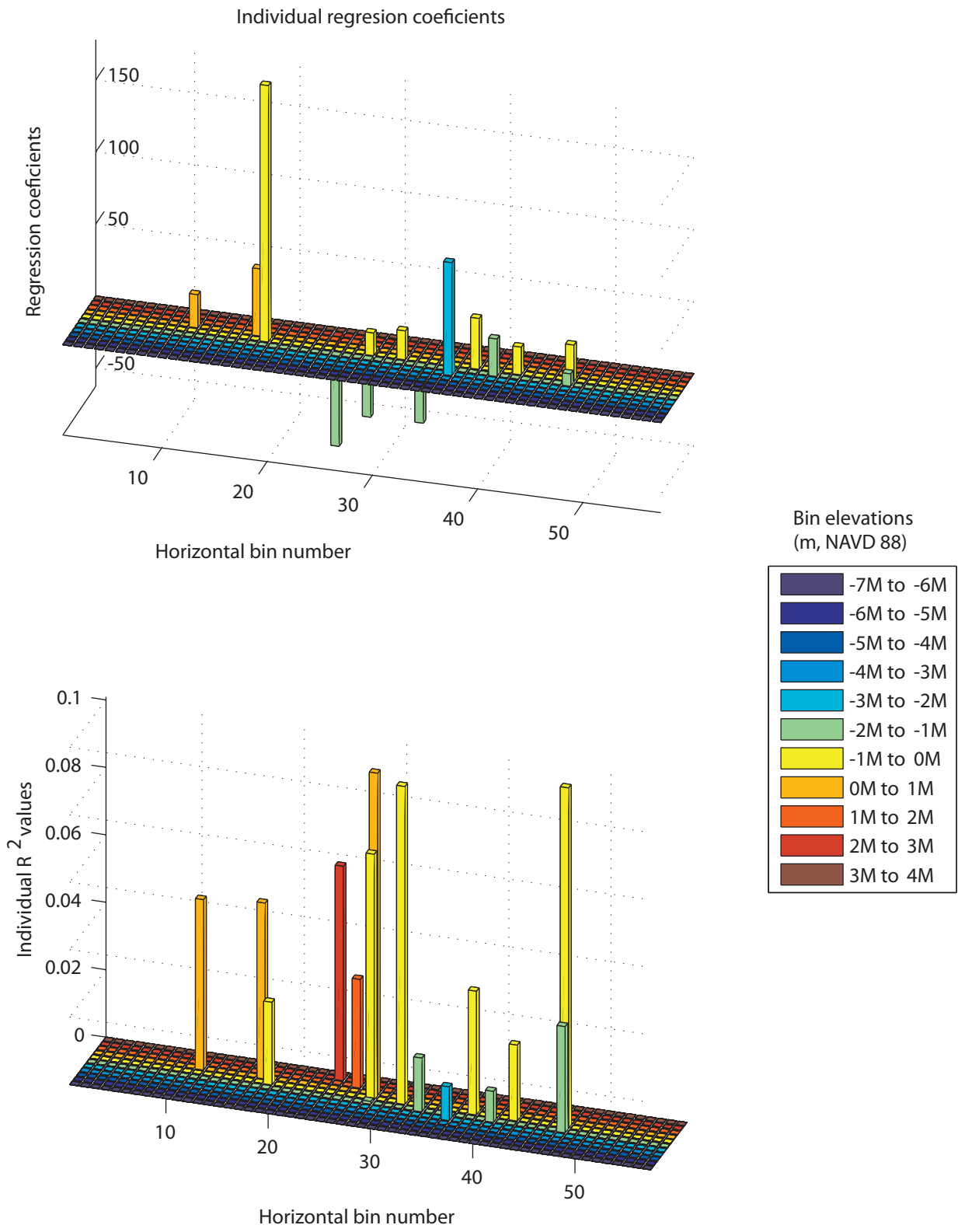


Figure 57. Cross correlation coefficients between individual DAG bin fish density signals, and downstream entrainment signals, shaded by correlation coefficient. Pink areas are areas in the beams with now significant correlation, grey areas are wet areas with no beam coverage.

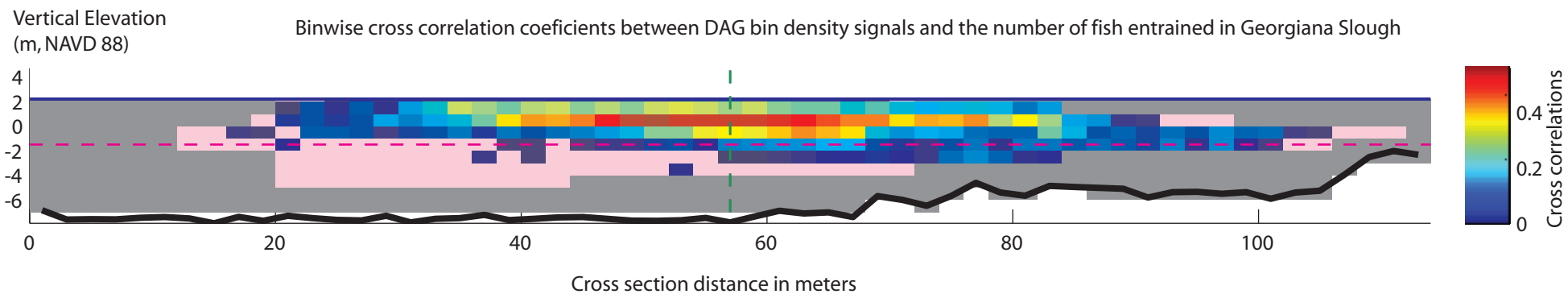
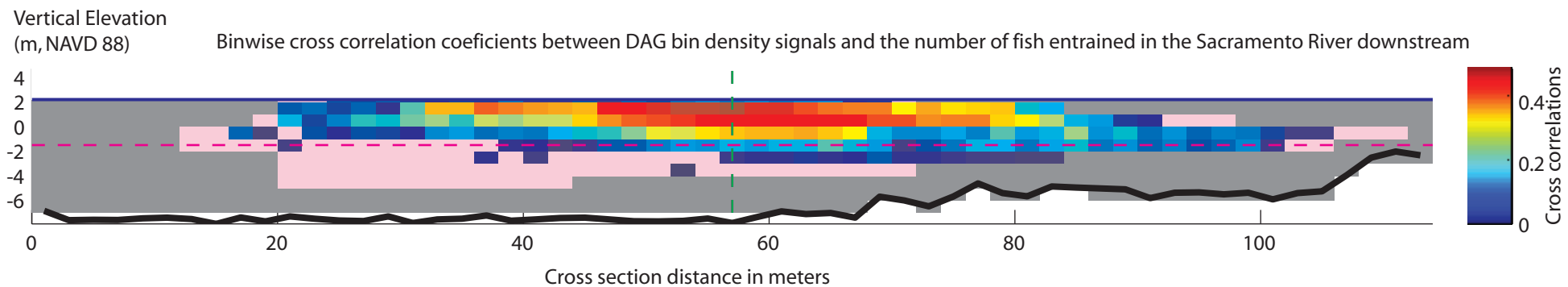
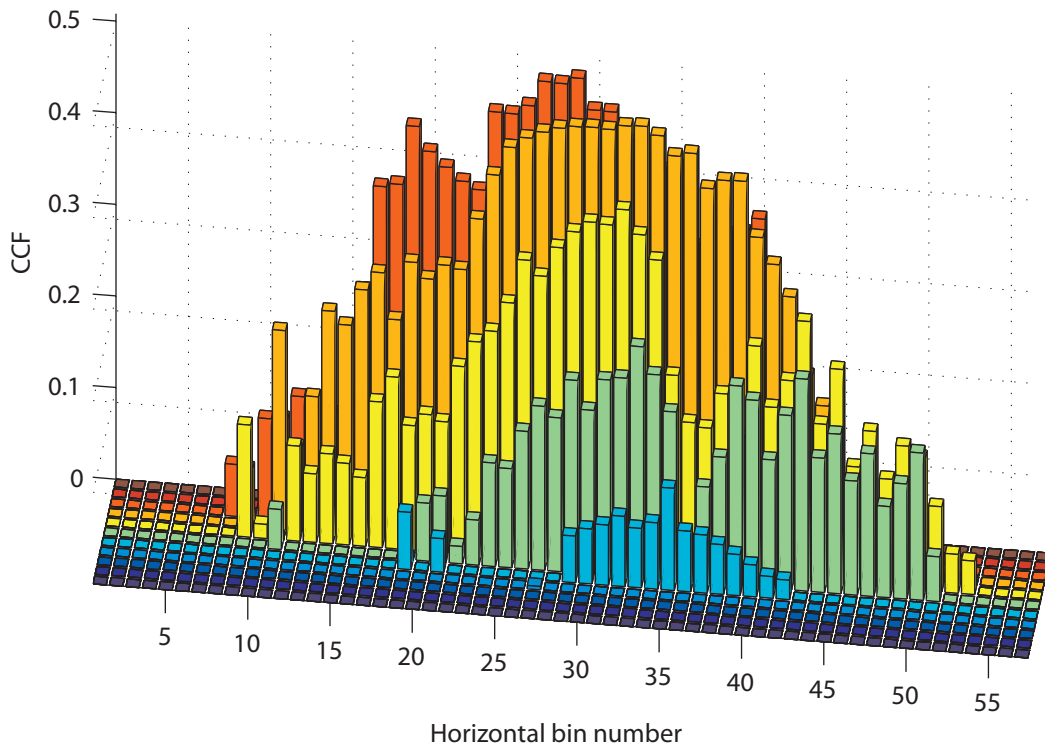


Figure 58. Correlations between fish density signals for individual bins at DAG, and downstream entrainment

Distribution of cross correlation coefficients between DAG individual bin detections over time and SACDS detections



Distribution of cross correlation coefficients between DAG individual bin detections over time and GS detections

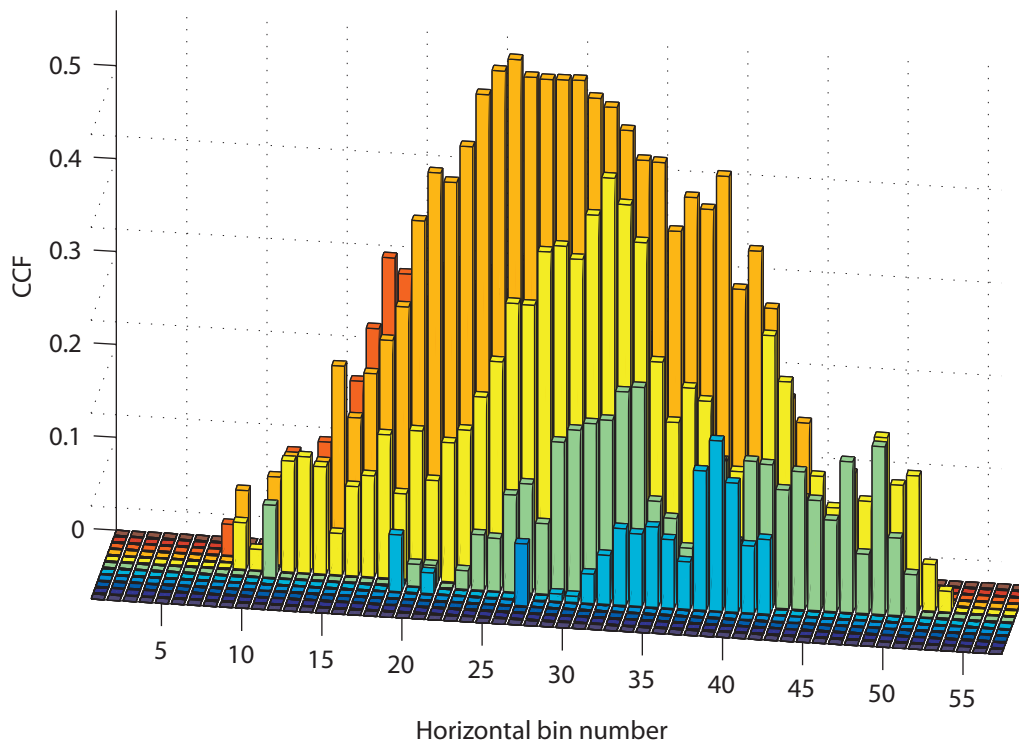


Figure 59. Total fish densities entering and leaving the control volume

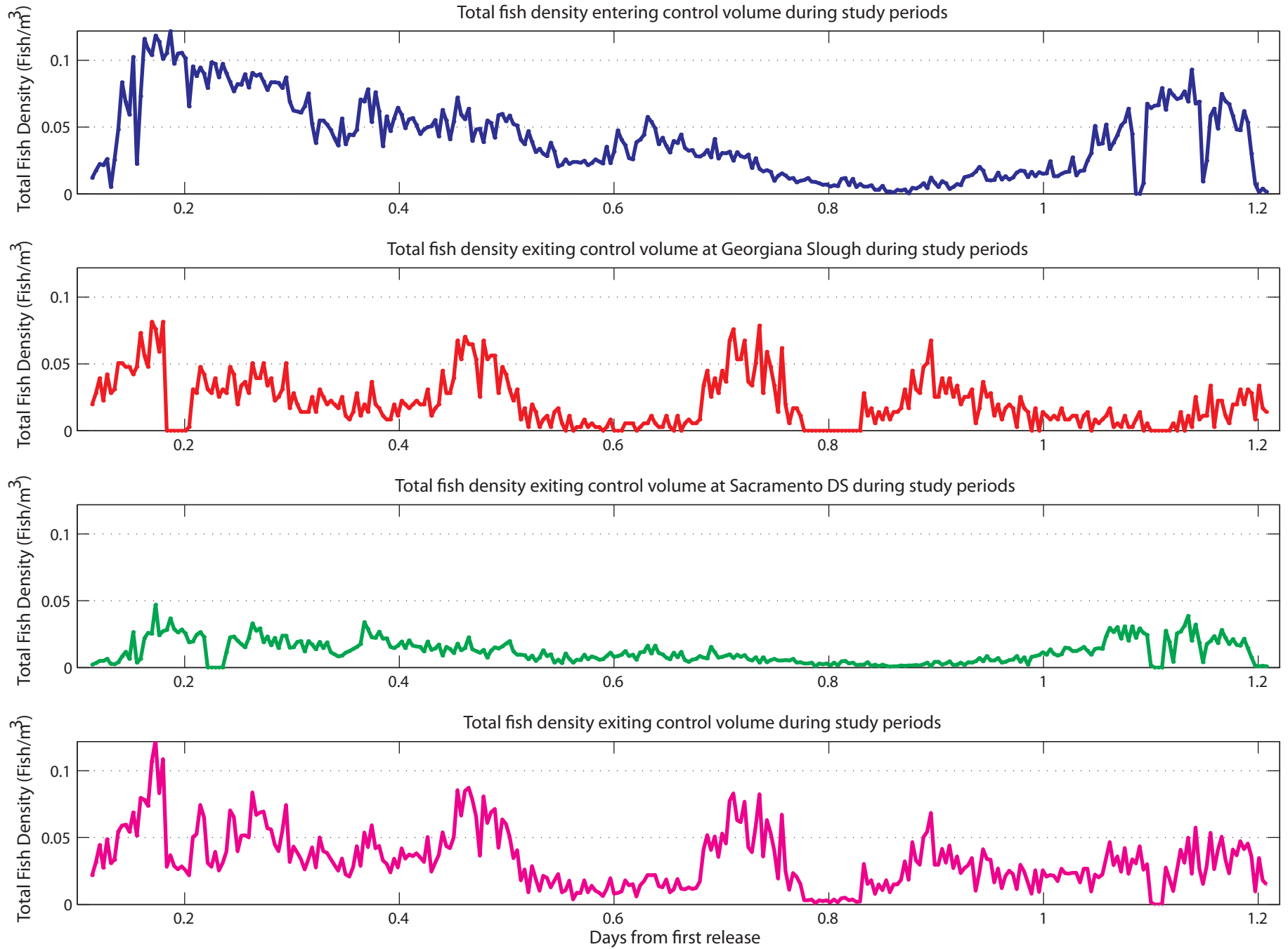


Figure 60. Total fish densities in each branch computed by deviding the total number of fish detected per 5 minute bin in each branch by the total volume of water moving through the branch in that 5 minute period

